Analog-Model Analysis of Regional Three-Dimensional Flow in the Ground-Water Reservoir of Long Island, New York

GEOLOGICAL SURVEY PROFESSIONAL PAPER 982

Prepared in cooperation with
the Nassau County Department of Public Works,
the Suffolk County Department of Environmental Control,
the Suffolk County Water Authority, and
the New York State Department of Environmental Conservation

Analog-Model Analysis of Regional Three-Dimensional Flow in the Ground-Water Reservoir of Long Island, New York

By RUFUS T. GETZEN

GEOLOGICAL SURVEY PROFESSIONAL PAPER 982

Prepared in cooperation with
the Nassau County Department of Public Works,
the Suffolk County Department of Environmental Control,
the Suffolk County Water Authority, and
the New York State Department of Environmental Conservation

UNITED STATES GOVERNMENT PRINTING OFFICE, WASHINGTON : 1977

UNITED STATES DEPARTMENT OF THE INTERIOR

THOMAS S. KLEPPE, *Secretary*

GEOLOGICAL SURVEY

V. E. McKelvey, *Director*

Library of Congress Cataloging in Publication Data

Getzen, Rufus T.
Analog-model analysis of regional three-dimensional flow in the ground-water reservoir of Long Island, New York

(Geological Survey Professional Paper 982)
Bibliography: p. 47-49.
Supt. of Docs. no.: I 19.16:982
1. Groundwater flow–New York (State)–Long Island–Electromechanical analogies. 2. Groundwater flow–New York (State)–Long Island–Data processing. 3. Water, Underground–New YOrk (State)–Long Island–Electromechanical analogies. 4. Water, Underground–New York (State)–Long Island–Data processing. I. Nassau Co., N. Y. Dept. of Public Works. II. Title: Analog-model analysis of regional three-dimensional flow in the groundwater reservoir of Long Island. . . II. Series: United States Geological Survey Professional Paper 982.
TC176.G48 551.4'9'0974721 76-608323

For sale by the Superintendent of Documents, U.S. Government Printing Office
Washington, D.C. 20402

Stock Number 024-001-02936-7

CONTENTS

ILLUSTRATIONS

TABLES

SYMBOLS AND ABBREVIATIONS

[Basic physical dimensions given in parentheses]

A_1, A_2, A_3, A_4	similarity coefficients for relating hydrologic quantities to their electronic counterparts
amp	amperes
C	capacitance (coulombs/volt)
cm	centimetres (length)
cm^{-1}	reciprocal centimetres (1/length)
cm/s	centimetres per second—Darcy velocity (length/time)
cm/d	centimetres per day (length/time)
coul	coulombs
E	electromotive potential (volts)
ft	feet (length)
ft/d	feet per day (length/time)
ft^3/s	cubic feet per second ($length^3$/time)
$(gal/d)/ft^2$	gallons per day per square foot (=1 Meinzer Unit; unit gradient and prevailing ground-water temperature presumed)
h	head, ground-water potential (length)
I	electric current (coulombs/time)
K	hydraulic conductivity (length/time)
K_x, K_y, K_z	hydraulic conductivity in x, y, z directions, respectively; gradient and discharge are assumed to be measured in same direction (length/time)
K_{xx}, K_{xy}, K_{xz}, K_{yy}, K_{yz}, K_{zz}	hydraulic conductivity in various directions; first subscript denotes direction of discharge, second subscript direction of gradient. K is a symmetric tensor, so no change in quantity results from reversing subscript (length/time)
K_A	maximum principal hydraulic conductivity (length/time)
K_B	minimum principal hydraulic conductivity (length/time)
m	metres (length)
m^3/s	cubic metres per second—volumetric discharge ($length^3$/time)
mA	milliamperes ($10^{-3}\times$coulombs/sec)
Mgal/d	million gallons per day ($length^3$/time)
$(Mgal/d)/mi^2$	million gallons per day per square mile—volumetric recharge rate (length/time)
pf	picofarads ($10^{-12}\times$coulombs/volt)
Q	volumetric discharge rate ($length^3$/time)
q	electric charge (coulombs)
q_x, q_y, q_z	components of Darcy velocity (length/time)
R	resistance (ohms)
S_s	specific storage; storage per unit volume (1/length)
S_y	specific yield (dimensionless)
s	second (time)
T	transmissivity ($length^2$/time)
t	time
t'	model time (as opposed to real time)
V	volume ($length^3$)
x, y, z	dimensions in arbitrary directions (length)
x', y', z'	dimensions corresponding to principal conductivities
Δ	finite-difference operator, $\Delta x=x_1-x_0$

CONVERSION TABLE

[The following conversions are given to four significant digits. Equivalent metric and English units in the text, however, have the same relative accuracy]

Metric	*Multiply by*	*English*
centimetres (cm)	3.937×10^{-1}	inches (in.)
centimetres (cm)	3.281×10^{-2}	feet (ft)
centimetres per second (cm/s)	2.835×10^{3}	feet per day (ft/d)
centimetres per second (cm/s)	2.223×10^{4}	gallons per day per square feet [(gal/d)/ft^2]
centimetres per year (cm/yr)	1.868×10^{-2}	million gallons per day per square mile [(Mgal/d)/mi^2]
cubic metres per second (m^3/s)	3.531×10	cubic feet per second (ft^3/s)
cubic metres per second (m^3/s)	2.282×10	million gallons per day (Mgal/d)
kilometres (km)	6.214×10^{-1}	miles (mi)
metres (m)	3.281	feet (ft)
square kilometres (km^2)	3.861×10^{-1}	square miles (mi^2)
square metres (m^2)	1.076×10	square feet (ft^2)
metres per kilometre (m/km)	5.280	feet per mile (ft/mi)

ANALOG-MODEL ANALYSIS OF REGIONAL THREE-DIMENSIONAL FLOW IN THE GROUND-WATER RESERVOIR OF LONG ISLAND, NEW YORK

By RUFUS T. GETZEN

ABSTRACT

A three-dimensional analog model of the ground-water system beneath Long Island, N.Y., provides a practical means for studying anisotropic flow on a regional scale. Constructional and operational techniques influence the simulation almost as much as model design does. Usefulness and accuracy of the model depend on (1) inherent and practical limitations of the finite-difference method, (2) accuracy and completeness of the data base, and (3) accuracy of the assumptions and approximations that were made in applying the simulation technique to this particular ground-water reservoir.

Reliable data used in design of the model are (1) horizontal hydraulic conductivity and thickness of three major aquifers, (2) extent of confining beds, (3) specific yield, and (4) locations of streams. Estimates of vertical hydraulic conductivity and specific storage were applied to the model. Most spatially fixed model boundaries are good representations of prototype (real-world) boundaries. Most dynamic boundaries are only approximately represented, and some dynamic boundaries require application of unproved assumptions. The simulated ground-water reservoir generally agrees with prototype hydrology, and the model is being used for predictive studies.

INTRODUCTION

BACKGROUND

More than one-third of the 7.3 million people on Long Island are wholly dependent on ground water as a source of water, and the remaining two-thirds use some ground water. More significantly, Nassau and Suffolk Counties, which together constitute more than 85 percent of the land area of Long Island, depend entirely upon ground water for all their water needs. The populations of Nassau and Suffolk Counties are growing rapidly, and the governing bodies of these counties are already planning for a time in the foreseeable future when the consumptive-use rate will reach the rate of total recharge to the ground-water reservoir.

Use of ground-water resources presents several problems that differ from those encountered in use of surface-water supplies. Most of these problems arise from or can be reduced to three basic conditions: (1) The properties of ground-water reservoirs, or aquifers, are fundamentally geologic and their investigation proceeds with great expense, great difficulty, and much guesswork; (2) ground-water reservoirs are interconnected over large areas, and seemingly isolated human activities and natural events can influence water quantity and quality over wide areas; (3) ground water moves at such slow rates that movement from the point of recharge to the point where the water is ultimately discharged typically requires decades or centuries, and direct observation of this movement is usually impossible.

One of the most powerful tools available to the ground-water hydrologist for predicting the behavior of large, complex aquifer systems such as the one on Long Island is a model—a mathematical or physical-mathematical technique for simulating the physics of ground-water flow. Such models require much simplification of the geometry and properties of the aquifers. The most frequent simplification is that the aquifer material is isotropic; that is, its hydraulic conductivity is the same in all directions at any given point. This simplification is seldom even approximately correct (Hubbert, 1940, p. 826), but because of flow geometry, it is commonly assumed to have little adverse effect on the accuracy of flow predictions.

The present study, investigating ground-water flow on Long Island, indicates that the anisotropy of the aquifers is a major factor controlling the effects of ground-water development and that these effects must be considered in managing Long Island's water resources. One of the principal goals of this report is to provide a physically sound practical basis for analyzing anisotropic flow on a regional scale.

PURPOSE AND SCOPE

This report discusses design, construction, and operation of a three-dimensional electrical analog model of the ground-water system beneath Long Island, N.Y. Because the streams of Long Island are important as boundaries within the aquifer system, some aspects of stream hydrology are also represented by this model, but the design of the model limits its major uses to predicting regional or general changes in ground-water head or flow. This report describes sources and types of data used in designing the model, some of the

basic concepts and assumptions that underlie its operation, calibration of the model in terms of historical hydrologic data, probable sources of inaccuracy in its results, and certain conclusions on the behavior of anisotropic aquifers.

A prime use of the model will be to anticipate the response of the flow system to various expected and proposed stresses. These stresses can take the form of pumping or recharge through wells, streams, or basins. A model of this type cannot be used for water-quality predictions, although crude estimates and general trends in water quality can be derived from hydrologic information gained from the model. Several of the proposed water-management schemes have been modeled; results of some of this modeling are the subject of additional reports in this series of publications.

PREVIOUS WORK

Previous research, on which this study is dependent, is of two types: (a) Development of theory and techniques for analysis of ground-water flow; and (b) studies of Long Island's water resources, which have provided (1) information on the geologic background, (2) hydrologic data, and (3) general understanding of the hydrologic situation on Long Island.

The geology of Long Island has been studied extensively since the mid-nineteenth century, and a massive literature has accumulated. Some of the more important early papers are those by Mather (1843), Upham (1879), Dana (1890), Hollick (1893, 1894), Woodworth (1901), and Salisbury (1902). DeVarona (1896) and Freeman (1900) studied the water resources of the western part of Long Island. The report by Veatch, Slichter, Bowman, Crosby, and Horton (1906) is a comprehensive study of the geology and the water resources of the entire island but does not include quantitative data on the hydrologic properties of the ground-water reservoir.

Few quantitative data on aquifer properties were available before 1950, but some controlled pumping tests were made by C. E. Jacob, J. G. Ferris, W. V. Swarzenski, M. A. Warren, and N. J. Lusczynski at various times between 1935 and 1950 (Jacob, 1939, 1941, 1945; McClymonds and Franke, 1972) and yielded data of varying quality and quantity. McClymonds and Franke (1972), working with lithologic logs and acceptance tests from about 1,300 wells, compiled estimates of the transmissivity and the bed-parallel hydraulic conductivity for the major aquifers of Long Island. These estimates have been used in the current study.

Geologic and hydrogeologic features of Long Island have been described in comprehensive reports by other authors since the 1906 report by Veatch, Slichter, Bowman, Crosby, and Horton (Fuller, 1914; Suter and others, 1949). Detailed geology of smaller areas is described in reports by Isbister (1966), Lubke (1964), Perlmutter and Geraghty (1963), Pluhowski and Kantrowitz (1964), Swarzenski (1963), Soren (1971), and Jensen and Soren (1974).

The present investigation is not the first U.S. Geological Survey study of Long Island's water resources to use analog modeling techniques, but with some exceptions, the previous studies were not published, largely because of inadequacies or inaccuracies in the models. In October 1964, plans were begun for constructing an analog model of Long Island's aquifers. These plans resulted in the construction of a two-layer regional flow model of the western half of Long Island. Attempts to verify this model against historical and synthetic data produced inconsistent results. Experimentation over a period of 2 years with this model failed to bring it into tolerable agreement with all known aspects of Long Island's hydrology. This model indicated that a two-layered concept was inadequate for describing the ground-water flow system beneath Long Island. Part of the difficulty in obtaining an adequate representation of the hydrologic system was insufficient data on the confining beds that overlie parts of the Magothy aquifer.

In 1966, a steady-state axisymmetric analog of flow to a single well was used in the interpretation of pumping tests at Bay Park, Long Island. Experimentation with cross-sectional models of the aquifer system was begun in 1968. Results from a model of this type were used by Franke and Cohen (1972) to compute regional rates of ground-water movement. Additional cross-sectional modeling was done by Franke and Getzen (1975). A series of modeling experiments, in which the vertical and the horizontal conductivities of aquifers and confining beds, rates of recharge, and other hydrologic parameters were varied systematically, demonstrated the importance of anisotropy in controlling regional ground-water flow on Long Island. Some of the results of this series of experiments serve as basic starting points for the design of the three-dimensional model discussed in this report.

In 1971, work was begun on the model that is the subject of the present report. Construction of the model was completed in less than 4 months, but testing and modification of the model were not completed until early 1974. This analog model represents three-dimensional regional flow in the ground-water reservior on Long Island. The digital modeling techniques that were available at the time this model was begun could not supply the needed accuracy and resolution when used on computers of the size commonly avail-

able. Existing analog techniques could be easily adapted to simulate three-dimensional, anisotropic flow; because development of an adequate digital model would require much experimentation, the author chose the analog approach.

Two Long Island modeling studies that were not done by the Geological Survey were (a) a cross-sectional Hele-Shaw model (Wilson, 1970) and (b) a single-aquifer digital model of the southeastern part of Long Island (Fetter, 1971). The Hele-Shaw model is sophisticated in concept and design and uses composite anisotropic permeabilities (Collins and others, 1972; Collins and Gelhar, 1970).

LOCATION AND GENERAL PHYSIOGRAPHY OF STUDY AREA

Long Island is bounded on the north by Long Island Sound, on the east and south by the Atlantic Ocean, and on the west by New York Bay and the East River (fig. 1). The island parallels the New York and Connecticut coasts for about 190 kilometres (120 miles) and has an area of about 3,600 square kilometres (1,400 square miles), including several smaller islands that are within the same political boundaries. The eastern end of Long Island is divided into two narrow forks by the Peconic Bay, and the southern edge of the island is fringed with an almost continuous line of barrier beaches. The forks and barrier beaches are not included in the primary study area shown in figure 1. Data from the barrier beaches were used in designing and testing the model, but no predictive capability was developed for these areas. The area of the two forks (east of Shinnecock Canal and Mattituck Creek) was not used.

The island is divided into four counties, two of which (Kings and Queens Counties) are within the political boundaries of New York City. Kings, Queens, Nassau, and Suffolk Counties have areas of 202, 298, 754, and 2,390 square kilometres (78, 115, 291, and 923 square miles), respectively.

ACKNOWLEDGMENTS

Parts of this report were included in the author's Ph.D dissertation, Department of Geology, University of Illinois. Publication rights have been given to the Geological Survey.

Prof. O. L. Franke of City College, New York City University, assisted the author in gathering the data for this report. Prof. Franke also examined the report for technical accuracy.

Mr. D. E. Vaupel provided unpublished stream data. He and several of his assistants provided qualitative and quantitative information about Long Island streams, both orally and written, on several occasions during 1971–73.

Laboratory assistants B. H. Cohen, M. E. Eskenazi, Daniel Gillen, Natale Guadagnino, and R. F. Lingner built the model; they and A. W. Harbaugh and Donald

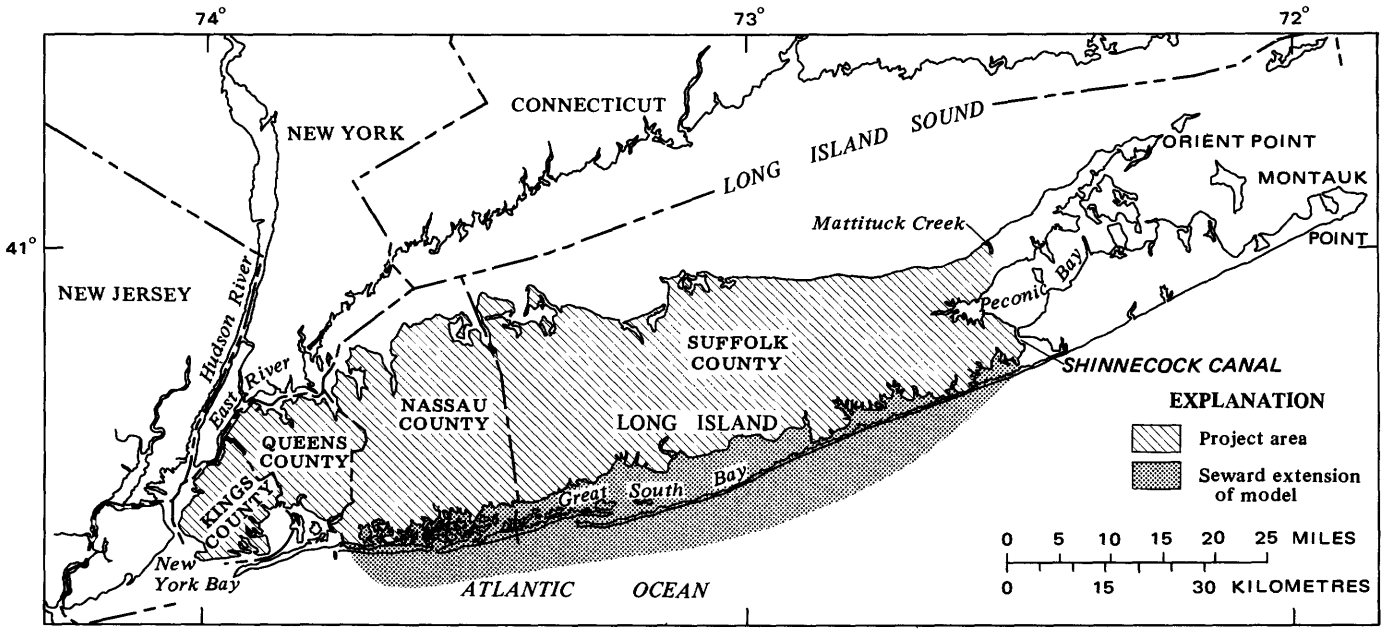

Base from U.S. Geological Survey, 1:250,000 series:
Scranton, Hartford, 1962; New York, 1957;
Newark, Providence, 1947

FIGURE 1.—Long Island, N.Y., showing area of investigation.

Hockheiser assisted in testing and modifying the model.

UNITS OF MEASURE

Metric units were used in this study, but not for field data and not until after most of the model design and construction were completed. Metric units have been given preference in the text, but some illustrations, adapted from other sources, could not be easily modified and are reproduced here in their original units. Where these illustrations are referred to in the text, the original units in the illustrations are mentioned first. This inconsistency seems unavoidable.

HYDROGEOLOGY OF LONG ISLAND

The hydrologic cycle on Long Island, as in most places, tends towards a state of dynamic equilibrium. That is, the naturally occurring outputs of water tend to balance the inputs, and the pattern of flow remains fairly constant over long periods of time. The sun provides the energy to maintain the hydrologic cycle by evaporating water at low altitudes and releasing it at higher altitudes in the form of precipitation. Precipitation is indicated by (A) in figure 2, which outlines the major components of the hydrologic cycle; evaporation is shown by (B). Rates of evaporation are greatest where bodies of surface water are directly exposed to sun and wind, but some evaporation occurs across the entire surface of the island.

Some of the precipitation occurs over bodies of surface water or within such a short distance from them that the water reaches these surface-water bodies without infiltrating the soil. Such direct runoff accounts for a small percentage of the total precipitation on Long Island, and, except in areas with storm sewers, is an infrequent event.

Water is also transpired to the atmosphere by plants (C). On Long Island, the sum of the quantities of transpiration and evaporation is almost always less than precipitation. Net natural recharge to the ground-

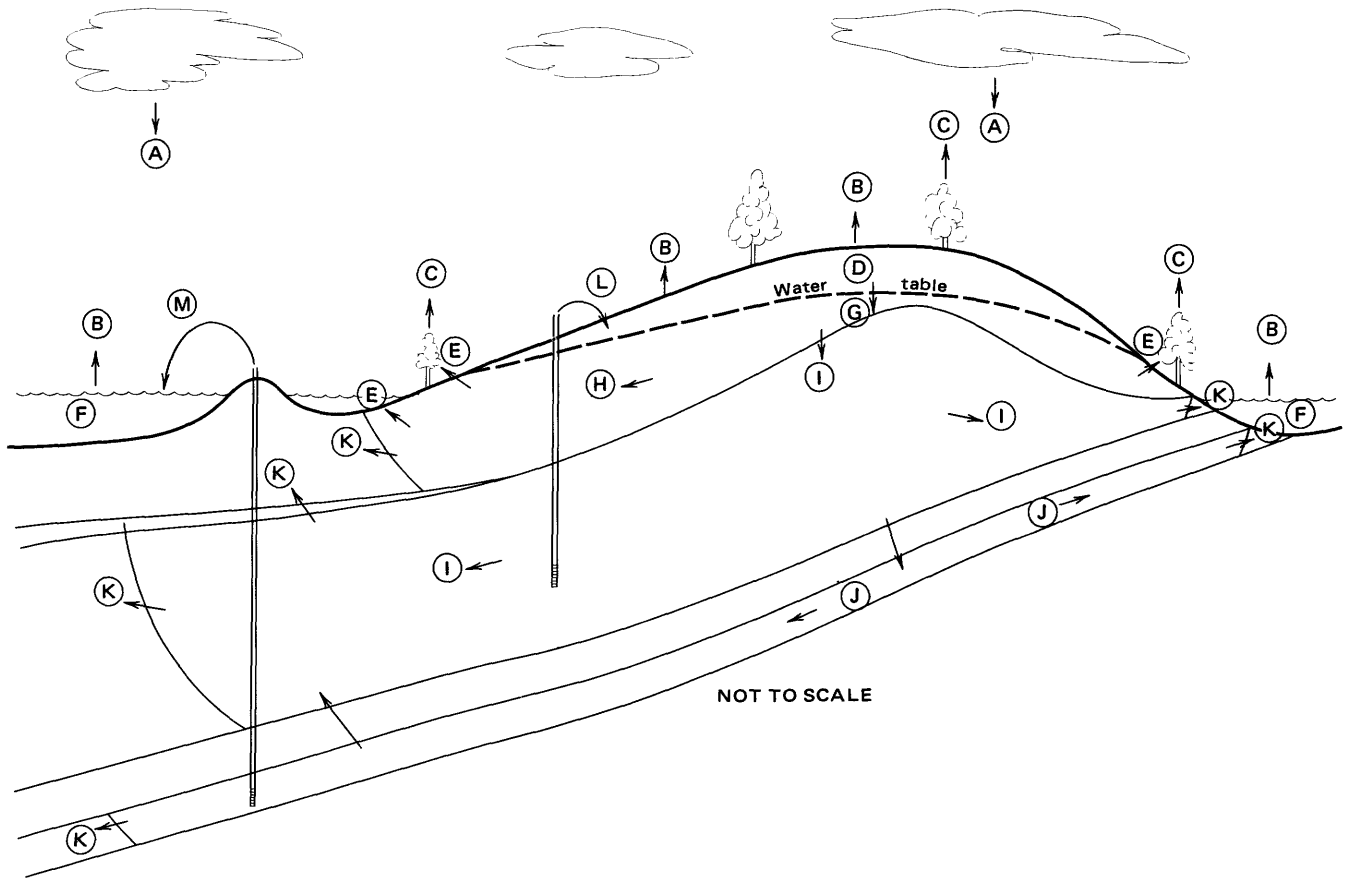

FIGURE 2.—Major components of the hydrologic cycle on Long Island: (A) precipitation, (B) evaporation, (C) transpiration, (D) unsaturated ground-water flow, (E) surface seepage, (F) salty water, (G) saturated ground-water flow, (H) glacial aquifer, (I) Magothy aquifer, (J) Lloyd aquifer, (K) dispersion into salty ground water, (L) deep pumpage returned to surface, and (M) deep pumpage returned to salty water. Arrows show inferred direction of water movement.

water reservoir is the difference between precipitation and the sum of evaporation and direct runoff. The ground-water reservoir is that part of Long Island's rocks and sediments that is saturated with freshwater (G), but recharge does not usually enter this saturated zone without first passing through an unsaturated zone (D) in which the interstices (openings between sedimentary particles) are only partly filled with liquid water. Part of the interstitial volume is occupied by water vapor and other gases. The ground-water reservoir is separated from the unsaturated zone by the water table—a surface along which the interstitial pressure is equal to atmospheric pressure. The top part of the reservoir (H), the glacial aquifer, is a water-table aquifer; its upper surface is the water table. Some of the water in the water-table aquifer is discharged directly to the surface as springs and as seepage to streams, lakes, and marshes. Collectively, these discharge points (E) are known as seeps. The remainder of the water in the water-table aquifer flows into other hydrogeologic units (I and J). The Magothy aquifer (I) and the Lloyd aquifer (J) are distinguished from the glacial aquifer (H) by differences in lithology and geologic origins, by differences in physical properties, or by the fact that water flows within each aquifer more readily than from one aquifer to another.

Water from all three aquifers (H, I, and J) is eventually discharged to salty surface water, either directly or through intervening sediments containing mixed freshwater and salty water (K). This discharge and most other components of the hydrologic cycle are inputs and outputs in relation to the ground-water reservoir. These inputs and outputs form the natural stresses and boundary conditions to the reservoir.

Flow within the ground-water reservoir is controlled by three factors—driving forces, resistive forces, and changes in storage. A flow system in dynamic equilibrium maintains a constant flow rate and a flow pattern that does not change with time; hence, there are no changes in storage. Although the Long Island flow system tends towards dynamic equilibrium, such equilibrium is not perfectly achieved. There are small, local changes in flow patterns (and in storage) resulting from waves and tides and daily fluctuations in precipitation. There are larger changes in flow resulting from climatic changes and human activities; these are discussed later in this section. Driving forces within the reservoir result from differences in the potential energy at different points within the reservoir. Two sources of potential energy are pressure and direct action of gravity. The sum of the gravitational potential and pressure potential at any point is the ground-water head at that point, and the driving force equals the gradient of head. Both the direction and the magnitude of the driving force differ from point to point within the reservoir. On a macroscopic scale (a scale that includes a statistically significant number of interstices), the spatial variation in head can be described by piecewise continuous functions.

Resistive forces result from friction between the moving fluid and the surfaces of the sedimentary particles. The forces are described by the term hydraulic conductivity, which includes such factors as density and viscosity of the water and microscopic geometry of the sedimentary fabric. Not only does the geometry of the sedimentary fabric differ from point to point in the reservoir, but the fabric usually has a directional aspect, so that the hydraulic conductivity perpendicular to bedding at any point is less than the conductivity parallel to bedding. The first characteristic is described as nonhomogeneity, the second as anisotropy; both characteristics are true of the sediments that compose the Long Island ground-water reservoir.

The glacial aquifer (H in fig. 2) shows the least nonhomogeneity and the least anisotropy of any Long Island aquifer. At the other extreme, the hydraulic conductivity in the direction of bedding in the Magothy aquifer ranges through an order of magnitude or more along any bedding plane and through several orders of magnitude from top to bottom. The conductivity of the latter aquifer is also significantly lower perpendicular to bedding than it is along the bedding. Very little is known about the hydraulic conductivity of the Lloyd aquifer (J), but very little water flows through this aquifer (Franke and Getzen, 1975).

Properties of the water throughout a reservoir are usually assumed to be constant, and differences in hydraulic conductivity are assumed to be the result of differences in the medium (the sediments); but these assumptions cannot always be made. Salty water has a density different from that of freshwater; hot water is less dense and less viscous than cool water, and water flowing through sanitary landfills may have a viscosity and density quite different from those of the native ground water.

Flux (flow per unit area) through any part of the reservoir is equal to the product of the hydraulic gradient and the hydraulic conductivity. For isotropic aquifers, direction of flow is directly downgradient; but for anisotropic aquifers, such as those that constitute the Long Island ground-water reservoir, direction of flow may diverge from the direction of the gradient.

More than half the natural discharge from the reservoir is through seepage to streams and marshes. The remainder of the natural discharge is to salty surface water, either directly or through mixing with the salty ground water that surrounds Long Island. The mechanism through which this mixing occurs is poorly

understood; theoretical models, such as Cooper (1959) and the Gheyben-Herzberg theory (Glover, 1959), do not seem to fit the Long Island situation (Upson, 1966). Beneath the barrier islands along Long Island's south shore, fresh ground water is found at depths where it should be salty according to both equilibrium models. Two explanations for this have been proposed—(1) that the salty ground water is not in equilibrium with present-day heads along Long Island's south shore and that the fresh ground water there is a relic of the island's last glaciation; or (2) that the salty water is in equilibrium with the heads but that the conditions for equilibrium are modified by the osmotic effects of clay within the lower part of the reservoir. Neither of these explanations can be wholly proved or disproved. Other possible explanations are that presently observed heads reflect human influences or that Long Island's climate is significantly drier than it was a few centuries ago. However, observed heads in the water-table aquifer indicate little or no change during the past 70 years throughout most of the eastern half of Long Island, and there is very little evidence to support the hypothesis of much greater precipitation at any time since the last major glaciation.

Human influences on the hydrologic cycle are of three types: (1) Reduction of recharge through paving and storm sewers, (2) removal of water from deeper aquifers through wells and recharge to the water-table aquifer through cesspools and basins, and (3) removal of ground water through wells and discharge to the ocean through sewers. These last two are shown as new components to the hydrologic cycle (L and M, fig. 2). All three human influences result in immediate changes in the amount of ground water in storage, followed by spreading changes in head and flow patterns as the system seeks a new equilibrium. All three human influences were active in Kings and western Queens Counties from the mid-nineteenth century until the early 1940's. The flow system responded to this stress by (1) reduced heads, (2) reduced streamflow, and (3) intrusion of salty water into the more highly conductive parts of the reservoir. Human influences of all three types have been active in Queens and Nassau Counties since the 1940's, and the system has responded by (1) reduced heads and (2) reduced streamflow. Seepage to the bottoms of the surrounding saltwater bodies has been reduced somewhat, but to date (1975) little saltwater intrusion has been observed. Human influences in Suffolk County have generally been limited to removal of water from deep aquifers and recharge to the water-table aquifer. The only observed response has been a decline of head at depth in the western one-third of Suffolk County.

Human activities have also affected quality of ground water on Long Island. Cesspool effluent, industrial wastes, road salt, contaminated runoff from highways and parking lots, decomposing wastes in sanitary landfills, chemical fertilizers and pesticides, animal feces, and leaking sewer mains have all degraded the quality of recharge water. Large parts of the ground-water reservoir now contain water of less than desirable quality. The glacial aquifer is affected over most of the western half of the island and the Magothy aquifer in the west-central part of the island where the movement of ground water is predominantly in a downward or down-and-lateral direction. Pumping from the lower part of the Magothy aquifer is accelerating the downward movement of the contaminated recharge water. This study, although it analyzes movement of ground water, does not attempt to explain or predict changes in water chemistry.

PROMINENT PHYSIOGRAPHIC FEATURES AND THEIR ROLE IN THE HYDROLOGY OF LONG ISLAND

The physiographic features of Long Island are a result of its geologic history; there is a conspicuous geographic relationship between many of these features and the hydrologic features of Long Island, not only because of their role in determining the gross geometry of the flow system but also because of the close connection between the topographic features and the underlying geology. The most prominent physiographic features are related to Pleistocene glaciation. These are (1) the east-west trending hills in the northern and central parts of the island and their eastward extensions, which form the north and south forks, (2) the gently sloping plain that extends southward from the hills, and (3) the deeply eroded headlands along the north shore. Other important features are the barrier beaches along the south shore, the shoreline, and the major streams.

The Harbor Hill Moraine, which forms the northern line of east-west trending hills, extends from Kings County to Orient Point on the north fork (fig. 3). The southern line of hills, which make up the Ronkonkoma Moraine, extends from northwestern Nassau County eastward to Montauk Point. These moraines were deposited near the southern terminus of glacial ice sheets and have an altitude ranging from 70 to 90 m (210 to 270 ft) in most places.

GEOLOGIC FEATURES

The consolidated bedrock that underlies Long Island in overlain by a wedge-shaped body of unconsolidated sediments (fig. 4). The bedrock is at or near land sur-

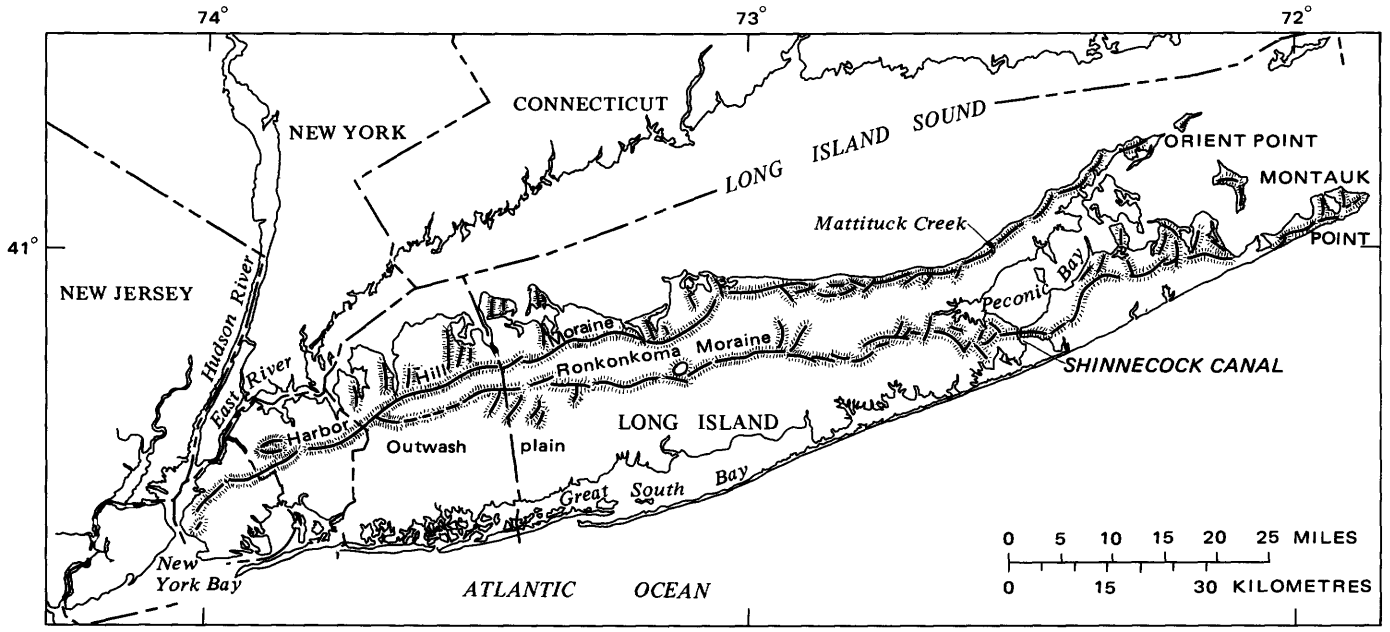

Base from U.S. Geological Survey, 1:250,000 series:
Scranton, Hartford, 1962; New York, 1957;
Newark, Providence, 1947

FIGURE 3.—Physiographic features that influence Long Island hydrology.

face in the northwestern part of Long Island and has a regional southeastward slope of about 0.7 degrees (about 12 m/km or 63 ft/mi). The bedrock has an extremely low hydraulic conductivity (not measured); the contact between it and the Cretaceous sediments can be considered to be the lower boundary of the ground-water flow system. The Cretaceous sediments and overlying deposits that are saturated with fresh, moving ground water constitute the ground-water reservoir.

Pertinent information on the reservoir rocks is summarized in table 1. Figures 4–8 show what was known of the gross geometry of the reservoir rocks at the time the three-dimensional model was constructed (1971). These illustrations are regional, hydrogeological interpretations used in the current study. Additional geologic data were acquired after the study began; improper model performance suggested some discrepancies in the geologic data before the new data were acquired. Other recently acquired geologic data are insignificant to the regional hydrology but would have to be considered in hydrologic analyses of small areas.

The lowermost aquifer, the Lloyd, directly overlies the bedrock. The Lloyd consists mainly of gravelly sand with lenses of silty sand and clay. Seepage into the Lloyd aquifer is limited by the overlying Raritan clay, which has a fairly uniform thickness of 60–90 m (200–300 ft) and probably has a very low hydraulic conductivity (Franke and Getzen, 1975). The Raritan clay, even though silty and sandy in places, appears dense and well-compacted almost everywhere it has been seen, but it has been seen at only a few widely scattered localities. The Raritan is penetrated by only a few wells and is exposed in only a few places on the north shore of western Long Island. The clay is missing from the sequence in small areas of northwestern Long Island.

The Magothy aquifer, which probably includes parts of several poorly defined Cretaceous formations (Perlmutter and Todd, 1965), consists of a series of beds of fine to medium sand interbedded with clay and sandy or silty clay. Several of these beds seem to be fairly extensive, but none, apparently, can be traced for more than a few kilometres. The degree of consolidation of the sand beds varies from loose to moderately indurated, and their texture varies from silty to gravelly. Only rarely does the thickness of a single sand bed exceed 15 m (47 ft), but the thickness of some sandy zones that have only a few thin clay beds scattered through them are 50 m (160 ft) or more. Thickness of the clay beds range from a few millimetres to 20 m (66 ft); in many places, the beds are thicker in the upper part of the sequence than in the lower part.

The Magothy aquifer is overlain by several Cretaceous and post-Cretaceous units of low to very low hydraulic conductivity. Among these units are silty, sandy clay beds of the Monmouth Group along the south shore of Long Island. The beds thicken seaward.

Clays of the Monmouth Group are not found on western Long Island. There, the Magothy aquifer is overlain by the Jameco Gravel, evidently a fluvio-glacial deposit on an erosional surface in the Magothy. A fringe of Pleistocene clay that surrounds the island extends a few kilometres inland along much of the south shore and in several places on the north shore. This fringing clay is almost always referred to as the Gardiners Clay but may include material of diverse geologic origins (Upson, 1970). Material identified in well logs as Gardiners Clay generally ranges in thickness from 2 to 120 m (6 to 400 ft). The areas of the thickest parts of the clay are very small. The clay in the subsurface near the south shore seems to thicken slightly in a seaward direction, but its seaward extent is largely unknown.

The upper glacial aquifer consists primarily of sand and gravel, which is glaciofluvial and glaciodeltaic in origin. Even the end-morainal features on much of Long Island seem to be associated with deformed deposits of stratified drift rather than till (Mills and Wells, 1974). Several tills within and above the stratified drift have been identified in the northern part of the island, and several extensive clays, evidently glaciolacustrine in origin, are found within the stratified drift.

DISTRIBUTION OF HYDRAULIC CONDUCTIVITY AND STORAGE COEFFICIENT

Regional trends in the hydraulic conductivity of the upper glacial and Magothy aquifers on Long Island have been mapped by McClymonds and Franke (1972). These trends, shown in figures 9 and 10, are sufficiently accurate for a regional ground-water model, although the ground-water reservoir is not completely defined by them. The Jameco aquifer, which is highly conductive, is important in western Long Island. Figure 11 shows the areal extent and estimated hydraulic conductivity of the Jameco aquifer. Although the Jameco aquifer is a distinct geologic unit (Soren, 1971), it is continuous with the Magothy aquifer over much of its area and has been considered in this study as a high-permeability zone at the top of the Magothy aquifer. Several additional but minor hydrogeologic units are also part of the Long Island ground-water reservoir and are lumped here with major units.

Estimates of hydraulic conductivity mapped in figures 9–11 are for flow parallel to bedding (bed parallel) (McClymonds and Franke, 1972, p. E11). Similar estimates for flow perpendicular to bedding (bed normal) within each aquifer have not been published. Franke and Getzen (1975), in working with steady-state, cross-sectional models, conclude that an

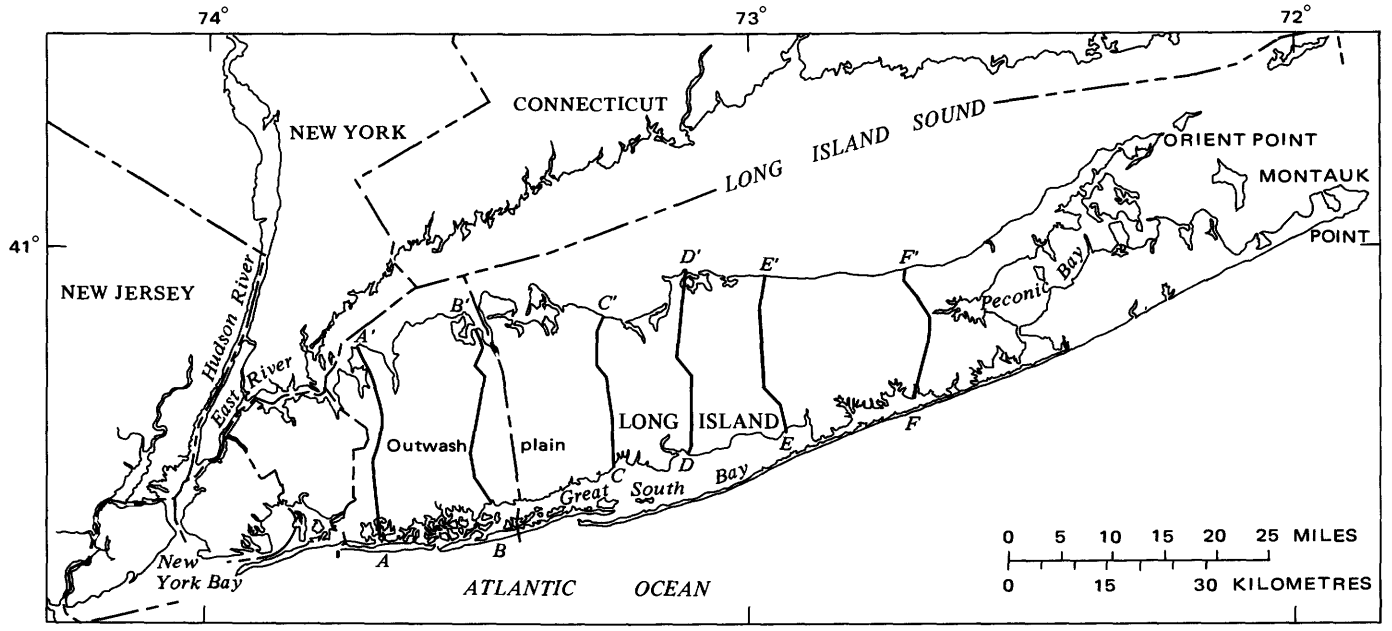

Base from U.S. Geological Survey, 1:250,000 series:
Scranton, Hartford, 1962; New York, 1957;
Newark, Providence, 1947

FIGURE 4.—Locations of and typical sections through the Long Island ground-water reservoir showing major hydrogeologic units. (Geology after Swarzenski, 1963; Isbister, 1966; Jensen and Soren, 1974.)

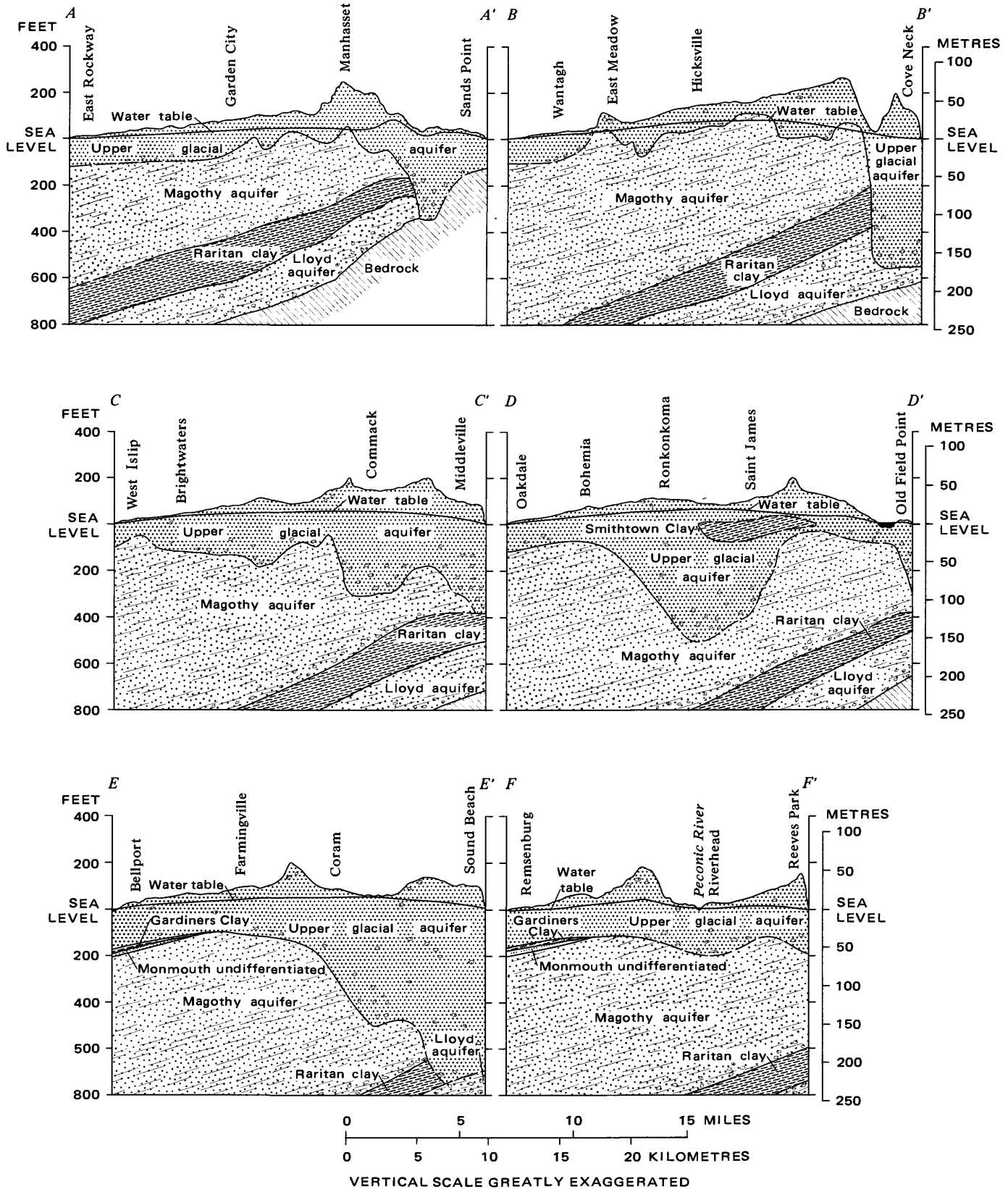

FIGURE 4.—Continued.

TABLE 1.—*Hydrogeologic units of Long Island*
[From McClymonds and Franke, 1972, p. E5–E6]

System	Series	Geologic unit[1]	Hydrogeologic unit	Approximate maximum thickness (metres)	Depth from land surface to top (metres)	Character of deposits	Water-bearing properties
Quaternary	Holocene	Recent deposits: Artificial fill, salt marsh deposits, stream alluvium, and shoreline deposits.	Recent deposits	15	0	Sand, gravel, clay, silt, organic mud, peat, loam, and shells. Colors are gray, brown, green, black, and yellow. Recent artificial-fill deposits of gravel, sand, clay, and rubbish.	Permeable sandy beds beneath barrier beaches yield fresh water at shallow depths, brackish to salty water at greater depth. Clay and silt beneath bays retard saltwater encroachment and confine underlying aquifers. Stream floodplain and marsh deposits may yield small quantities of water but are generally clayey or silty and much less permeable than the underlying upper glacial aquifer.
	Pleistocene	Upper Pleistocene deposits	Upper glacial aquifer	180	0–15	Till (mostly along north shore and in moraines) composed of clay, sand, gravel, and boulders forms Harbor Hill and Ronkonkoma terminal moraines. Outwash deposits (mostly between and south of terminal moraines, but also interlayered with till) consist of quartzose sand, fine to very coarse, and gravel, pebble to boulder sized. Glaciolacustrine deposits (mostly in central and eastern Long Island) and marine clay (locally along south shore) consist of silt, clay, and some sand and gravel layers; includes the "20-foot clay" in southern Nassau and Queens Counties. Colors are mainly gray, brown, and yellow; silt and clay locally are grayish green. Contains shells and plant remains, generally in finer grained beds; also contains Foraminifera. Contains chlorite, biotite, muscovite, hornblende, olivine, and feldspar as accessory minerals; "20-foot clay" commonly contains glauconite.	Till is poorly permeable; commonly causes perched-water bodies and impedes downward percolation of water to underlying beds. Outwash deposits are moderately to highly permeable; specific capacities of wells tapping them range from about 10 to more than 200 gal/min per ft (gallons per minute per foot) of drawdown. Good to excellent infiltration characteristics. Glaciolacustrine and marine clay deposits are mostly poorly permeable but locally have thin, moderately permeable layers of sand and gravel; generally retard downward percolation of ground water. Contains freshwater except near the shore lines. Till and marine deposits locally retard saltwater encroachment.
		Unconformity?					
		Gardiners Clay	Gardiners Clay	90	15–120	Clay, silt, and few layers of sand and gravel. Colors are grayish green and brown. Contains marine shells, Foraminifera, and lignite; also locally contains glauconite. Altitude of top generally is 50–80 feet below mean sea level. Occurs in Kings, Queens, and southern Nassau and Suffolk Counties; similar clay occurs in buried valleys near north shore.	Poorly permeable; constitutes confining layer for underlying Jameco aquifer. Locally, sand layers yield small quantities of water.
		Unconformity?					
		Jameco Gravel	Jameco aquifer	90	15–170	Sand, fine to very coarse, and gravel to large-pebble size; few layers of clay and silt. Gravel is composed of crystalline and sedimentary rocks. Color is mostly dark brown. Contains chlorite, biotite, muscovite, hornblende, and feldspar as accessory minerals. Occurs in Kings, Queens, and southern Nassau Counties; similar deposits occur in buried valleys near north shore.	Moderately to highly permeable; contains mostly freshwater, but brackish water and water with high iron content occurs locally in southeastern Nassau and southern Queens Counties. Specific capacities of wells in the Jameco range from about 20 to 150 gal/min per ft of drawdown.
		Unconformity					

adequate representation of aquifer properties near the center of Long Island must include a substantial degree of anisotropy; bed-normal conductivities one-tenth to one-twenty-fourth of bed-parallel conductivity are suggested for the upper glacial aquifer, and bed-normal conductivities one-thirtieth to one-sixtieth of bed-parallel conductivity are suggested for the Magothy aquifer. These ranges of anisotropy are supported by four recent aquifer tests. One test in the Magothy aquifer indicated an anisotropy of 1:30; three in the upper glacial aquifer indicated anisotropy ranging from 1:1.8 to 1:2.8. These tests, however, are inconclusive and may not be representative of the aquifers.

Reliable data for the conductivity of the confining beds (Gardiners Clay and other clays in the deposits of Cretaceous-Quaternary age that overlie the Magothy aquifer) are not available. A vertical conductivity of 2.5×10^{-5} cm/s (0.07 ft/d), characteristic of similar clay beds in Connecticut and Maryland, is reasonable for these units. Subsequent sensitivity tests conducted on the cross-sectional models of Long Island (Franke and Getzen, 1975) indicate that this estimate may be about one order of magnitude too high but that relative to the other parameters tested regional flow is insensitive to the conductivity of these beds. On a regional scale, horizontal flow in the confining beds is probably negligible.

Field data for storage coefficients of Long Island aquifers are meagre. The few data that are available indicate that the specific yield of the unconfined

TABLE 1.—*Hydrogeologic units of Long Island*—Continued

System	Series	Geologic unit[1]	Hydrogeologic unit	Approximate maximum thickness (metres)	Depth from land surface to top (metres)	Character of deposits	Water-bearing properties
Tertiary (?)	Pliocene(?)	Mannetto Gravel	(Commonly included with upper glacial aquifer.)	90	0–35	Gravel, fine to coarse, and lenses of sand; scattered clay lenses. Colors are white, yellow, and brown. Occurs only near Nassau-Suffolk County border near center of island.	Highly permeable, but occurs mostly above water table. Excellent infiltration characteristics.
		Unconformity					
Cretaceous	Upper Cretaceous	Magothy (?) Formation[2]	Magothy aquifer	340	0–180	Sand, fine to medium, clayey in part; interbedded with lenses and layers of coarse sand and sandy and solid clay. Gravel is common in basal 50–200 feet. Sand and gravel are quartzose. Lignite, pyrite, and iron oxide concretions are common; contains muscovite, magnetite, rutile, and garnet as accessory minerals. Colors are gray, white, red, brown, and yellow.	Most layers are poorly to moderately permeable; some are highly permeable locally. Specific capacities of wells in the Magothy generally range from 1 to about 30 gal/min per ft of drawdown, rarely are as much as 80 gal/min per ft of drawdown. Water is unconfined in uppermost parts; elsewhere is confined. Water is generally of excellent quality but has high iron content locally along north and south shores. Constitutes principal aquifer for public-supply wells in western Long Island except Kings County, where it is mostly absent. Has been invaded by salty ground water locally in southwestern Nassau and southern Queens Counties and in small areas along north shore.
		Unconformity					
		Raritan Formation — Clay Member	Raritan Clay	90	20–460	Clay, solid and silty; few lenses and layers of sand; little gravel. Lignite and pyrite are common. Colors are gray, red, and white, commonly variegated.	Poorly to very poorly permeable; constitutes confining layer for underlying Lloyd aquifer. Very few wells produce appreciable water from these deposits.
		Raritan Formation — Lloyd Sand Member	Lloyd aquifer	150	60–550	Sand, fine to coarse, and gravel, commonly with clayey matrix; some lenses and layers of solid and silty clay; locally contains thin lignite layers and iron concretions. Locally has gradational contact with overlying Raritan clay. Sand and most of gravel are quartzose. Colors are yellow, gray, and white; clay is red locally.	Poorly to moderately permeable. Specific capacities of wells in the Lloyd generally range from 1 to about 25 gal/min per ft of drawdown, rarely are as much as 50 gal/min per ft of drawdown. Water is confined under artesian pressure by overlying Raritan clay; generally of excellent quality but locally has high iron content. Has been invaded by salty ground water locally in necks near north shore, where aquifer is mostly shallow and overlying clay is discontinuous. Called "deep confined aquifer" in some earlier reports.
		Unconformity					
Precambrian		Bedrock	Bedrock		0–820	Crystalline metamorphic and igneous rocks; muscovite-biotite schist, gneiss, and granite. A soft, clayey zone of weathered bedrock locally is more than 100 feet thick.	Poorly permeable to virtually impermeable; constitutes virtually the lower boundary of ground-water reservoir. Some hard, freshwater is contained in joints and fractures but is impractical to develop at most places; however, a few wells near the western edges of Queens and Kings Counties obtain water from the bedrock.

[1]Names are those used in reports by the Geological Survey.
[2]The use of the term "Magothy(?) Formation" has been abandoned. The post-Raritan Cretaceous deposits are divided into the Magothy Formation and Matawan Group undifferentiated and the Monmouth Group undifferentiated.

aquifer north of the Harbor Hill terminal moraine is generally less than it is in the outwash plain south of the moraine (unpublished data in Geological Survey files). A specific yield (water-table storage coefficient) of 0.10 was estimated for the area north of the line shown in figure 12 and a coefficient of 0.18, south of this line. Water-table storage coefficients were assumed for the upper glacial aquifer throughout most of Long Island. In two small areas in the north-central part of the island, the top of the saturated zone is below the glacial deposits and the top of the Magothy aquifer is unconfined with a storage coefficient of 0.10. These specific yields are minimal for sediments with a porosity of 25–30 percent. A minimal value of 2×10^{-8} cm^{-1} (6×10^{-7} ft^{-1}) for compressive storage was also assumed. These estimates were based on a general appraisal of the lithology; subsequent aquifer tests tend to corroborate these values.

SURFACE WATER

LAKES

As described by Veatch, Slichter, Bowman, Crosby, and Horton (1906), lakes and ponds on Long Island occur in three different hydrologic environments. Lake Success is an example of a perched lake. This type of lake is separated from the main water table by nearly impervious strata and is common on the ground-morainal deposits that form the more elevated parts of

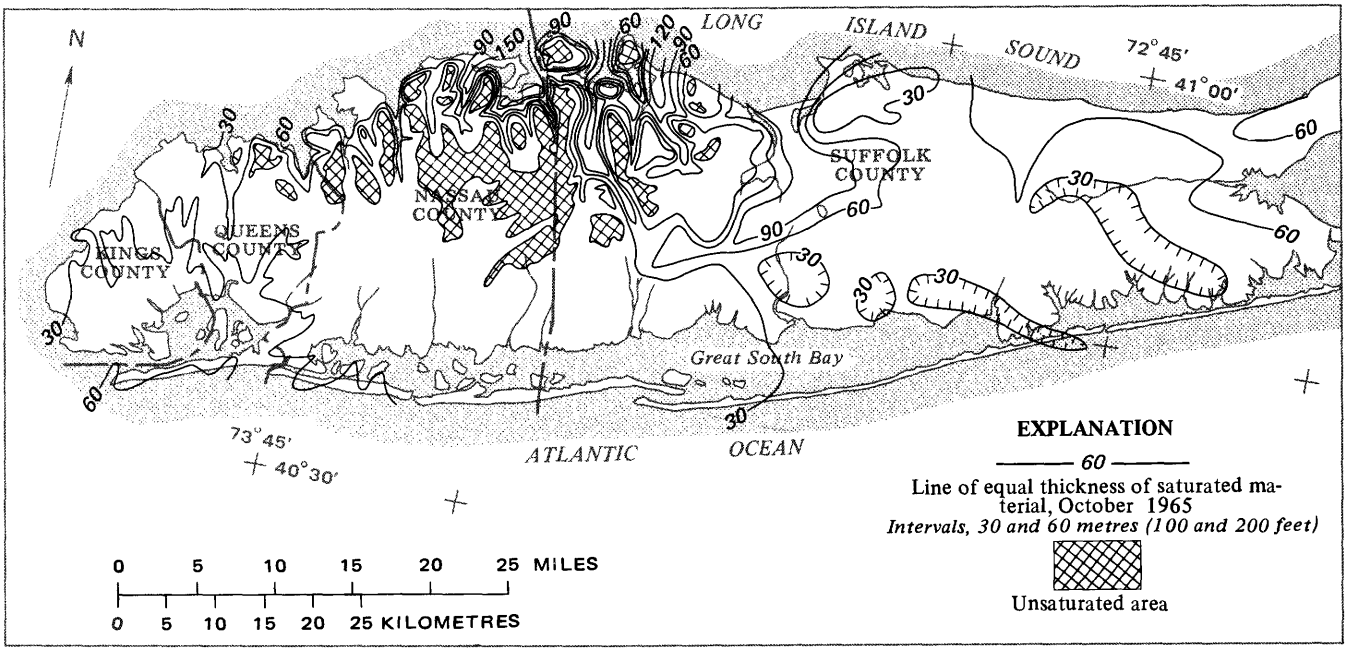

Base from U.S. Geological Survey, 1:250,000 series:
Hartford, 1962; New York, 1957; Newark, 1947

FIGURE 5.—Saturated thickness of the upper glacial aquifer on Long Island. (After McClymonds and Franke, 1972, pl. 1.)

the island. These lakes do not influence, nor, for the most part, are they influenced by the main water table.

A second type of lake, one that is dependent on the regional water table, is much more abundant on eastern Long Island. Lake Ronkonkoma is the largest lake of this type, but Artist Lake, Long Pond, Deer Pond, Swan Pond, Great Pond, Big Fresh Pond, and Poxabogue Pond are other examples (Veatch and others, 1906, p. 63). Water is exchanged more or less freely between this type of lake and the ground-water reservoir, and when water is pumped from a lake of this type or evaporates from its surface, the lake becomes a ground-water sink; it is a large "natural well." Both types of lakes are unimportant to the regional ground-water system.

Dammed streams constitute a third class of lakes (fig. 13). Depending on whether the water level in such lakes is maintained above or below the surrounding ground-water table, such lakes can function as either ground-water sources or sinks of a local nature. Figure 13 shows that dammed streams retard the seepage of ground water into the streams along the lakeshore. The basic effect of these lakes on the ground-water reservoir is to modify the regional gradients in their vicinities—decreasing the shorewards gradients in the areas above the dams and increasing gradients below the dams. Such a lake causes a reversal in the water table slope adjacent to the stream, which prevents ground-water seepage into the stream, but the effect on both streamflow and the water table is small a short distance upstream or downstream of the lake. In the regional analysis, each lake of this type is treated as a stream reach with little or no ground-water seepage.

STREAMS

The Nissequogue River, which has the highest average flow of any Long Island stream, had an average discharge of 1.18 m^3/s (40.3 ft^3/s) between 1943 and 1970 (U.S. Geological Survey, 1972, p. 37). There are four other major streams with discharges greater than 0.5 m^3/s (17 ft^3/s)—Peconic, Carmans, Connetquot, and Carlls Rivers. Most of the larger streams and all those with an average discharge greater than 0.3 m^3/s (10 ft^3/s), except the Nissequogue and Peconic Rivers, discharge along the south shore. Except for a few in the western part of the island, the streams of Long Island receive most of their flow from ground-water seepage (Cohen and others, 1968, p. 62). Seventy-five of these streams (fig. 14) are large enough so that each affects the water table and patterns of flow within the ground-water reservoir over an area greater than 2 km^2; all together, these streams drain more than 13.4 m^3/s (300 Mgal/d) from the ground-water reservoir.

The streams are of interest because of the way in which they are affected by changing ground-water levels and because of their changing rates of seepage from the ground-water reservoir. Even small fluctuations in water-table elevation can cause pronounced changes in stream discharge. Changes in stream dis-

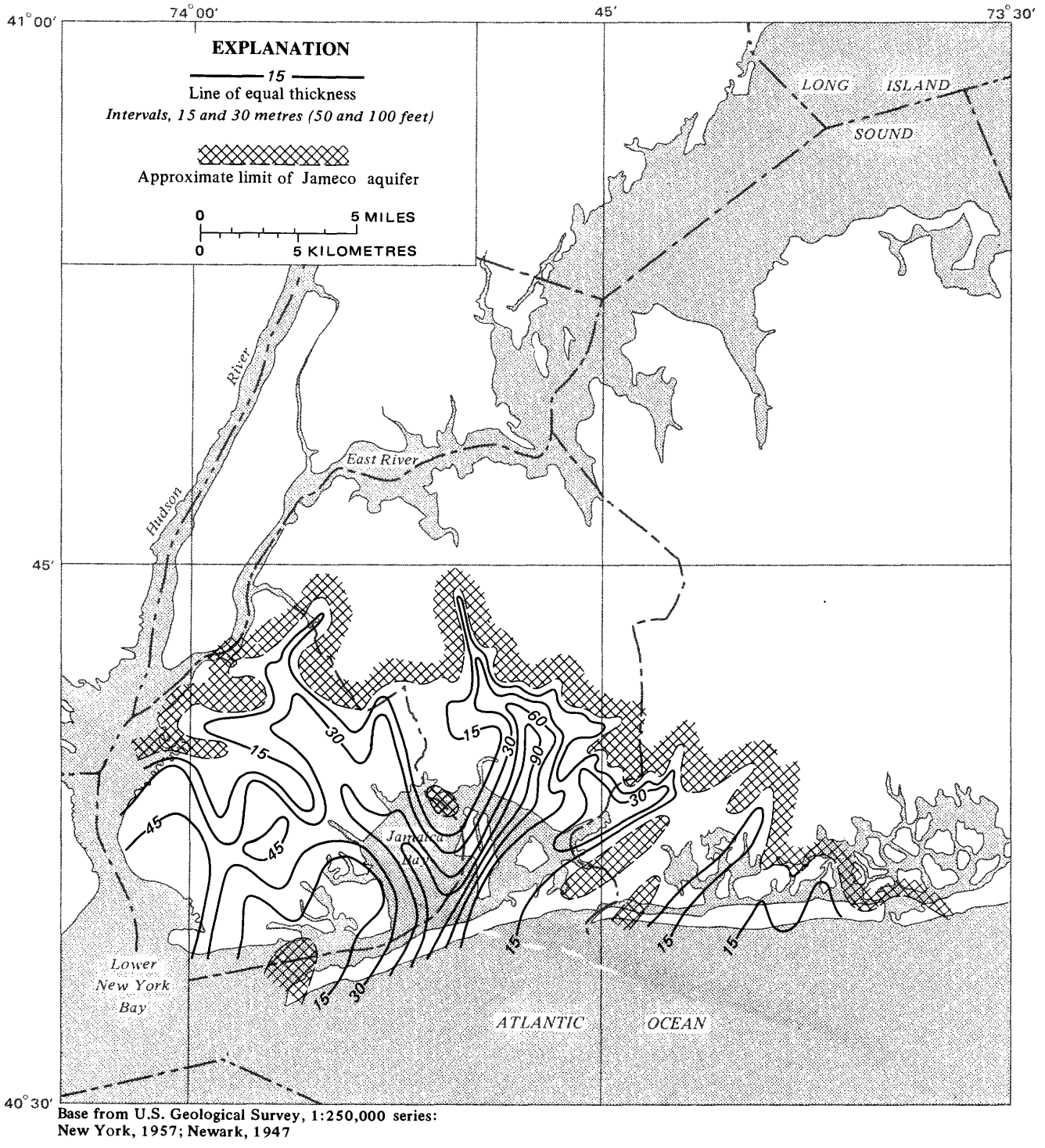

FIGURE 6.—Thickness of the Jameco aquifer. (After McClymonds and Franke, 1972, fig. 13).

charge are of interest because of (a) recreational uses of freshwater lakes, (b) the influence of stream discharge on the salinity of the brackish-water bodies surrounding Long Island and the resulting effects on shell fishing and general marsh ecology, and (c) the large amounts of ground water that are diverted from streams to wells where pumping of the wells causes a slight lowering of the regional water table.

BOUNDARIES BETWEEN SALTWATER AND FRESH GROUND WATER

Fresh ground water comes into contact with both

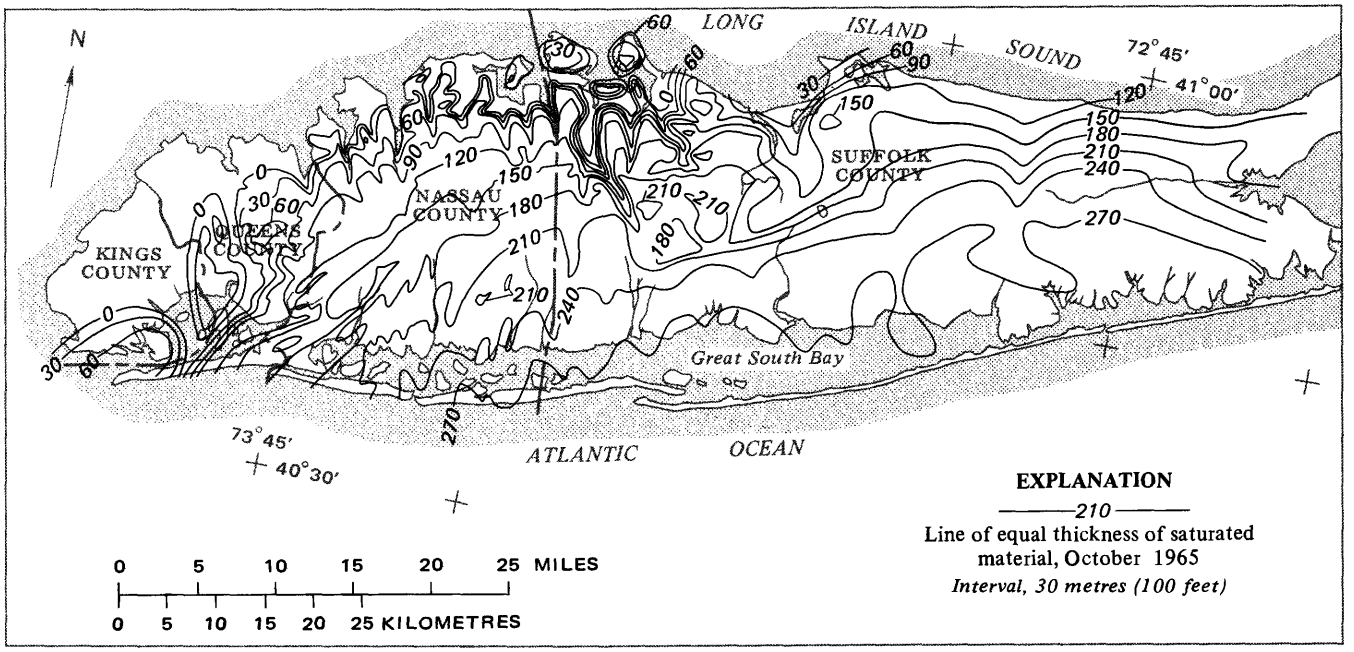

Base from U.S. Geological Survey, 1:250,000 series: Hartford, 1962; New York, 1957; Newark, 1947

FIGURE 7.—Saturated thickness of the Magothy aquifer. (After McClymonds and Franke, 1972, pl. 2.)

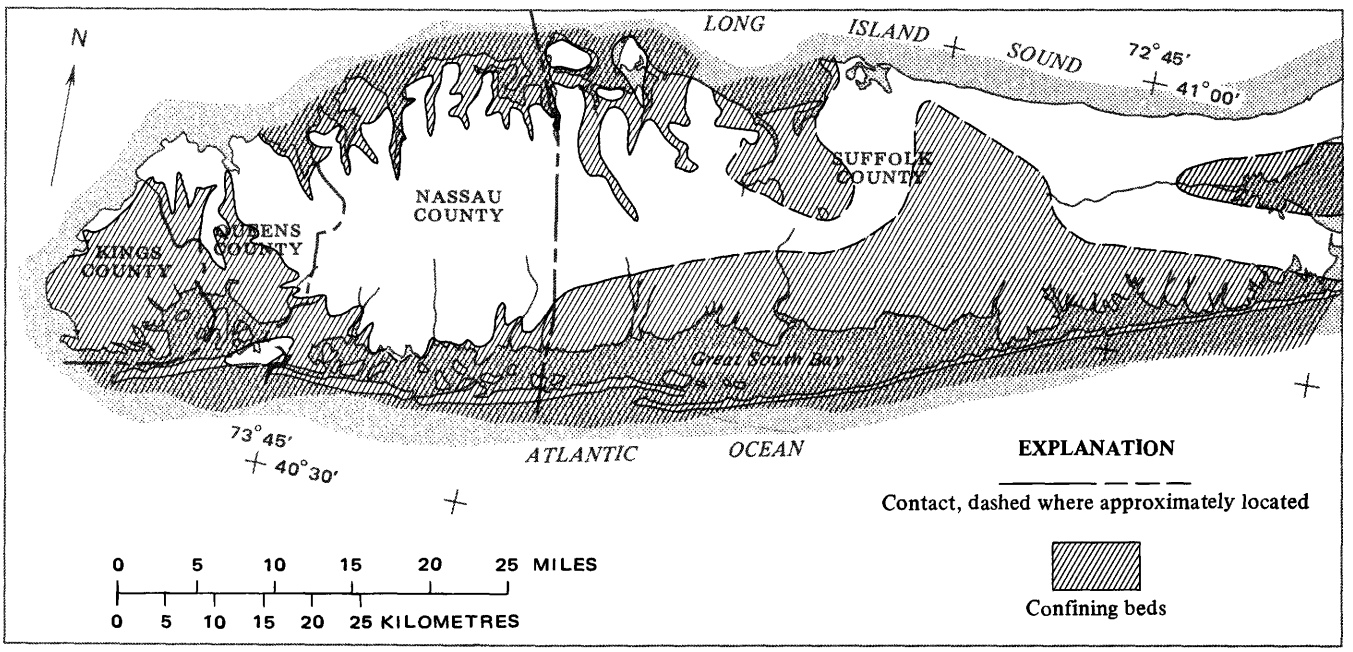

Base from U.S. Geological Survey, 1:250,000 series: Hartford, 1962; New York, 1957; Newark, 1947

FIGURE 8.—Extent of Gardiners Clay and other Cretaceous-Pleistocene deposits that constitute a composite confining bed overlying the Magothy aquifer. (Geology after Perlmutter and Geraghty, 1963 and N. E. McClymonds, written commun., 1970.)

salty surface water and salty ground water. The salty surface water surrounding Long Island is a significant boundary to the ground-water reservoir. Any fluctuations in head along the bottoms of the surface-water bodies are independent of head within the ground-water reservoir; the bottom is said to be a specified-potential boundary. Waves and tides fluctuate so rapidly that the fluctuations are usually ignored, and the boundary is treated as one along which the head is constant, or invariant with time and horizontal direc-

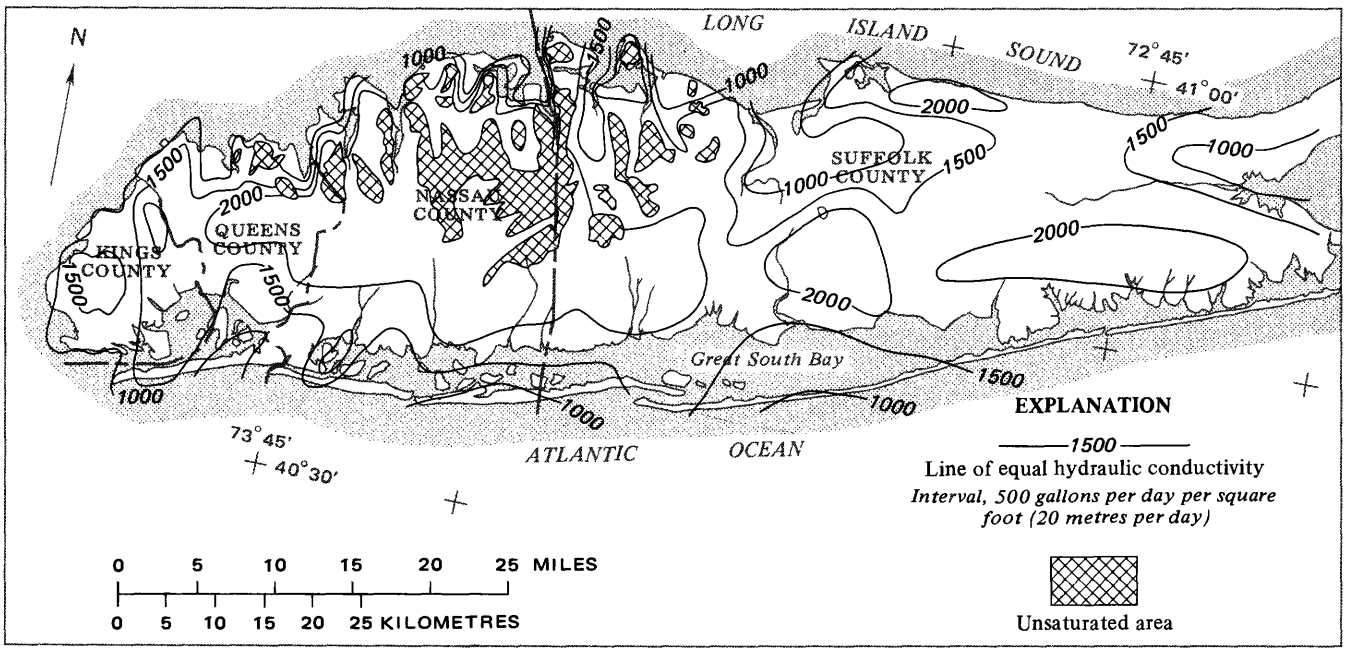

Base from U.S. Geological Survey, 1:250,000 series:
Hartford, 1962; New York, 1957; Newark, 1947

FIGURE 9.—Estimated hydraulic conductivity of the upper glacial aquifer. (After McClymonds and Franke, 1972, pl. 1.)

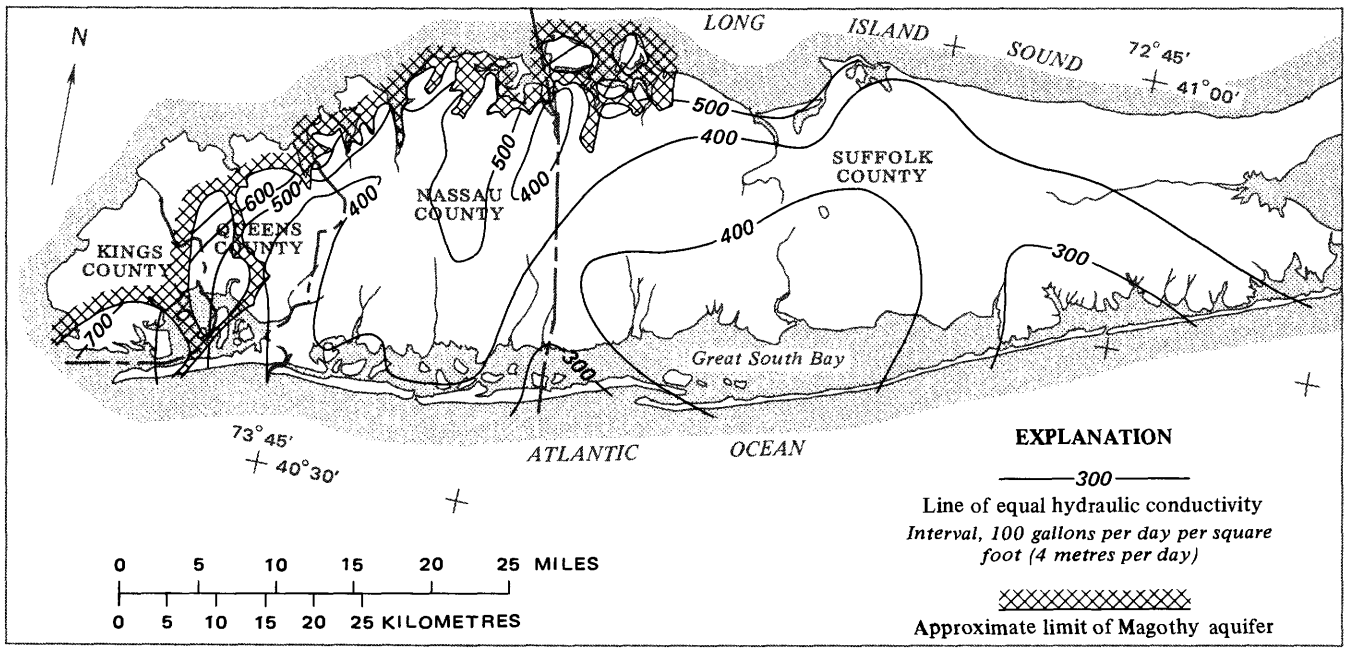

Base from U.S. Geological Survey, 1:250,000 series:
Hartford, 1962; New York, 1957; Newark, 1947

FIGURE 10.—Estimated hydraulic conductivity of the Magothy aquifer. (After McClymonds and Franke, 1972, pl. 2.)

tion. Because salty water is more dense than freshwater, the head along the boundary is a function of saltwater depth. At the bottoms of bays and oceans, freshwater heads at the sediment-water interface must balance the head resulting from the density difference—about 2.5 percent of the surface-water depth if the body is seawater, proportionately less if the surface water is less dense than seawater. The head condition just described must always be met along the boundary between fresh ground water and salty surface water, regardless of whether the system is in equilibrium. The same head condition must be

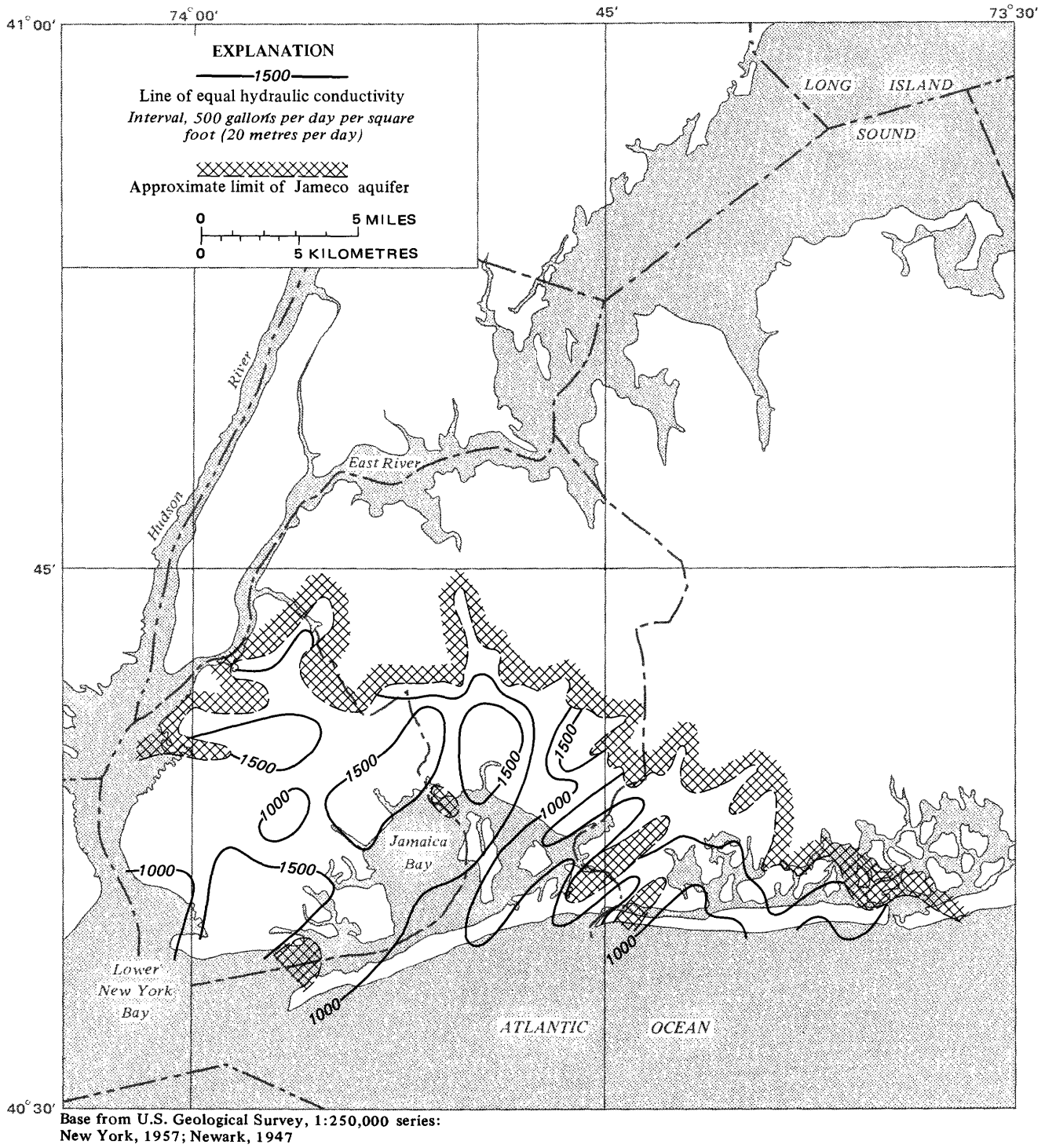

FIGURE 11.—Estimated average hydraulic conductivity of the Jameco aquifer. (After McClymonds and Franke, 1972, fig. 14.)

met for the boundary between fresh ground water and salty ground water if dynamic equilibrium is to be maintained, if the salty ground water is assumed to be static, and if the only net forces acting on the ground water are head gradients arising from gravitational forces (Hubbert, 1940, p. 868–870, 924–926).

Figure 15 is a diagram of the seaward boundary of fresh ground-water flow on Long Island showing (*A*) the surface along which freshwater head must balance the head caused by density differences between freshwater and saltwater and (*B*) the surface along which freshwater head seems to balance saltwater heads and

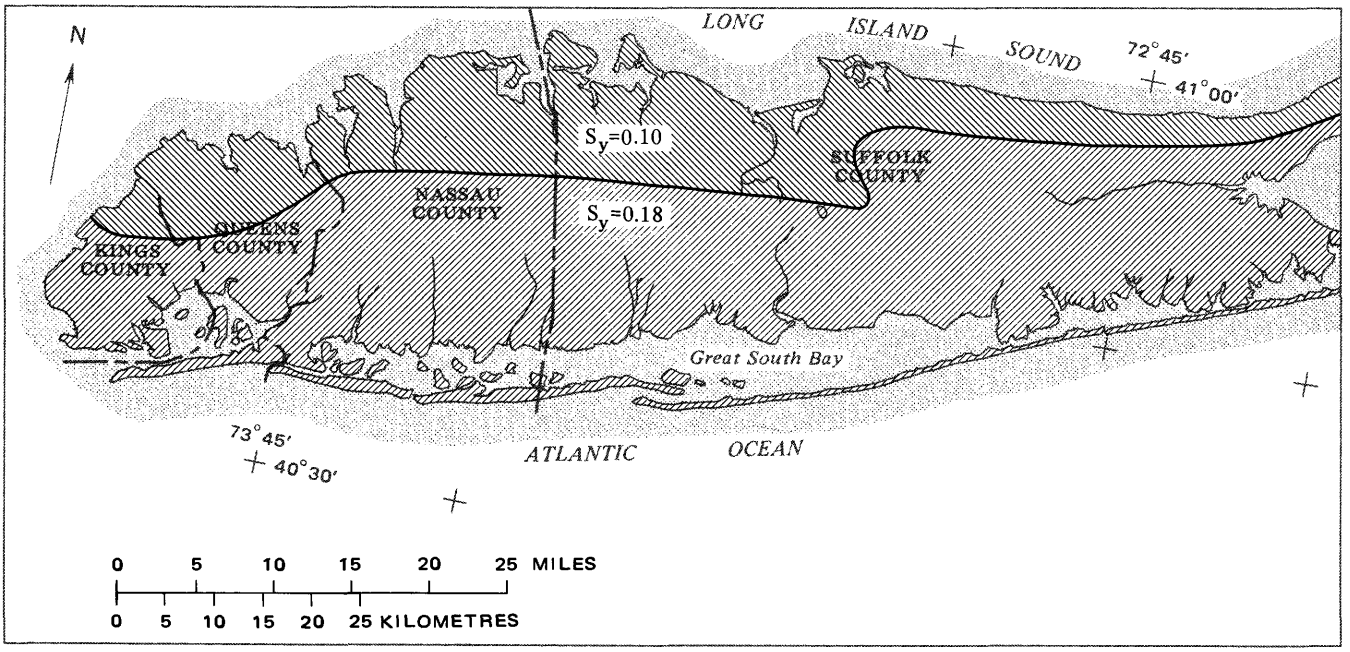

Base from U.S. Geological Survey, 1:250,000 series: Hartford, 1962; New York, 1957; Newark, 1947

FIGURE 12.—Values of specific yield estimated for the water table.

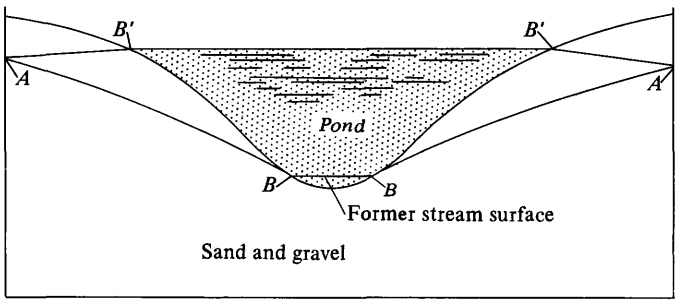

FIGURE 13.—Section across a stream valley showing water table before (A–B) and after (A–B') pond is created by damming a stream. The pond causes a reversal in the water-table slope which prevents ground-water seepage into the stream. (After Veatch and others, 1906.)

meets conditions for a classical equilibrium interface as described by Hubbert (1940, p. 868–870); (*C*) indicates that surface along which freshwater head seems not to balance saltwater head and along which conditions for a classical equilibrium interface are not met. An earlier discussion (p. 6) indicated that failure of heads along surfaces marked (*C*) to meet the conditions for a classical equilibrium interface could result from either (1) nonequilibrium conditions or (2) modification of the conditions for equilibrium by osmotic effects of the clays at and below the top of the Magothy aquifer.

The difference in density between fresh and salty water tends to keep the two separated with the fresh ground water on top; under steady-state conditions, the interface is represented by limiting flowlines of the fresh and salty water flow systems. A limiting flowline is mathematically equivalent to a no-flow or impermeable boundary, although there is no physical impermeable boundary. Fresh or salty ground water can move across the interface through two processes—(a) bulk displacement of one type of fluid by the other or (b) dispersion or mixing of the two fluids. Under nonsteady flow conditions, either process can cause movement of the interface, but the interface would move at velocities several orders of magnitude less than the velocity at which potential transients are transmitted through the confined parts of the ground-water reservoir. Transient changes in head are transmitted across the interface as though the interface were nonexistent, but because the interface is generally some distance offshore in the confined aquifers of Long Island, head changes at the interface resulting from human activities on the island will generally be small. Movement of the interface resulting from onshore pumping would accordingly be slow. Cooper (1959) provides a useful discussion of the physics of saltwater intrusion, and Lusczynski and Swarzenski (1966) describe the occurrence of intrusion on Long Island.

Although the preceding conclusion is true for the interface in the confined aquifer along most of the south shore of Long Island, it is not true everywhere. In parts of Kings, Queens, and Nassau Counties, the interface is landward of the shoreline and adjacent to

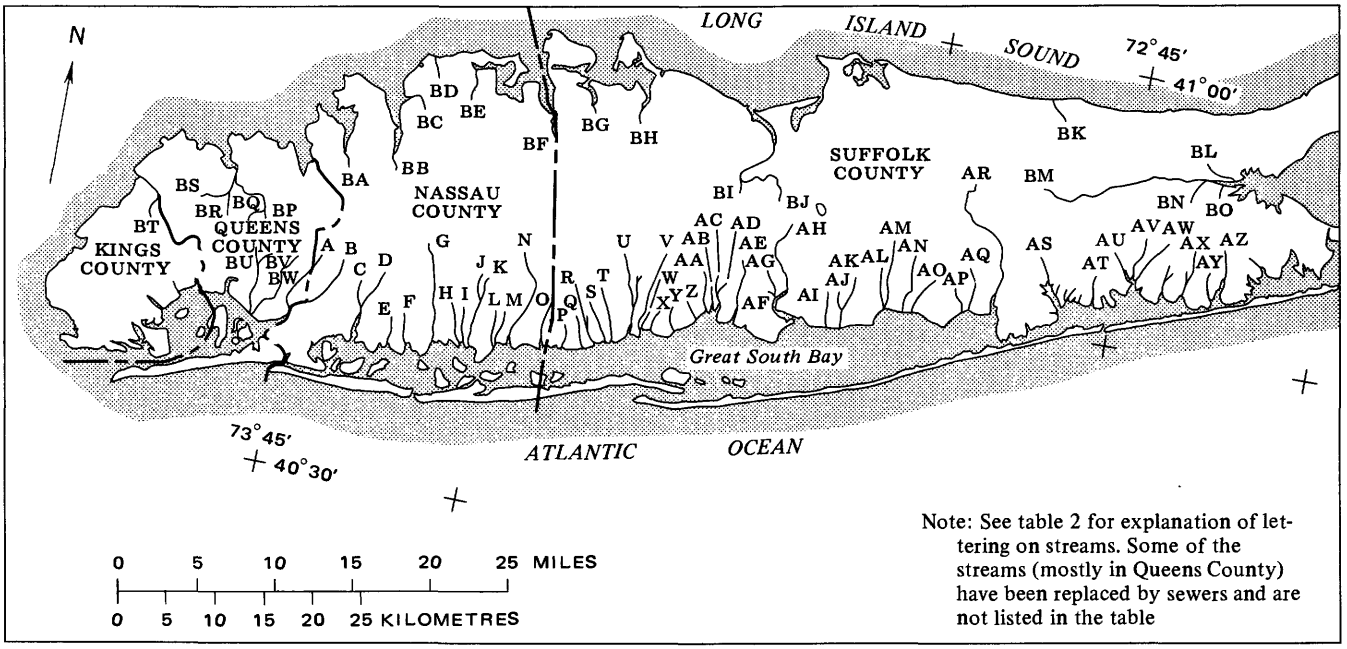

Note: See table 2 for explanation of lettering on streams. Some of the streams (mostly in Queens County) have been replaced by sewers and are not listed in the table

Base from U.S. Geological Survey, 1:250,000 series: Hartford, 1962; New York, 1957; Newark, 1947

FIGURE 14.—Locations and letter designations used for major Long Island streams.

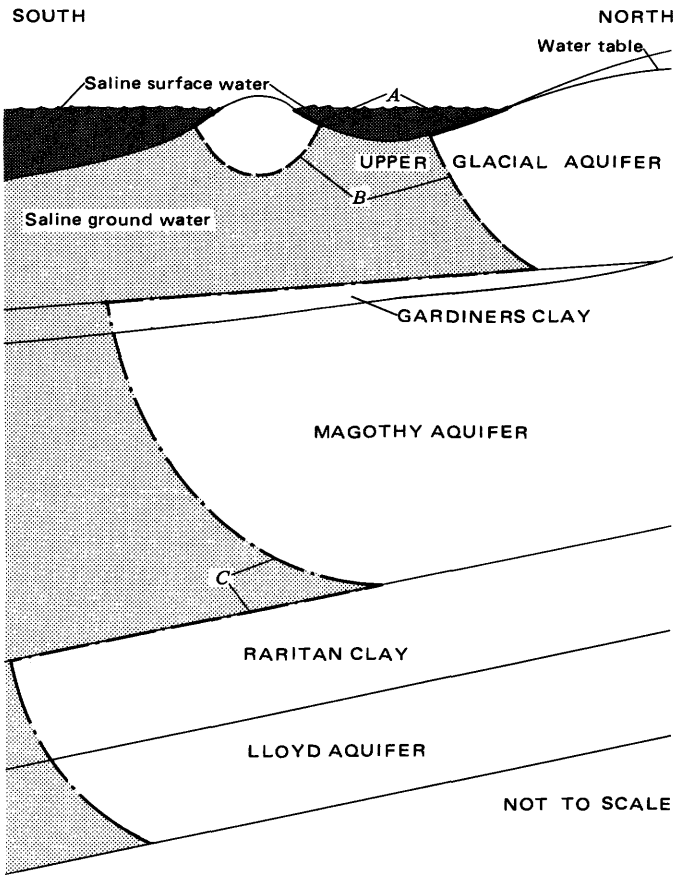

major pumping centers, the aquifers are thinner and more highly permeable than average for Long Island, and the confining unit is discontinuous; consequently, the interface can move rapidly (locally in excess of 10 m/yr or 33 ft/yr) in response to onshore pumping.

WATER TABLE

The water table, or free surface, is a boundary to the ground-water reservoir that can move in time. In recharge areas on Long Island, the flux (rate of flow per area) to the water table generally occurs as unsaturated flow and, therefore, is not affected by heads within the reservoir. In discharge areas, the rate at which water leaves the reservoir at the water table is related to heads within the reservoir but is ultimately controlled by evapotranspiration rates. One way of treating the water table is to ignore the how and the why of changes in flux across it and to treat it as a surface across which the flux is entirely controlled by events external to the aquifer except at points where

FIGURE 15.—Schematic hydrologic section of seaward boundary of fresh ground-water flow on the south shore of Long Island showing (*A*) the surface along which freshwater head must balance the head caused by the density difference between freshwater and salty surface water, (*B*) the surface along which freshwater head seems to balance saltwater head in the aquifer, and (*C*) the surface along which freshwater head seems not to balance static saltwater head.

the water table intersects seeps (streams and springs). At those seeps, flow out of the upper surface of the aquifer is a linear function of the gradient towards the seep; the seep is maintained at a potential defined by its altitude.

MODEL DESIGN

BASIC ANALOG CONCEPTS AND SIMILARITY COEFFICIENTS

The sediments of the Long Island aquifer system are clearly anisotropic in their hydraulic conductivity, which is maximum parallel to the bedding and minimum at right angles to it. They are likewise heterogeneous, with extreme variations in hydraulic conductivity from place to place. The flow of ground water of uniform density and viscosity through a medium of this sort can be described in terms of two equations, as follows:

$$\begin{bmatrix} K_{xx} & K_{xy} & K_{xz} \\ K_{yx} & K_{yy} & K_{yz} \\ K_{zx} & K_{zy} & K_{zz} \end{bmatrix} \begin{bmatrix} \partial h/\partial x \\ \partial h/\partial y \\ \partial h/\partial z \end{bmatrix} = \begin{bmatrix} q_x \\ q_y \\ q_z \end{bmatrix} \quad (1)$$

and

$$\frac{\partial q_x}{\partial x} + \frac{\partial q_y}{\partial y} + \frac{\partial q_z}{\partial z} = S_s \frac{\partial h}{\partial t}, \quad (2)$$

where $K_{xx}, K_{xy}, \ldots$, are the components of the hydraulic conductivity tensor; h represents hydraulic head; q_x, q_y, and q_z are the components of the Darcy velocity, or flow per unit area; t is time; and S_s is the specific storage. In this formulation, both the hydraulic conductivity tensor and the specific storage are considered functions of position—that is, the medium is considered heterogeneous as well as anisotropic. The coordinate directions, x, y, and z, are chosen arbitrarily. (See, for example, Collins, 1961, p. 63 and 72.)

Direct electrical simulation of equations 1 and 2 could be accomplished by using complex circuitry; for example, by using certain negative resistance elements. But this would be a difficult and costly procedure. A considerable simplification is possible if the medium can be considered orthotropic—that is, having three perpendicular principal axes of conductivity along at least one of which the conductivity attains its maximum value and along at least one of which the conductivity has its minimum value—and if the coordinate axes can be taken along these principal axes of conductivity. In the Long Island system, two of the principal axes can be taken parallel to the bedding. In these directions, designated x' and y', the hydraulic conductivity has its maximum value, K_A. The third principal axis, designated z', can be taken at right angles to the bedding. In this direction, the conductivity has its minimum value, K_B. If the coordinate axes are taken along x', y', and z', equations 1 and 2 can be reduced to:

$$\frac{\partial}{\partial x'}\left(K_A \frac{\partial h}{\partial x'}\right) + \frac{\partial}{\partial y'}\left(K_A \frac{\partial h}{\partial y'}\right) + \frac{\partial}{\partial z'}\left(K_B \frac{\partial h}{\partial z'}\right) = S_s \frac{\partial h}{\partial t}. \quad (3)$$

Equation 3, which is easily simulated electrically, accounts for the heterogeneity of the system—that is, variation of K_A, K_B, and S_s with position—but assumes that the directions of maximum and minimum conductivity remain the same throughout the system. This is not strictly true in the Long Island aquifers because the dip of the sediments varies slightly with map location and with depth. The electrical simulation used in this analysis approximates equation 3 at each individual point in the aquifer but also partly accounts for variation in direction of the principal axes. In this sense, the simulation represents the ground-water system more accurately than does equation 3. In the process, however, additional errors are introduced. The errors are described later in this section.

Electrical simulation is accomplished by dividing the aquifer into blocks as shown in figure 16. Figure 16*A* represents a typical hydrologic section through the island; figure 16*B* illustrates the division of the aquifer into blocks along this section. The two uppermost layers of blocks represent the upper glacial aquifer, and the three lower layers represent the Magothy aquifer. The layers are aligned along the high-conductivity axes; that is, they are parallel to the bedding at all points. Because of the exaggeration of the vertical scale, both the dip of the various layers and the differences in dip between the layers seem to be much greater in figure 16 than they are. All dips are on the order of 1 degree.

Figure 16*C* shows one of the blocks of figure 16*B* and an array of seven nodal points in the neighborhood of this block. The head at each nodal point is indicated by the subscript notation shown in the figure. The central node lies at the centroid of the block shown in the figure, and the surrounding nodes are assumed to lie at the centroids of the six surrounding blocks. In terms of finite differences in head, the equation for approximate inflow along the x' axis is

$$Q_{x_1}' \approx K_{A_1} \frac{h_1 - h_0}{(\Delta x')_1} (\Delta y' \Delta z')_1, \quad (4)$$

where the subscript 1 indicates that the various terms are taken between node 1 and node 0. The hydraulic conductivity, K_{A_1}, is an average value for this interval, as is the flow area $(\Delta y'\Delta z')_1$. The symbol $(\Delta x')_1$ is simply the distance between node 1 and node 0. Equation 4 can be obtained by applying Darcy's law to flow through the right face of the block, expressing the derivative $\frac{\partial h}{\partial x}$ by a Taylor series expansion, and neglecting terms of higher order than the first in the resulting series.

The equation for approximate outflow along the x' axis is

$$Q_{x_2}' \approx K_{A_2} \frac{h_0-h_2}{(\Delta x')_2} (\Delta y'\Delta z')_2 , \qquad (5)$$

where subscript 2 indicates values for the interval between node 0 and node 2. Therefore, inflow minus outflow in the x' direction is approximately

$$Q_{x_1}' - Q_{x_2}' \approx \left(\frac{K_{A_1}(\Delta y'\Delta z')_1}{(\Delta x')_1} (h_1-h_0)\right) - \left(\frac{K_{A_2}(\Delta y'\Delta z')_2}{(\Delta x')_2} (h_0-h_2)\right) \qquad (6)$$

Similar expressions, using parallel subscript notation, can be developed for inflow minus outflow in the y' and z' directions. When this is done, the total inflow minus outflow may be equated approximately to the rate of accumulation of fluid in storage in the block, $S_s(\Delta V)\frac{\partial h}{\partial t}$ where ΔV represents the volume of the block.

This leads to the equation

$$\frac{K_{A_1}(\Delta z'\Delta y')_1}{(\Delta x')_1} (h_1-h_0) - \frac{K_{A_2}(\Delta z'\Delta y')_2}{(\Delta x')_2} (h_0-h_2)$$

$$+ \frac{K_{A_3}(\Delta z'\Delta x')_3}{(\Delta y')_3} (h_3-h_0) - \frac{K_{A_4}(\Delta z'\Delta x')_4}{(\Delta y')_4} (h_0-h_4)$$

$$+ \frac{K_{B_5}(\Delta x'\Delta y')_5}{(\Delta z')_5} (h_5-h_0) - \frac{K_{B_6}(\Delta x'\Delta y')_6}{(\Delta z')_6} (h_0-h_6)$$

$$\approx S_{s_0} \left(\frac{(\Delta x')_1 + (\Delta x')_2}{2} \times \frac{(\Delta y')_3 + (\Delta y')_4}{2} \times \frac{(\Delta z')_5 + (\Delta z')_6}{2}\right) \frac{\partial h}{\partial t} . \qquad (7)$$

Equation 7 is simplified considerably by making $\Delta x'=\Delta y'$ for all blocks. In this case,

$$K_{A_1} (\Delta z')_1 (h_1-h_0) - K_{A_2} (\Delta z')_2 (h_0-h_2)$$

$$+ K_{A_3} (\Delta z')_3 (h_3-h_0) - K_{A_4} (\Delta z')_4 (h_0-h_4)$$

$$+ \frac{K_{B_5} (\Delta x'\Delta y')}{(\Delta z')_5} (h_5-h_0) - \frac{K_{B_6} (\Delta x'\Delta y')}{(\Delta z')_6} (h_0-h_6)$$

$$\approx S_{s_0} \Delta x'\Delta y' \frac{(\Delta z')_5 + (\Delta z')_6}{2} \frac{\partial h}{\partial t} . \qquad (8)$$

Equation 8 may be regarded as a finite-difference (in space) approximation to equation 3, using the block configuration shown in figures 16 and 17 and keeping $\Delta x'=\Delta y'$ throughout. As suggested previously, however, equation 8 simulates conditions in the aquifer (equations 1 and 2) more closely than it simulates equation 3. Equation 3 requires that the principal conductivity axes remain fixed throughout the system, whereas in reality they do not. A simulation of field conditions that is superior in certain ways to one that would be given by a direct, finite-difference approximation of equation 3 can be obtained by changing the orientation of the blocks to follow approximately the changing directions of maximum and minimum conductivity.

Errors associated with a finite-difference approximation using a uniform rectangular mesh have received extensive attention in the literature; for example, Karplus, (1958, p. 103–108). If, as in this example, the mesh is not perfectly rectangular, additional errors are introduced. The increase in $\Delta z'$ in the downdip direction implies that the downdip flow through a block must diverge, rather than remain entirely parallel to x'; thus, it cannot be completely accounted for by a term approximating only $\frac{\partial h}{\partial x'}$. In addition, the upper or lower surface of a block may not be perfectly perpendicular to a line between the centroid of the block and that of the overlying or underlying block. In this case, flow across the surface cannot be exactly described in terms of a head difference between the centroids. Magnitude of the errors generated by these causes is difficult to estimate and would vary from place to place in the system. However, because the dip is very low and the changes in dip are both small and very gradual, errors of this sort would probably be negligible throughout the system.

A direct electrical analog of equation 8 is easily constructed. Karplus and Soroka (1959), Skibitzke (1961), Bermes (1960), and Walton and Prickett (1963) discuss both the theoretical basis and the technique of such electrical simulation. Figure 16*D* shows an electrical configuration in which six resistors are used to connect a central node, or junction, with six surrounding nodes.

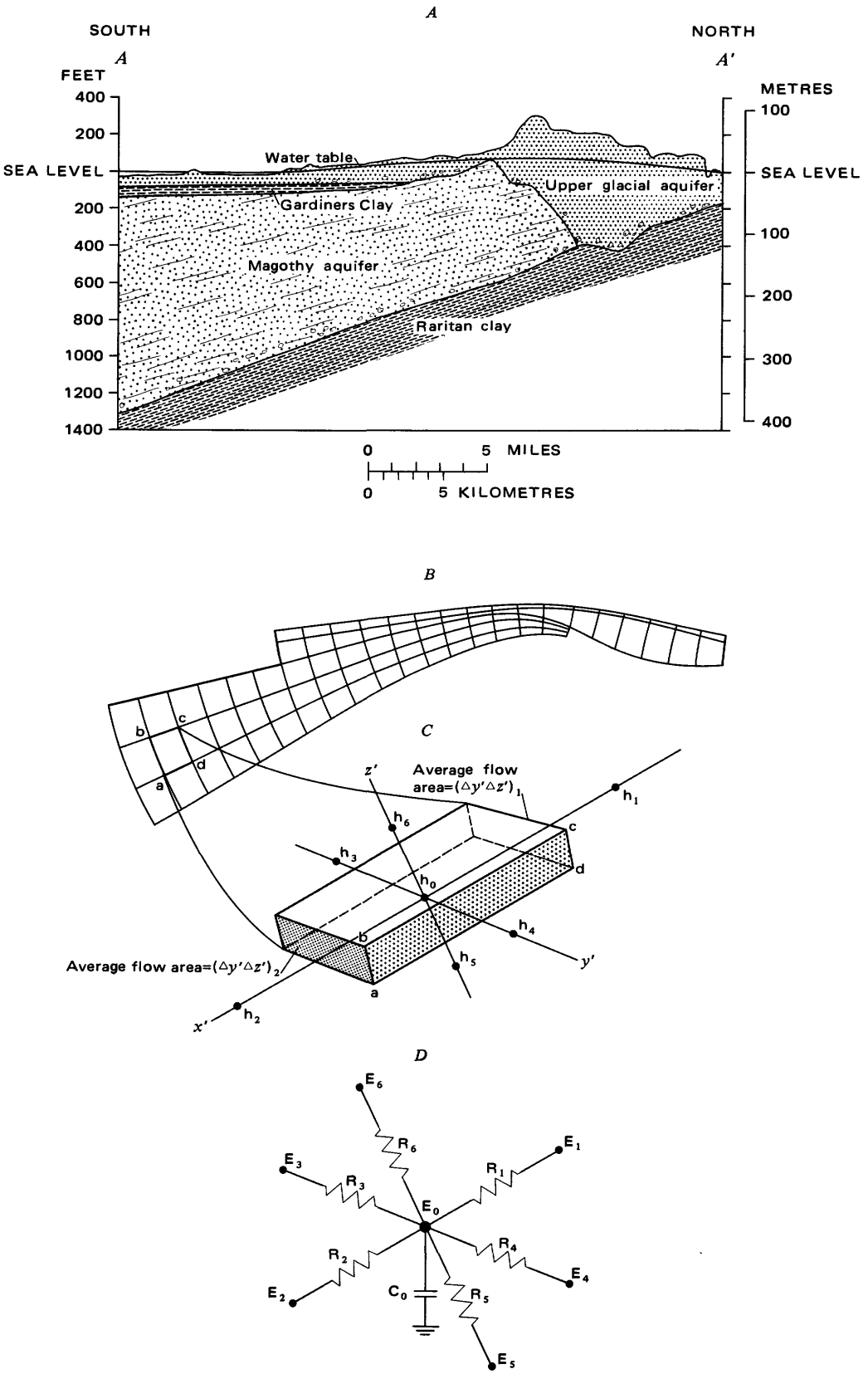

FIGURE 16.—Finite-difference representation and notation of hydrologic section through the Long Island ground-water reservoir (thickness greatly exaggerated): *A*, A typical hydrologic section. *B*, This section divided into blocks, or finite-differences. *C*, Expansion of one block from this section showing the principal conductivity axes, x', y', and z'; also head at the centroid of this block, h_0, and at the centroids of six surrounding nodes, $h_1, h_2, \ldots h_6$. *D*, An electrical analogy for flow in this block with voltages $E_0 \ldots E_6$ analogous to heads $h_0 \ldots h_6$, resistances $R_1 \ldots R_6$, and capacitance C_0.

A capacitor connected to the central node provides electrical storage at this point. Voltage at the central node is designated E_0, and voltages at the surrounding nodes are designated $E_1, \ldots E_6$, respectively, which parallels the notation used for heads in equations 4 through 8. The current (I_1) toward the central node through resistor R_1 is given by Ohm's law as

$$I_1 = \frac{1}{R_1}(E_1 - E_0), \tag{9}$$

where R_1 is the resistance between the central node and node 1. The current (I_2) from the central node to node 2 is similarly given by

$$I_2 = \frac{1}{R_2}(E_0 - E_2). \tag{10}$$

Expressions similar to equations 9 and 10 can be obtained for the currents toward and away from the central node in the other directions. The algebraic sum of these currents must equal the rate of accumulation of charge on the capacitor at the central node, which is given by $\frac{C_0 dE_0}{dt}$, where C represents the capacitance. This leads to the equation

$$\begin{aligned}\frac{1}{R_1}(E_1 - E_0) - \frac{1}{R_2}(E_0 - E_2) + \frac{1}{R_3}(E_3 - E_0) \\ - \frac{1}{R_4}(E_0 - E_4) + \frac{1}{R_5}(E_5 - E_0) \\ - \frac{1}{R_6}(E_0 - E_6) = C_0 \frac{dE_0}{dt}.\end{aligned} \tag{11}$$

Equation 11 is of the same form as 8, where voltage is analogous to head, the terms $\frac{1}{R_1} \ldots \frac{1}{R_4}$ are analogous to the terms $K_{A_1}(\Delta z')_1 \ldots K_{A4}(\Delta z')_4$, the terms R_5 and R_6 are analogous to $\frac{K_{B_5}(\Delta x' \Delta y')}{(\Delta z')_5}$ and $\frac{K_{B_6}(\Delta x' \Delta y')}{(\Delta z')_6}$, and C_0 is analogous to $S_{s_0} \Delta x' \Delta y' \frac{(\Delta z')_5 + (\Delta z')_6}{2}$.

Thus, if a three-dimensional network of resistors and capacitors is constructed and subjected to electrical stresses that are proportional to hydraulic stresses in the ground-water system, the voltage of each node of the network should vary in proportion to the head in the corresponding block of figure 16*B*. Equation 11 provides a means by which head changes in response to proposed or assumed stresses can be predicted without resort to extended field experiment.

For the uppermost layer of a three-dimensional analog network, the term K_{B_5} of equation 8 is zero; the term $\frac{1}{R_5}$ of equation 11 is similarly taken as zero. For the lowermost layer, the terms K_{B_6} and $\frac{1}{R_6}$ are zero. If the uppermost layer corresponds to a water-table zone, the capacitance C at each node in this layer is taken to represent the term $S_y \Delta x' \Delta y'$, where S_y represents specific yield, rather than the specific storage term of equation 8; in an interval that includes the water table, virtually all withdrawal from storage is sustained by dewatering rather than by release from compressive storage.

The electrical analogy may be summarized in terms of four similarity coefficients, any three of which may be considered independent. These are as follows:

$$\begin{aligned} V &= A_1 q \\ h &= A_2 E \\ Q &= A_3 I \\ t &= A_4 t', \end{aligned}$$

where the quantities left of the equal sign are prototype[1] (real world) quantities and those on the right are model quantities. V is volume of water, q is electrical charge, h is head, E is electrical potential, Q is rate of discharge of water, I is electrical current, t is prototype time compared with model time t'; and the coefficients A_1–A_4 have the dimensions necessary for the appropriate conversions. The model study is described in terms of the following units:

V (cubic metres)	$= 2.484 \times 10^{13}(m^3/\text{coul}) \times q$ (coulombs)
h (metres)	$= 2.0(m/\text{volt}) \times E$(volts)
Q (cubic metres/day	$= 4.967 \times 10^7(m^3/d/\text{amp}) \times I$ (amperes)
t (days)	$= 5 \times 10^5(d/s) \times t'$ (seconds).

MODEL MATRIX

This model was designed around the similarity coefficients (A_1–A_4) and the data presented earlier in this report. The aquifers were split into several zones. The five levels of the model correspond to five zones of the prototype. None of these zones or levels corresponds to a distinct sand unit within an aquifer. In order to comply with the restrictions discussed in the section on basic analog concepts, the zones are approximately parallel to bedding within each aquifer, and, therefore, they vary in thickness and altitude from point to point. The bed-normal spacing, $\Delta z'$, between finite-difference nodes ranges from zero (where an aquifer pinches out)

[1]The term "prototype" is used to designate the real-world hydrologic system as opposed to the model hydrologic system.

up to about 120 m (400 ft). The bed-parallel node spacings, $\Delta x'$, and $\Delta y'$, are both 6,000 ft (1,829 m) for all the zones. The finite-difference grid in figures 16*B* and 17 shows the even-numbered rows and columns that are spaced at 6,000-ft (1,829–m) intervals. The nodes are "volume centered"; that is, they are at the centroids of the volumes they represent.

On the basis of the values of hydraulic conductivity in figures 9–11 and of aquifer thicknesses in figures 5–7, the model area for each of the five levels was subdivided into areas in which the bed-parallel hydraulic conductivity and thickness could be assumed to be reasonably uniform. Figures 18 and 19 show the distribution of transmissivity (product of thickness and bed-parallel hydraulic conductivity) about each node in levels 1 and 2 of the model, which represent the upper glacial aquifer. Specified-potential boundaries are shown by the symbol "*", and impermeable or no-flow boundaries by "ϕ"on these maps. Figure 20 shows the transmissivity assigned to level 3; this level includes the Jameco aquifer and the upper third of the Magothy aquifer. Distribution of transmissivity in levels 4 and 5, representing the middle third and lower third of the Magothy aquifer, are mapped in figures 21 and 22.

All vertical resistances were computed on a node-by-node basis because of the complex variations in thickness, aquifer conductivities, and confining beds that they represent. In computing vertical resistances, an anisotropy of 1:10 was assumed for the upper glacial and Jameco aquifers and 1:40 for the Magothy aquifer. Thickness of the confining beds overlying the Magothy aquifer is divided between levels 2 and 3. Figures 23–25 show the distribution of estimated values of $(\Delta z'/K_B)$. Because R_z' is directly proportional to $\frac{1}{\Delta x'\Delta y'} \times \frac{\Delta z'}{K_B}$ and $\Delta x'\Delta y'$ is constant throughout the model, R_z' can be computed directly from the values mapped in figures 23–25. The distribution of estimated values of $(\Delta z'/K_B)$ between levels 4 and 5 is the same as that given in figure 25 for levels 3 and 4, except that the lower level is not quite as extensive.

The Lloyd aquifer (table 1; fig. 4) was not included in this model. The aquifer is well isolated from the remainder of the ground-water reservoir by the Raritan clay (Franke and Getzen, 1975), and its hydrologic properties are poorly known (McClymonds and Franke, 1972; Jensen and Soren, 1974). The Lloyd aquifer is used as a source of water in only a few places on Long Island. Thus, its inclusion is not necessary either for utilization or for correct operation of the model. The top of the Raritan clay was treated as an impermeable bottom for the flow system.

Lack of detailed information on specific storage of the aquifers required a somewhat more general assignment of capacitance. Two different values of capacitors, corresponding to the two areas shown in figure 12, were used in level 1. In a few places where the upper glacial aquifer is not saturated (figs. 4, 5), capacitors appropriate to water-table storage coefficients were used for the corresponding nodes in level 3 (fig. 16). Level 2 was assigned a compressive storage coefficient where it represents saturated material. Because level 2 is closely connected, both electronically and hydrologically, to level 1, it exhibits all the characteristics of a water-table aquifer except when subjected to very fast transient stresses.

Figure 8 and the geologic cross sections in figure 4

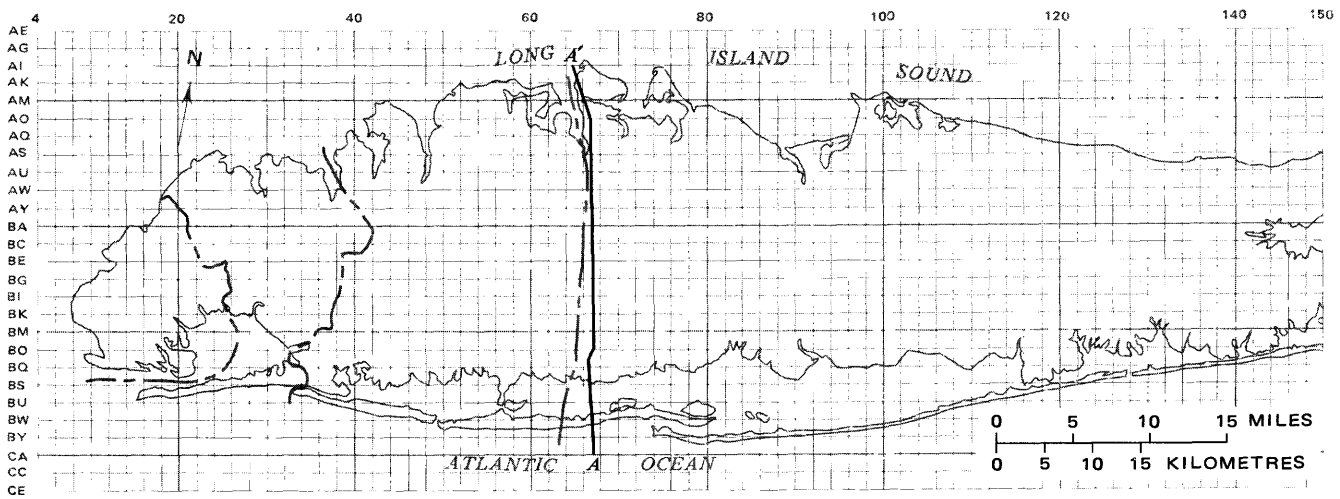

Base from U.S. Geological Survey, 1:250,000 series:
Hartford, 1962; New York, 1957; Newark, 1947

FIGURE 17.—Finite-difference grid used for constructing the three-dimensional model of Long Island, and location of section *A–A'*.

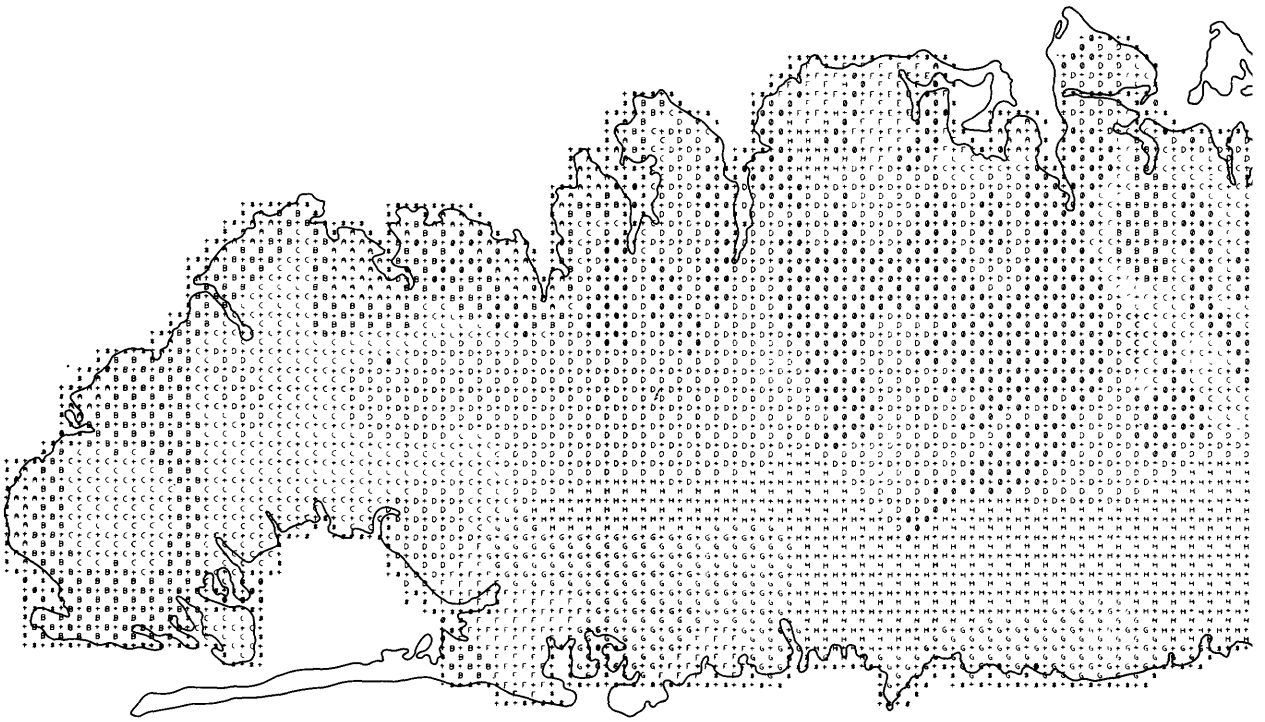

FIGURE 18.—Distribution of transmissivity (product of thickness and bed-parallel hydraulic conductivity) about each node in level 1 (uppermost level) of the model.

show that there are no continuous island-wide confining beds stratigraphically above the Raritan clay. Upper Cretaceous sandy clays (correlated with the Monmouth Group by Jensen and Soren, 1972), the Gardiners Clay, and the Pleistocene Smithtown and "20-ft" clays together comprise an aggregate confining unit that is stratigraphically above the Magothy aquifer around the fringes of Long Island. The Magothy aquifer and deeper parts of the glacial aquifer exhibit confined hydrologic behavior.

Compressive storage controls short-term response of confined aquifers such as the Magothy aquifer and deeper parts of the glacial aquifer on Long Island; water-table, or gravity, storage controls long-term response. Compressive storage contributes to the total storage in all aquifers but is usually of negligible importance in unconfined aquifers. None of the Long Island aquifer tests before construction of the model provide data that are adequate for separating the two types of storage. An average specific storage of 2×10^{-8} cm^{-1} (6.1×10^{-7} ft^{-1}) was assumed. This value, multiplied times an average thickness of 200 m (650 ft) yields the storage coefficient of 4×10^{-4}, which was distributed uniformly to all nodes except where water-table storage was assigned. Rigorously, the amount of storage assigned each node should be proportional to the volume represented by the node. This was not done because of the lack of data to support the storage coefficient that was assumed. The author considered that the assigned storage would have to be modified during model testing, so one value of capacitor was used throughout. During testing, this assignment of storage seemed adequate.

Four aquifer tests after the construction of the model indicate a specific storage for these semiconfined aquifers ranging from 10^{-7} to 10^{-6} cm^{-1} (3×10^{-6} to 3×10^{-5} ft^{-1}) (Getzen, 1974, p. 53), at least one order of magnitude greater than the values used in the model design. Even with the larger values, the effects of elastic storage on long-term response are insignificant when compared with water-table storage for most of the Long Island reservoir. Around the fringes of the island, where the confining unit is thickest and more nearly continuous and where the overlying units are saturated with seawater, model accuracy is more sensitive to the accuracy of the assumed value for specific storage. This sensitivity is one reason to question the model's predictive capability in the offshore area.

The large size of the model caused some concern about the effects of stray capacitance on performance of the model. The mechanics of construction require large amounts of wire connecting nodes on each level to the corresponding nodes on the levels above and below, and much of this wire (more than 70,000 ft or 21,000

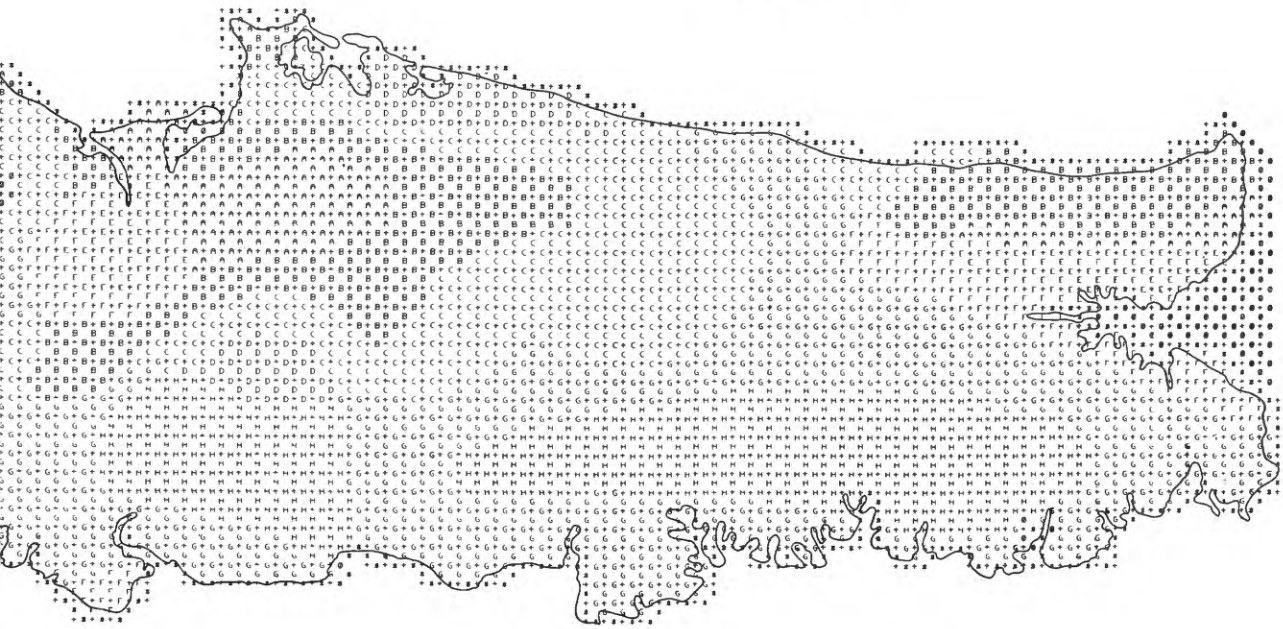

EXPLANATION

- Model node
- Specified-potential boundary
- Impermeable boundary (no transmissivity)
- A Transmissivity=93 square metres per day
- B Transmissivity=160 square metres per day
- C Transmissivity=220 square metres per day
- D Transmissivity=280 square metres per day
- E Transmissivity=330 square metres per day
- F Transmissivity=550 square metres per day
- G Transmissivity=760 square metres per day
- H Transmissivity=980 square metres per day

FIGURE 18.—Continued.

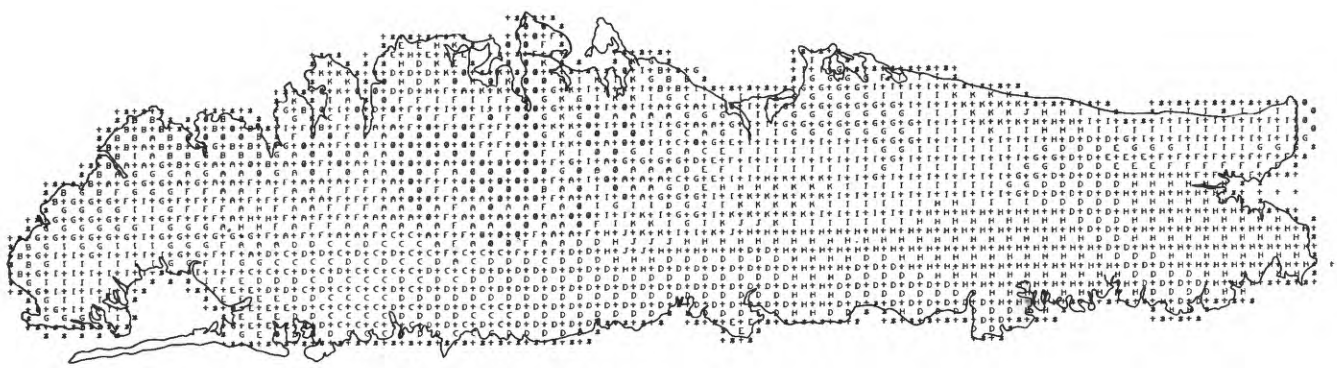

EXPLANATION

- Model node
- Specified-potential boundary
- Impermeable boundary (no transmissivity)
- A Transmissivity=370 square metres per day
- B Transmissivity=500 square metres per day
- C Transmissivity=930 square metres per day
- D Transmissivity=990 square metres per day
- E Transmissivity=1,200 square metres per day
- F Transmissivity=1,500 square metres per day
- G Transmissivity=1,700 square metres per day
- H Transmissivity=3,000 square metres per day
- I Transmissivity=3,700 square metres per day
- J Transmissivity=5,300 square metres per day
- K Transmissivity=5,900 square metres per day

FIGURE 19.—Distribution of transmissivity (product of thickness and bed-parallel hydraulic conductivity) about each node in level 2 of the model.

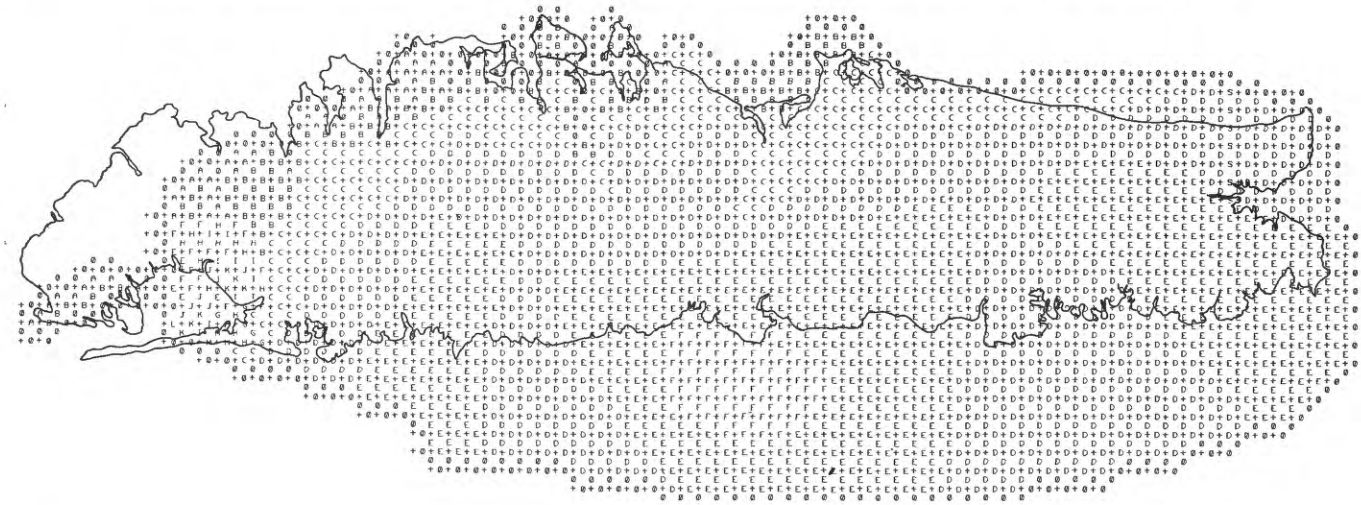

EXPLANATION

- Model node
- Impermeable boundary
- A Transmissivity=120 square metres per day
- B Transmissivity=310 square metres per day
- C Transmissivity=620 square metres per day
- D Transmissivity=990 square metres per day
- E Transmissivity=1,550 square metres per day
- F Transmissivity=1,740 square metres per day
- G Transmissivity=2,200 square metres per day
- H Transmissivity=3,600 square metres per day
- I Transmissivity=5,500 square metres per day
- J Transmissivity=6,300 square metres per day
- K Transmissivity=9,100 square metres per day
- L Transmissivity=15,000 square metres per day

FIGURE 20.—Distribution of transmissivity (product of thickness and bed-parallel hydraulic conductivity) about each node in level 3 of the model.

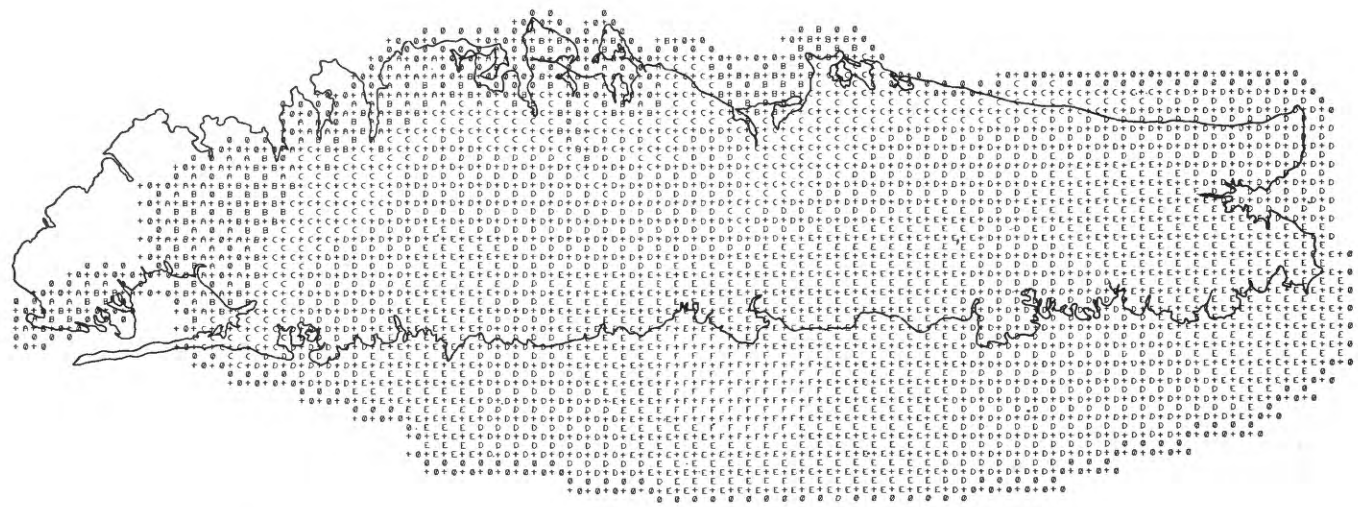

EXPLANATION

- Model node
- Impermeable boundary (no transmissivity)
- A Transmissivity=120 square metres per day
- B Transmissivity=310 square metres per day
- C Transmissivity=620 square metres per day
- D Transmissivity=990 square metres per day
- E Transmissivity=1,600 square metres per day
- F Transmissivity=1,700 square metres per day

FIGURE 21.—Distribution of transmissivity (product of thickness and bed-parallel hydraulic conductivity) about each node in level 4 of the model.

m) must be bundled into tight cables. Preconstruction estimates of the capacitance between adjacent nodes were on the order of 3–10 pf (picofarads). Postconstruction measurements have indicated that stray capacitance may be as high as 15 pf between some nodes. Although some nodes near boundaries show a total capacitance to ground of 45 pf, most of the nodes in the interior part of the model have a total capacitance of 26–31 pf with respect to ground. Therefore, some variation in aquifer storage is not accounted for in design

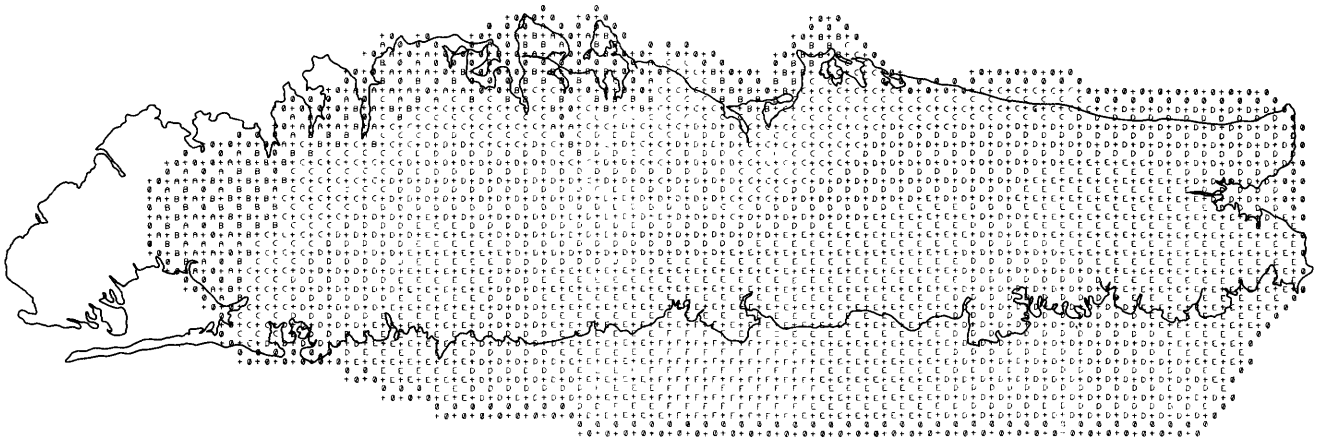

EXPLANATION

- Model node
- Impermeable boundary (no transmissivity)
- A Transmissivity=120 square metres per day
- B Transmissivity=310 square metres per day
- C Transmissivity=620 square metres per day
- D Transmissivity=990 square metres per day
- E Transmissivity=1,500 square metres per day
- F Transmissivity=1,700 square metres per day

FIGURE 22.—Distribution of transmissivity (product of thickness and bed-parallel hydraulic conductivity) about each node in level 5 of the model.

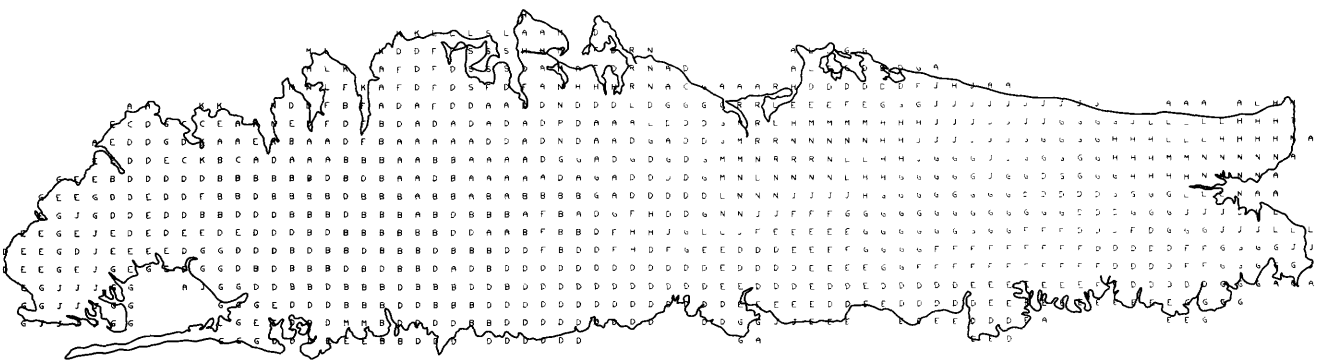

EXPLANATION

Bed-normal thickness/bed-normal hydraulic conductivity

A 5.6 days	E 22 days	J 57 days	N 130 days
B 6.8 days	F 26 days	K 68 days	P 170 days
C 10 days	G 39 days	L 81 days	R 220 days
D 15 days	H 48 days	M 99 days	S 290 days

FIGURE 23.—Distribution of estimated values of $(\Delta z'/K_B)$ between nodes in levels 1 and 2 of the model, where $(\Delta z'/K_B)$ is thickness divided by bed-normal hydraulic conductivity.

criteria, but the discrepancy seems negligible when compared with the design capacitance of 27 pf per node.

BOUNDARY CONDITIONS

Five types of boundary conditions are incorporated into model design: (1) Boundaries across which no flow occurs; (2) boundaries along which the potential is defined by potential sources external to the model; (3) boundaries across which the flow is defined by external sources; (4) internal stresses whose magnitude and location are defined by external sources; and (5) stream boundaries across which the flow is controlled by both internal and external events. (As used here, the only differences between a boundary of type 3 and one of type 4 are size and position. In other authors' terminology, all specified-flux boundaries are referred to as "stresses.")

1. *No-flow boundaries*—The top of the Raritan clay is assumed to be an impermeable or no-flow boundary as is the interface between freshwater and salty water in the Magothy aquifer. Unfortunately, the interface is not a fixed boundary for steady-state flow and is no boundary at all for unsteady flow. Even if it were a boundary, the position of the interface in the Magothy aquifer is virtually unknown. The assumption is that somewhere offshore is a point beyond which freshwater

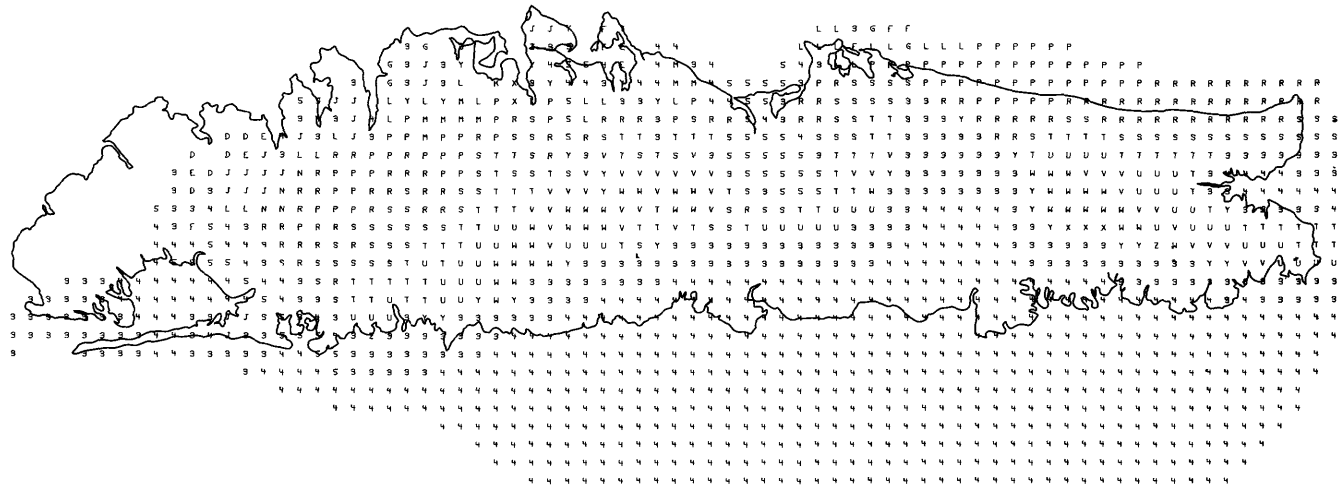

EXPLANATION

Bed-normal thickness/ bed-normal hydraulic conductivity

D 120 days	N 1,200 days	W 3,500 days
E 130 days	P 1,300 days	X 3,900 days
F 180 days	R 1,600 days	Y 15,000 days
G 220 days	S 1,900 days	Z 26,000 days
J 500 days	T 2,300 days	3 150,000 days
K 640 days	U 2,900 days	4 480,000 days
L 750 days	V 3,200 days	5 1,000,000 days
M 950 days		

FIGURE 24.—Distribution of estimated values of $(\Delta z'/K_B)$ between nodes in levels 2 and 3 of the model, where $(\Delta z'/K_B)$ is thickness divided by bed-normal hydraulic conductivity.

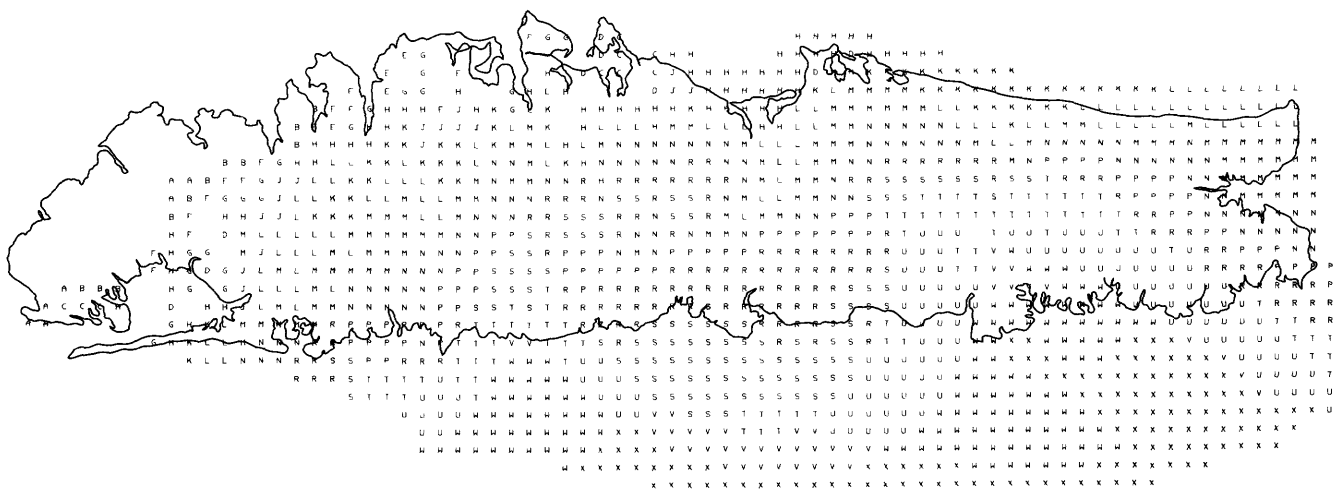

EXPLANATION

Bed-normal thickness/ bed-normal hydraulic conductivity

A 220 days	M 1,500 days	R 6,200 days
B 230 days	J 1,900 days	S 6,800 days
C 290 days	K 2,600 days	T 7,400 days
D 350 days	L 3,200 days	U 9,000 days
E 430 days	M 3,900 days	V 9,900 days
F 900 days	N 4,800 days	W 12,000 days
G 1,100 days	P 5,700 days	X 13,000 days

FIGURE 25.—Distribution of values of $(\Delta z'/K_B)$ between nodes in levels 3 and 4 and between nodes in levels 4 and 5 of the model, where $(\Delta z'/K_B)$ is thickness divided by bed-normal hydraulic conductivity.

flow and the effect of head changes on the island are negligible. The Magothy aquifer was simply terminated several miles offshore during construction of the model. Location of this termination was then adjusted

during calibration and verification procedures until the steady-state heads and vertical gradients resembled the prototype heads and gradients beneath the barrier beaches—as far seaward as prototype data permit.

2. *Known-potential boundaries*—The shoreline around the island is a specified-potential boundary for the upper glacial aquifer. This potential is determined by external voltage sources and serves as a reference altitude for most model measurements. The upper surface of the Gardiners Clay offshore is maintained at the same potential as the shoreline. This is equivalent to assuming that (a) the density of seawater is not significantly different from that of freshwater and (b) that head losses in the sea-bottom sediments above the clay are negligible. These assumptions are acceptable because the depths of salty water above the clay are small and because the quantity of freshwater leaking through the offshore part of the Gardiners Clay is small.

3. *Specified-flux boundaries*—Recharge to the upper surface of the model can be either steady-state or steady-state with superposed transients. In each of these recharge modes, this surface is a specified-flux boundary. The flux into each node is equal to the long-term average recharge for the area in the first mode, but in the second the flux varies with time as well as space. Flux across the water table is controlled by external current sources and resistor networks that divide the current into the proper proportions for each water-table node. Steady-state rates of recharge are controlled by current-regulated power supplies; recharge rates that vary with time are achieved by superposing a transient current on the steady-state current. In the latter case, op amps (operational amplifiers) with diode-protected low-impedence output and resistance networks are used to isolate the transient electronic sources from the steady-state source.

Most models are designed to analyze response to transient stresses without reference to steady-state recharge. The way in which the streams are simulated in the experiments described herein rendered such operation undesirable, as explained in (5).

4. *Internal stresses*—Sources and sinks at nodes that are not on a bounding surface of the model are referred to as internal stresses. Stresses of this type include pumping from the aquifer system and (or) injection through wells and basins. These stresses are supplied by pulse generators and function generators, whose output is buffered by op amps. The op amps isolate the outputs of the pulse generators from each other so that it is possible to produce "step" and "ramp" approximations for stresses that vary with time. "Step" and "ramp" approximations, in which stresses change either in discrete steps or as a linear function of time, can be good approximations for many stresses. Although "ramp" and "step" functions may be gross representations of historical prototype stresses that vary irregularly in time and space, the model reservoir, as the prototype, tends to smooth out the response to rapidly changing stresses. The results are usually acceptable. The electrical stress is provided by currents (equivalent to rates of recharge and discharge) that vary with time. The low output impedence of the op amps makes this possible. Figure 26 shows the system for producing transient stresses.

The slow-rate generator shown in figure 26 provides a common reference time for measuring instruments as well as the signal generating equipment. Delay units start different pulse generators at various times after this reference time.

5. *Stream boundaries*—Streams are nonlinear boundaries on the system; their effect varies as a function of head within the model. Streams in the model have been represented by several different types of electrical circuits, all of which have been developed empirically without any attempt to represent the equations for open-channel flow. For the steady-state calibration studies, the streams were modeled by simple resistor networks as is shown in figure 27.

In order for these steady-state streams to represent the prototype streams, two conditions must be met at each stream node: (1) Flow out of the model network through each node must represent seepage into the stream reach represented by the node, and (2) head at the node must represent an "average" elevation of the water table in the area represented by the node. (This average elevation is assumed to be equal to the elevation of the stream surface). In the model (fig. 27*A*), a string of resistors was connected in parallel with the stream nodes. Thus, the voltage drop across each resistor in the string equalled the voltage drop between successive stream nodes of the model. The current flowing into each junction along the string of resistors (that is, leaving each stream junction of the model network) represents the ground-water seepage into the stream reach. Current (I_R in fig. 27*A*) carried by any resistor in the string represents the sum of all the seepage currents upstream from that point. In Long Island, where streams derive almost all their flow from ground-water seepage, this current must increase downstream in a normal, steady-state configuration.

Each resistor was chosen so that when the voltage drop across the resistor (E_1–E_2) was proportional to the head drop (h_1–h_2) between successive node points in the steady-state prototype system (fig. 27*B*), the current I_{R1} through the resistor was proportional to the cumulative discharge Q_{R1} in the stream reach. This

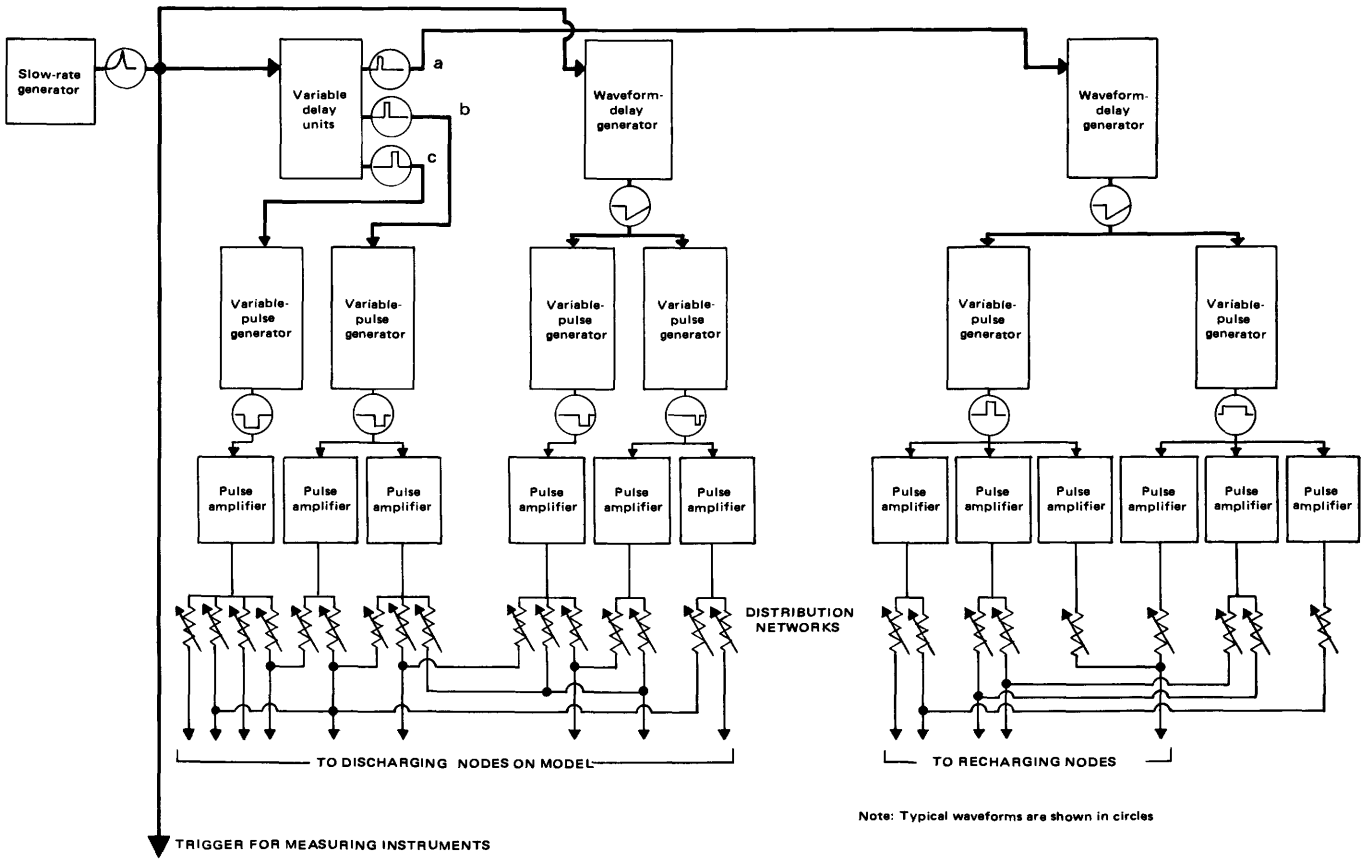

FIGURE 26.—Method for producing transient analog stresses. The distribution networks allow superposition of waveforms so that complex patterns of pumping and recharge can be approximated.

insured that, at every junction, the seepage currents I_S would be proportional to the ground-water seepage Q_S into the stream in the block represented by the junction. The configuration in figure 27A assures that, when the steady-state voltages, $E_1, E_2, \ldots E_n$, correctly represent steady-state heads, h_1, h_2, $\ldots h_n$, along the channel, the current out of each stream node will be proportional to the seepage into the stream in that reach.

The type of circuit in figure 27*A* can only represent ground-water seepage to a stream in the steady-state configuration for which the circuit was specifically designed, not in a transient situation in which heads beneath the stream may change with time. In the prototype system, seepage to streams rapidly decreases to zero as heads decline; when heads fall below stream level, the direction of seepage is reversed. If the flow in the affected stream reach is sustained by inflow to the stream in upstream areas, this seepage into the aquifer may continue; however, if the head in all upstream areas has similarly dropped below stream level, the stream will simply dry up everywhere above the first point at which ground-water head exceeds stream level. In the dried-up part of the stream, there will be no seepage in either direction between the stream and the ground-water system. Behavior of this type was observed in nearly all streams on Long Island during the drought of the 1960's.

To simulate the type of stream-aquifer condition observed during the drought, the circuit in figure 27 was modified by replacing each stream resistor with a resistor and diode in series. The diodes and resistors were chosen so that with potentials $E_1, E_2, \ldots E_n$ representing the prototype steady-state heads $h_1, h_2, \ldots h_n$, the forward resistance of each diode-resistor combination would be the same as the resistance of the resistor alone in figure 27*A*. If downstream gradients (that is, the voltage drop between successive nodes) were to decrease as a result of transient stresses, the diode resistance would increase and would effectively stop streamflow in the affected reach. If, for example, E_1 were to decline while E_2 remained constant, when E_1–E_2 dropped below the junction threshold voltage for the diode between nodes 1 and 2, the current I_{R1} would drop to zero. Reduction of I_{R1} would result in a reduction in I_{R2} and in the current carried by each subsequent reach of the simulated stream. As heads throughout the model aquifer continued to decline in

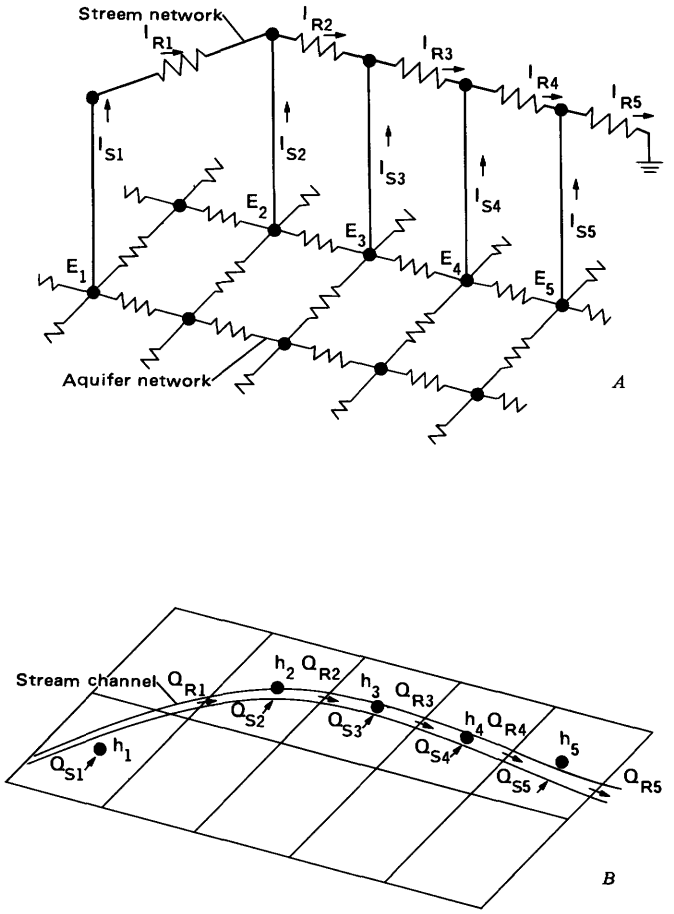

FIGURE 27.—Circuit diagram of a model stream (*A*) showing voltages $E_1, E_2, \ldots E_n$ and currents $I_{R1}, I_{R2}, \ldots I_{Rn}$ along the stream and currents $I_{S1}, I_{S2}, \ldots I_{Sn}$ into the stream. A prototype stream channel (*B*) indicates the values of head ($h_1, h_2, \ldots h_n$), represented by the voltages, and discharges Q_R and Q_S represented by the currents in the model. Each junction in the model network represents one of the aquifer blocks in the prototype.

response to a simulated drought, E_2 would eventually decline until E_2–E_3 was less than the threshold voltage for that diode and I_{R2} would decrease to zero. The stream would be shortened at its head.

Although model operation with the two stream circuits, as well as model operation without streams, proved useful for the model-performance analyses described in the section "Model-Prototype Comparisons," they were not adequate for some predictive studies. A third circuit, different in concept and more difficult in execution, has been used for predictive studies. Because the third circuit was not used in any of the analyses described in this report, a description of that circuit will be deferred to a later report (A. W. Harbaugh and R. T. Getzen, written commun., 1975).

SUMMARY OF DESIGN CRITERIA

Conditions of the ground-water reservoir that must be correctly represented by the model are as follows:

(1) Geometry and distribution of hydraulic conductivity in the reservoir rocks. For Long Island, distribution of conductivity is three dimensional, and magnitude of conductivity is direction dependent. The finite-difference network must be alined with the directions of the principal conductivities.

(2) Average magnitude of the specific storage of the reservoir rocks and spatial distribution of storage.

(3) Location of boundaries of the hydrologic system and nature of the boundaries. Where this is not completely possible, the boundaries were designed to have minimal effect on the internal parts of the model. The lower boundary of the Magothy aquifer and the saltwater-freshwater interface are not exactly represented by the model. The model attempts to minimize the effects of these boundaries.

(4) Historical data on internal stresses to the reservoir and electronic-exciting circuitry capable of representing these stresses.

(5) Ground-water discharge to surface-water bodies. Where this seepage is to streams and its magnitude is likely to change drastically as a function of small head changes within the ground-water reservoir, the model must be capable of correctly representing the change in seepage.

If the model can reproduce observed and calculated distributions of head in response to observed (historical) stresses and synthetic stresses, all the preceding conditions are assumed to have been met. The model is then said to be "calibrated" or "verified." Such a verification procedure does not prove that the model ground-water reservoir will respond correctly to all stresses; it only shows that the representation of responses to a certain range of stress situations seems to correlate with observed prototype response.

MODEL-PROTOTYPE COMPARISONS

PERFORMANCE CRITERIA

Model performance is generally evaluated in terms of the preceding design criteria. Most of these criteria cannot be adequately defined by prototype data. The best known of these criteria on Long Island is the general configuration of the water table. Historical data describing the water table are shown from Burr, Herring, and Freeman (1904); Veatch, Slichter, Bowman, Crosby, and Horton (1906); Jacob (1945); Isbister (1959); and Kimmel (1971). In a thin, isotropic aquifer, the configuration of the water table would be adequate for defining correct steady-state operation of the model. The same cannot be said for regional flow systems in thick, anisotropic sedimentary sequences (Freeze and Witherspoon, 1967, p. 632–633). Sufficient data to

permit description of the head distribution at other depths have been acquired only recently (Kimmel, 1971; Jensen and Soren, 1974). Because measurements are almost never made before ground-water development begins, data that reflect human as well as climatological influences on the ground-water system must be used to estimate and extrapolate the distribution of steady-state head.

Model performance is measured by two types of tests—steady-state tests, which measure the model's ability to represent average or predevelopment hydrologic conditions, and unsteady-state tests, which compare the model's response to transient stresses with prototype response to historical stresses.

Evaluation of unsteady (transient) model performance requires two types of data—quantitative measurements of the stress (pumping, recharge, fluctuating lake levels, and other boundary conditions) and historical responses (changes in head and discharge over long periods of time) of the system to those stresses. Two types of unsteady stresses were considered in evaluating model performances: (1) Changes in net recharge that resulted from the severe drought of the early 1960's and (2) historical pumping records from major wells or well fields in western Long Island. Data for magnitude of the type 1 stresses are from Cohen, Franke, and Foxworthy (1968), and for type 2 from records compiled by New York State Water Power and Control Commission and by county agencies. Simulated response to the climatological stress was compared with the observations by Cohen, Franke, and McClymonds (1969). Response and recovery of the simulated water table to pumping stresses was compared with water-table data compiled by Lusczynski (1952) and from other sources cited in the preceding paragraph. Data from several of these sources are reproduced in subsequent illustrations for comparison with model response.

In addition to stress and head data, records of stream discharge are compared with simulated stream discharge. Streams on Long Island are seldom gaged at more than one point along their length; except for a few seepage runs and qualitative information about tidal fluctuations and location of the heads of streams in varying hydrological circumstances, there is only one point on each stream at which the model can be compared with prototype data.

STEADY-STATE EVALUATION

The average annual ground-water recharge has been estimated to be 58 cm (23 in.) for a water-budget area that excludes the highly urbanized areas and low-lying coastal areas of Long Island (Cohen and others 1968, p. 44–45). This value was used as a starting point for steady-state calibration of the model but yielded unsatisfactory results. The estimate of Cohen, Franke,

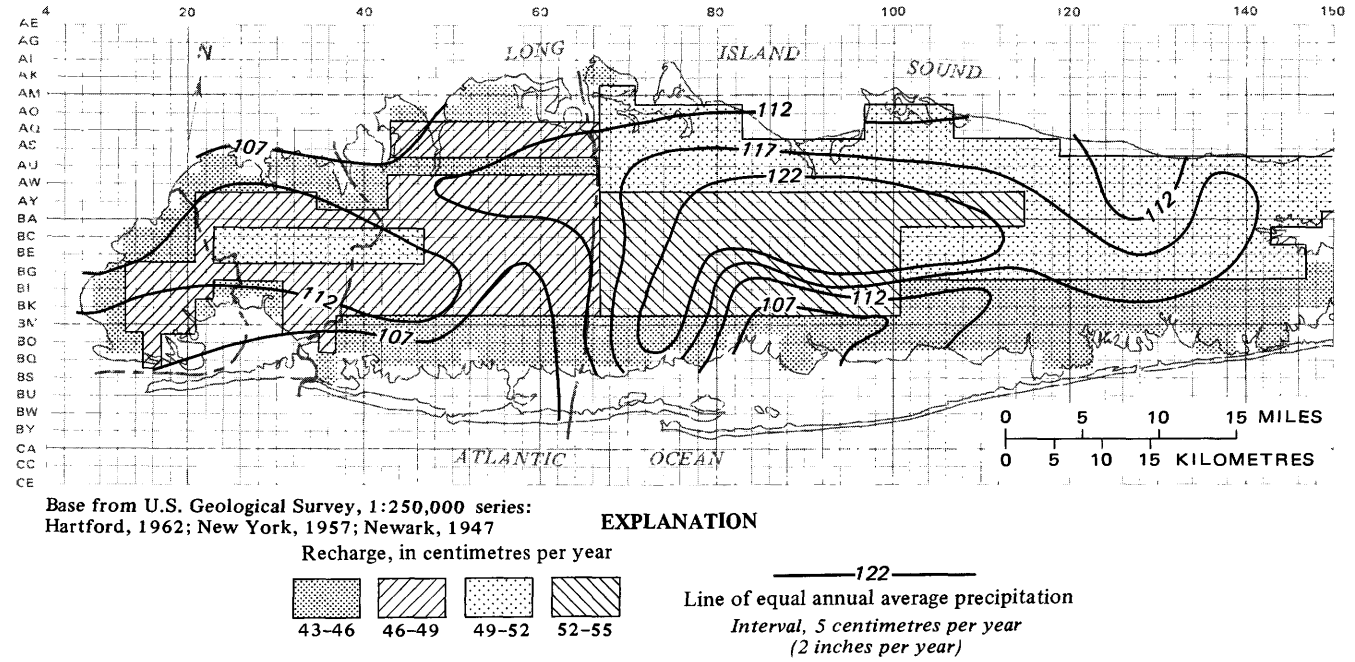

FIGURE 28.—Distribution of prototype mean annual precipitation, 1951–65, and of steady-state recharge to the model. (Mean annual precipitation modified from Miller and Frederick, 1969.)

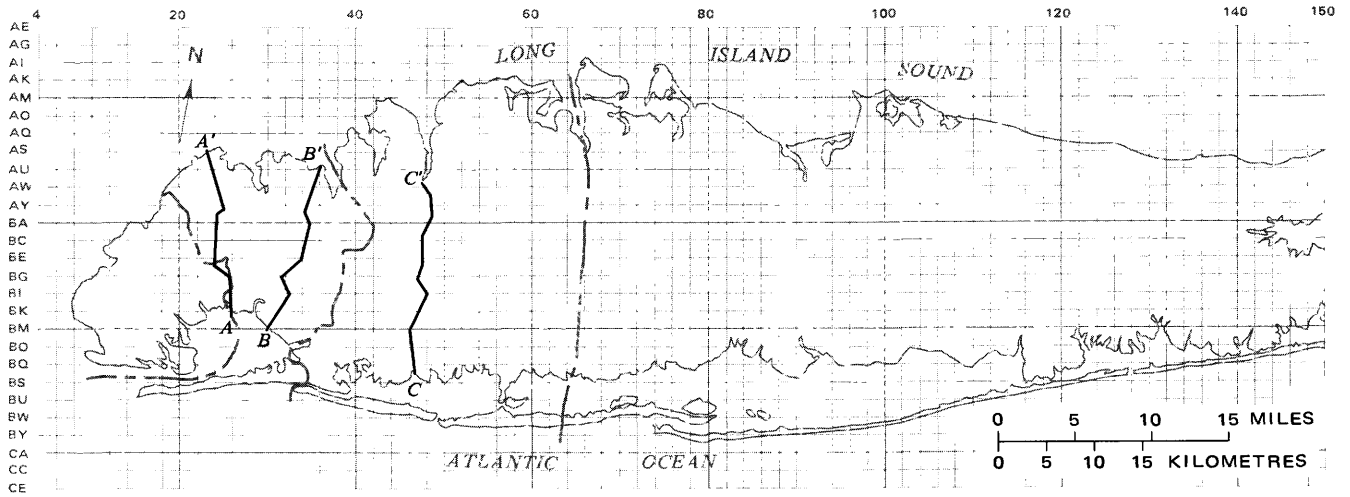

FIGURE 29.—Simulated, steady-state, water-table profiles and locations on western Long Island compared with 1903 prototype water-table profiles. Major production wells near profiles in 1903 are also shown. Prototype data from Burr, Hering, and Freeman (1904).

and Foxworthy (1968) seems to be too high if applied to the entire island. Several factors influence the rates of recharge; the most important seem to be (a) rate and duration of precipitation, (b) infiltration characteristics of the surficial sediments, (c) thickness of the unsaturated zone, and (d) local relief. Precipitation is not uniformly distributed over Long Island (fig. 28) but is noticeably greater near the center of the island than elsewhere. The soils of the morainal parts of Long Island tend to be less permeable than the soils of the outwash areas. Thus, there is a tendency for a greater proportion of the precipitation to run off near the north shore. Steep slopes, like those on the north shore, tend to cause precipitation to run off faster than it does on gentle slopes. Much more of the water that infiltrates the soil is lost to plant roots and to evaporation where the water table is close to the surface; a smaller proportion of rainfall becomes part of the ground-water reservoir in low-lying, swampy areas than in areas of greater altitude. The combination of all these factors does not reduce to an equation from which the steady-state recharge values shown in figure 28 could be calculated. These known factors make the recharge distribution in figure 28 seem reasonable, but other factors, unknown or misunderstood, could influence recharge rates in entirely different ways. The distribution of model recharge shown in figure 28 was obtained through a "tuning" process. The gross estimate by Cohen, Franke, and Foxworthy (1968) was assumed to be acceptable; distribution of this recharge was modified by trial and error until a reasonable water table was obtained.

With the recharge distribution shown in figure 28,

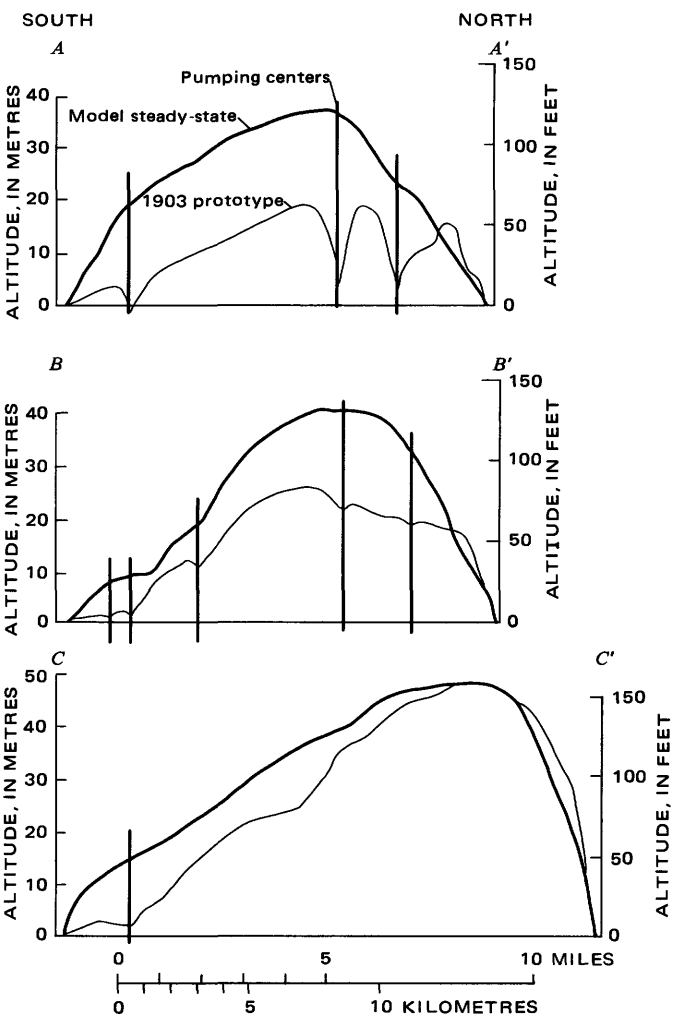

FIGURE 29.—Continued.

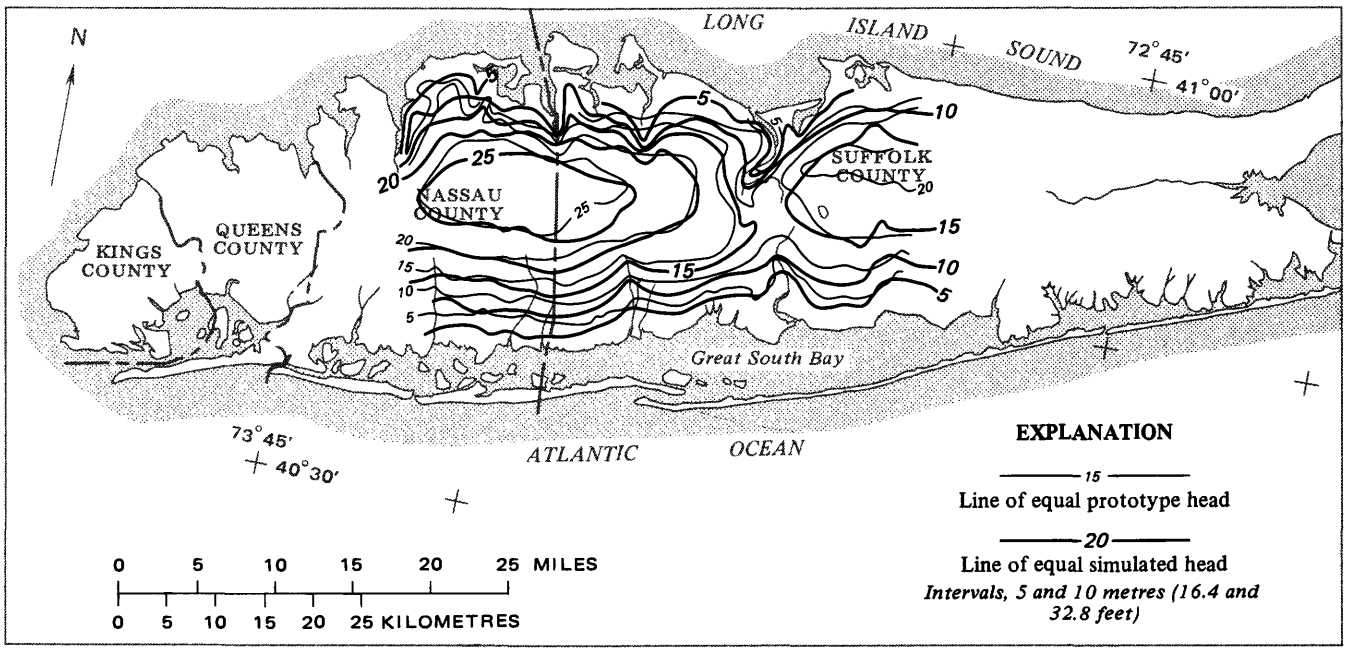

Base from U.S. Geological Survey, 1:250,000 series:
Hartford, 1962; New York, 1957; Newark, 1947

FIGURE 30.—Comparison of steady-state model water table with 1903 water table in central Long Island. (Prototype data from Veatch and others, 1906.)

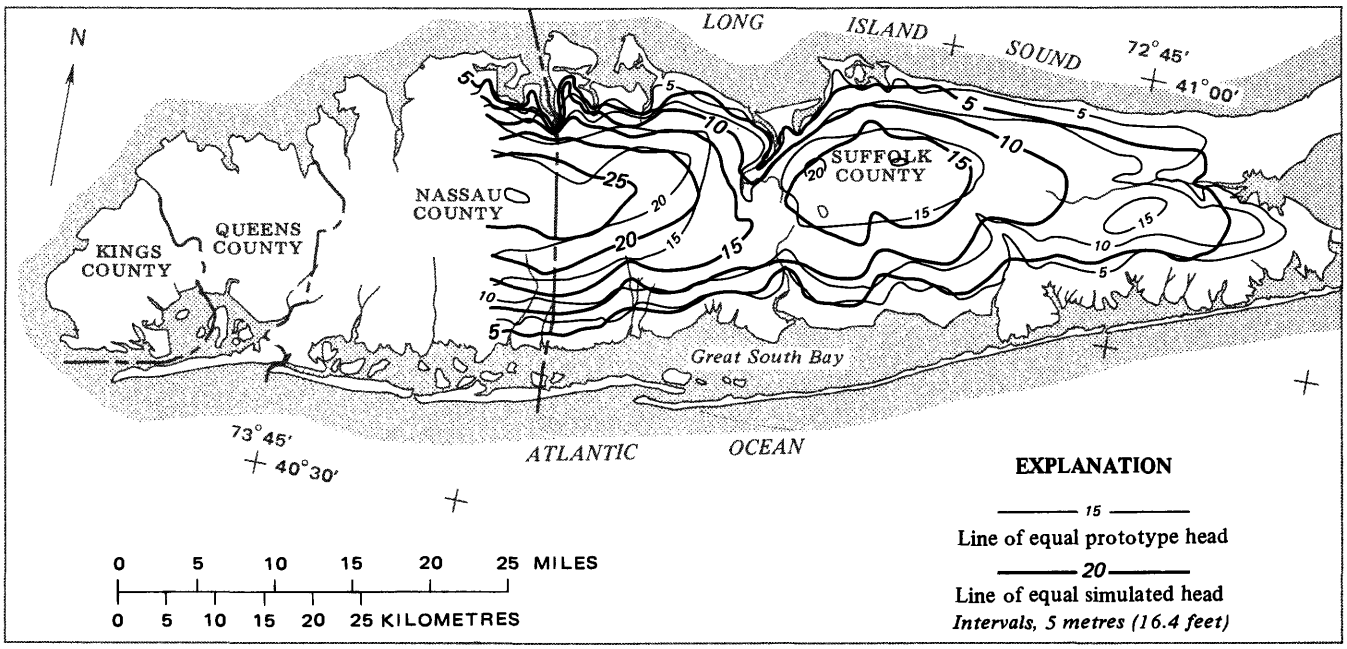

Base from U.S. Geological Survey, 1:250,000 series:
Hartford, 1962; New York, 1957; Newark, 1947

FIGURE 31.—Comparison of steady-state model water-table with 1970 water table in eastern Long Island. (Prototype data from Kimmel, 1972.)

the model produced the steady-state, water-table configuration that is compared with observed prototype water-table data in figures 29–31. Figure 29B shows water-table profiles along three lines of section in western Long Island; locations of these lines of section are shown in figure 29. Pumpage and other manmade hydrologic disturbances began in western Long Island and gradually spread eastward. The 1903 water levels for the westernmost part of the island reflect these manmade disturbances. The steady-state model analysis did not simulate these manmade effects, and, therefore, agreement between the model results and

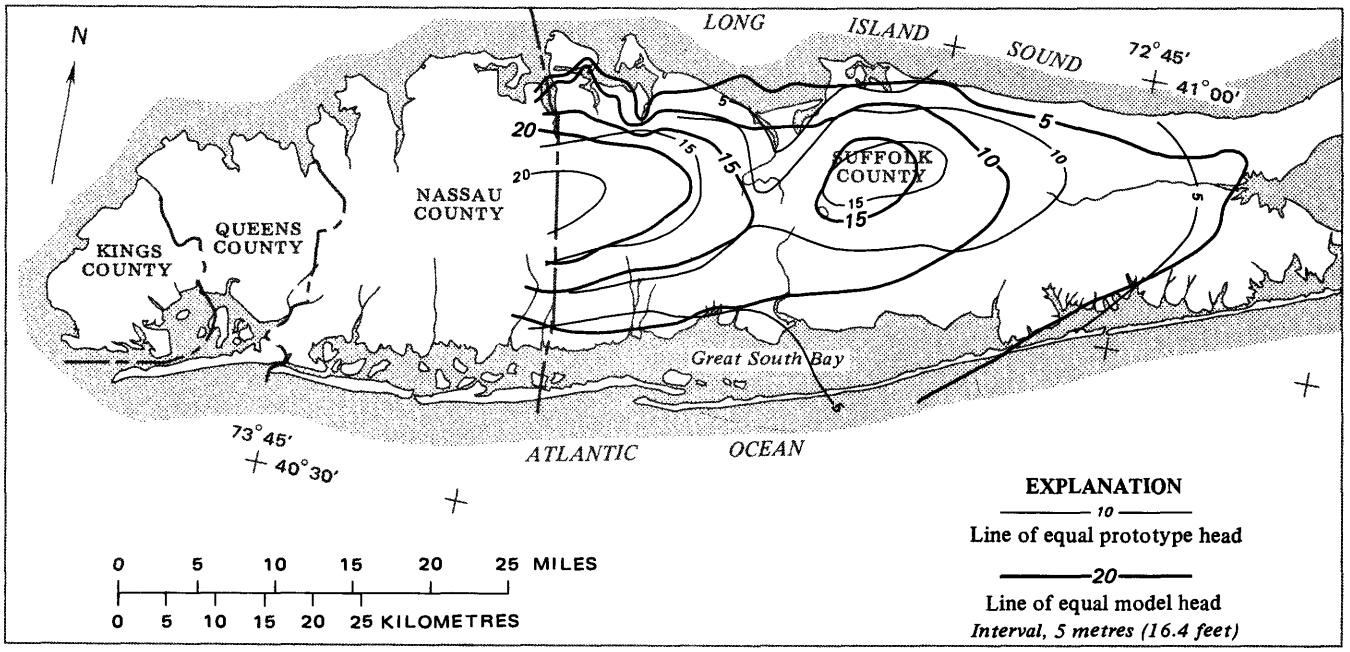

Base from U.S. Geological Survey, 1:250,000 series:
Hartford, 1962; New York, 1957; Newark, 1947

FIGURE 32.—Comparison of steady-state simulated head near the base of the Magothy aquifer with 1971 prototype head. (Prototype data from Jensen and Soren, 1974.)

the 1903 water levels is poor for the westernmost line of section *A–A'* in figure 29. The agreement improves progressively to the east as the manmade effects diminish. The poor agreement along line *A–A'* may also reflect that the model design is based on saturated thickness of the glacial aquifer in 1970; the saturated thickness in 1903 was considerably greater than it was in 1970 for part of Kings County. Model performance in the westernmost part of Long Island could not be justified by the preceding comparison but was justified by unsteady-state performance (next section).

For the eastern two-thirds of the modeled area, agreement between the prototype water table and model results was good, as shown by the maps of figures 30 and 31. Figure 30 shows a comparison of steady-state model results with a water-table map by Veatch, Slichter, Bowman, Crosby, and Horton (1906) covering eastern Nassau and western Suffolk Counties. Effects of pumpage were negligible in these areas at that time. Because the map by Veatch, Slichter, Bowman, Crosby, and Horton (1906) does not include the easternmost one-third of the modeled area, figure 31 shows a comparison of model results with 1970 water-table contours by Kimmel (1972) for Suffolk County. Again, the effects of pumpage on water levels in Suffolk County were small in 1970.

Comparison of heads near the base of the Magothy aquifer in 1971 with simulated steady-state head in model level 5 is shown in figure 32. Data for only the eastern half of the island are shown; heads in the lower part of the Magothy aquifer have been noticeably affected by pumping in the western half of the island.

Extent of agreement between prototype and model heads is not perfect but is within a few metres for most of the reservoir for which reliable data are available on undisturbed natural (predevelopment) potential. Some of the disagreement is probably due to differences in data interpretation; for example, other water-table maps such as that by Cohen, Franke, and Foxworthy (1968, plate 2E), do not show the same pronounced high in southeastern Suffolk County as that indicated by the 15–m (49–ft) closed contour in this area in figure 31.

Distribution of normal, steady-state head along two typical model hydrologic sections is shown in figure 33. Although there are no satisfactory prototype data for comparison, model head and flow data given in the hydrologic sections are useful for understanding the flow system.

Table 2 compares long-term average stream discharge with values of steady-state stream discharge from the model. Where a range of discharge is given for the simulated stream discharge, the prototype gage is near the division between two stream reaches on the model. Most pairs of model and prototype stream discharges agree within ±5 percent, and all pairs except for about ten streams agree within ±10 percent. Only short streams and streams that have extremely high or extremely low gradients have model discharges that differ significantly from prototype discharges. The difference between total stream discharge as modeled and the long-term average for all prototype streams com-

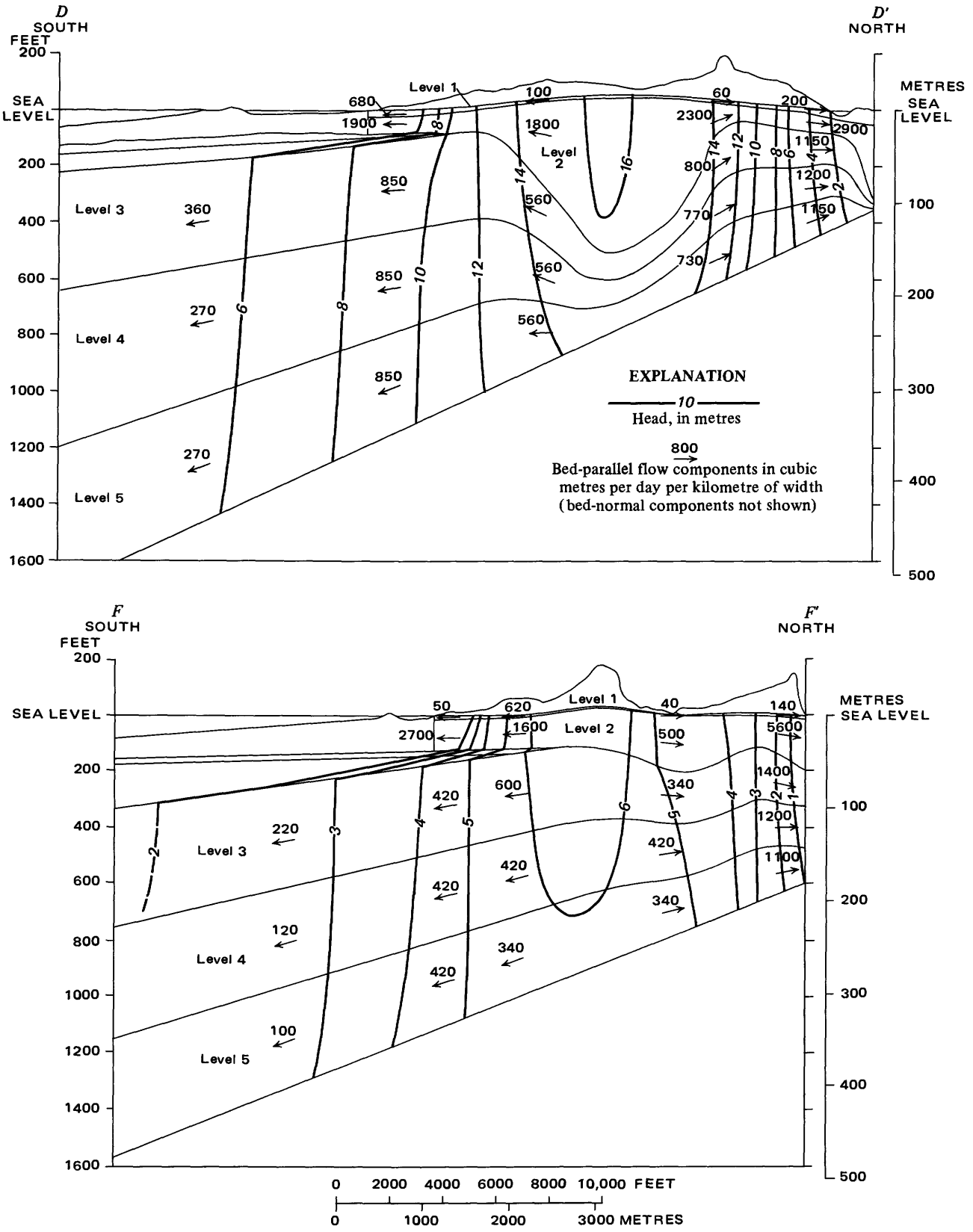

FIGURE 33.—Distribution of head and bed-parallel components of ground-water flow along two hydrologic sections through the model Long Island ground-water reservoir. Rates of flow are for a 1-kilometre-wide strip. Locations of sections are shown in figure 4.

TABLE 2.—*Streamflow comparisons*

Code shown for streams in figure 14[1]	Stream name	Average discharge (cubic metres per second)	Model discharge (cubic metres per second)
B	Valley Stream	0.165	0.186
C	Pines Brook	.141	.150
D	South Pond	.083	.094
E	Parsonage Creek	.117	.100
F	Milburn Creek	.242	.271
G	East Meadow Brook	.473	.575
H	Cedar Swamp Creek	.239	.265
I	Newbridge Creek	.066	[2].048 to .070
J	Bellmore Creek	.310	.435
L	Seamans Creek	.054	.050 to .058
M	Seaford Creek	.054	.064 to .084
N	Massapequa Creek	.339	.304 to .438
O	Carman Creek	.120	.136 to .154
P	Amityville Creek	.110	.059 to .102
Q	Great Neck Creek	.071	.075 to .142
R	Strongs Creek	.054	.052 to .082
S	Neguntatogue Creek	.108	.066
T	Santapogue Creek	.126	.165
U	Carlls River	.772	1.01
		.967	1.05
V	Sampawams Creek	.342	.397
W	Shookwams Creek	.031	.034 to .055
X	Willets Creek	.071	.074 to .100
Y	Trues Creek	.051	.058
Z	Cascade Creek	.071	.048 to .080
AA	Penataquit Creek	.175	.185 to .212
AB	Awixa Creek	.054	.063
AC	Orowoc Creek	.074	.080
AD	Pardees Pond	.174	.066 to .107
AE	Champlin Creek	.207	.247 to .343
AF	West Brook	.120	.096
AG	Rattlesnake Brook	.262	.248 to .277
AH	Connetquot River	1.10	1.02
AI	Green Creek	.128	.131
AJ	Brown Creek (west)	.231	.245
AK	Brown Creek (east)	.231	.245
AL	Tut Hills Creek	.174	.116 to .171
AM	Patchogue Creek	.595	.528 to .653
AN	Swan River	.365	.354
AO	Mud Creek	.153	.145 to .154
AP	Motts Brook	.051	.013 to .070
AQ	Beaverdam Creek	.046	.039
AR	Carmans River	.048	.055
		.678	.518
AS	Forge River	.274	.298
AT	Terrel River	.071	.069
AU	Little Seatuck	.128	.135
AV	Seatuck Creek	.162	.205
AW	East River	.071	.082
AX	Beaverdam Creek	.068	.055 to .057
AY	Aspatuck Creek	.063	.070
AZ	Quantuck Creek	.060	.069
BA	Whitney Lake	.071	.061
BB	Roslyn Brook	.051	.066
BC	Glen Cove Creek	.202	.206
BD	Island Swamp Brook	.026	.031
BE	Mill Neck Creek	.268	.121
BF	Cold Spring Brook	.126	.130
BG	Mill Creek	.085	.047
BH	Stony Hollow Run	.034	.046
BJ	NE Nissequogue	.051	.086
		.111	.114
		1.18	1.28
BK	Wading River	.028	.026
BL	Saw Mill Creek	.077	.042
BM	Peconic River	.986	1.00
BN	Little River	.125	.137 to .168
BO	White Brook	.077	.086

[1]Codes for only 64 of 75 streams plotted in figure 14 are listed. Eleven of the 75 streams, most of them in Queens County, have been replaced by sewers.
[2]A range of discharge indicates that prototype gage falls at or near division between two reaches on model.

bined is less than 5 percent. The ability of the simulated streams to represent prototype discharge correctly at one or two points (the gages) on each stream does not mean that the overall representation is correct. There are no prototype data relating changes in seepage along the entire length of each stream to changes in the water table, but the general agreement of the model response with the available historical data strongly suggest that the response of the prototype system is closely simulated by the model.

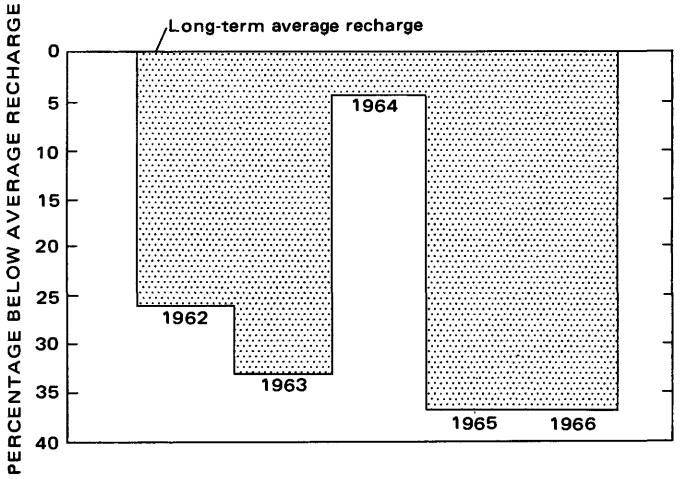

FIGURE 34.—Changes in annual recharge used to simulate the 1962–66 drought on Long Island.

UNSTEADY-STATE EVALUATION

Two historical stresses were used for unsteady-state evaluation. The first of these, the drought of 1962–66, was simulated by using estimates of the reduction in recharge during the drought (Cohen and others, 1968, plate 4E). Yearly deviation from the long-term, average annual recharge, derived from the estimates, is shown in figure 34. This stress has two causes: (1) Reduced precipitation and (2) sporadically occurring precipitation. During the drought, intense storms were the source of much of the precipitation. Although most precipitation on Long Island is rapidly absorbed by the soil, intense storms contribute large amounts of runoff to streams and fill surface ponds that evaporate. Very little of the storm precipitation becomes ground-water recharge.

The intensity of the drought stress, as given by Cohen, Franke, and Foxworthy (1968) and in figure 34, is a net or total stress. Just as was the case with average recharge distribution (fig. 28), the areal distribution of drought shown by the map in figure 35 was derived by a trial-and-error procedure aimed at reproducing the prototype response. Distribution of stress, mapped in figure 35 in terms of deviation from the islandwide areal average stress, was assumed to be constant from year to year during the drought. The trial-and-error method involved trying three different stress distributions: (1) Drought stress was uniformly distributed over the entire island; (2) stress in the low-lying parts of the island was five times greater than that in the higher, central part of the island; and (3) stress in the low-lying parts of the island was twice as great as that in the center of the island as depicted in figure 35. In each of these three stress distributions,

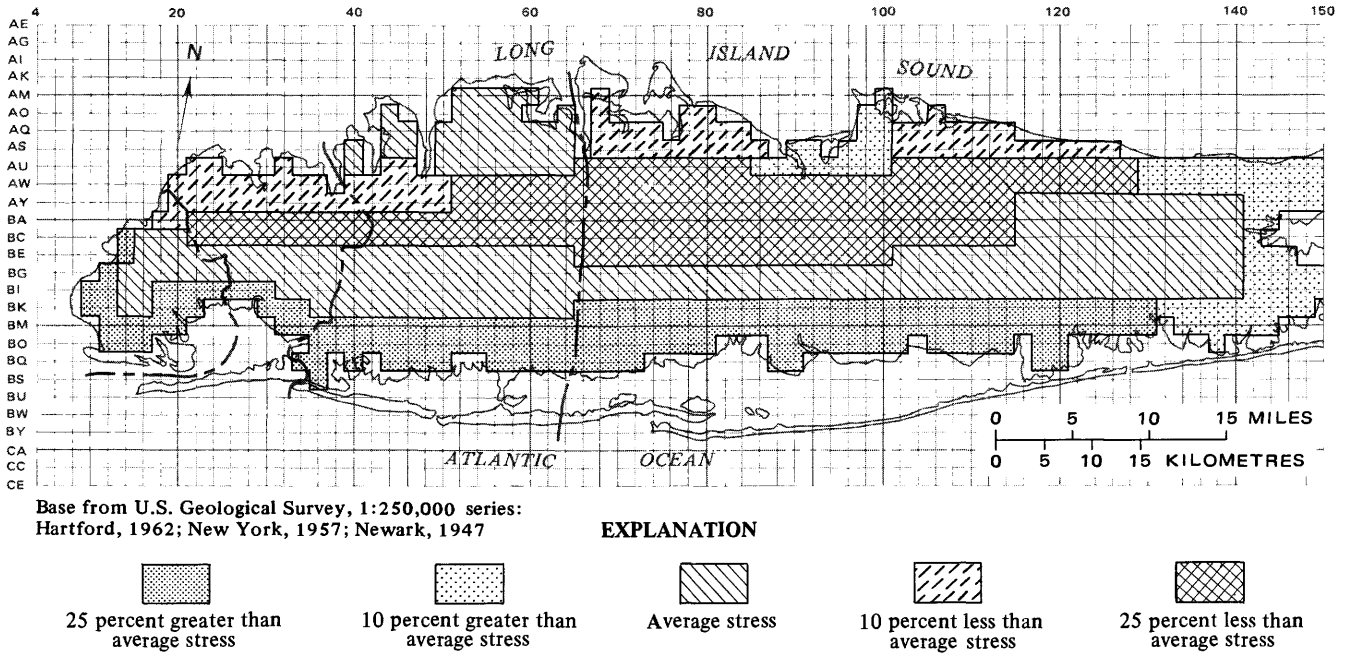

FIGURE 35.—Distribution of the decline in net recharge used to simulate the 1962–66 drought on Long Island. The distribution is given in terms of deviation from the islandwide areal average of the stress.

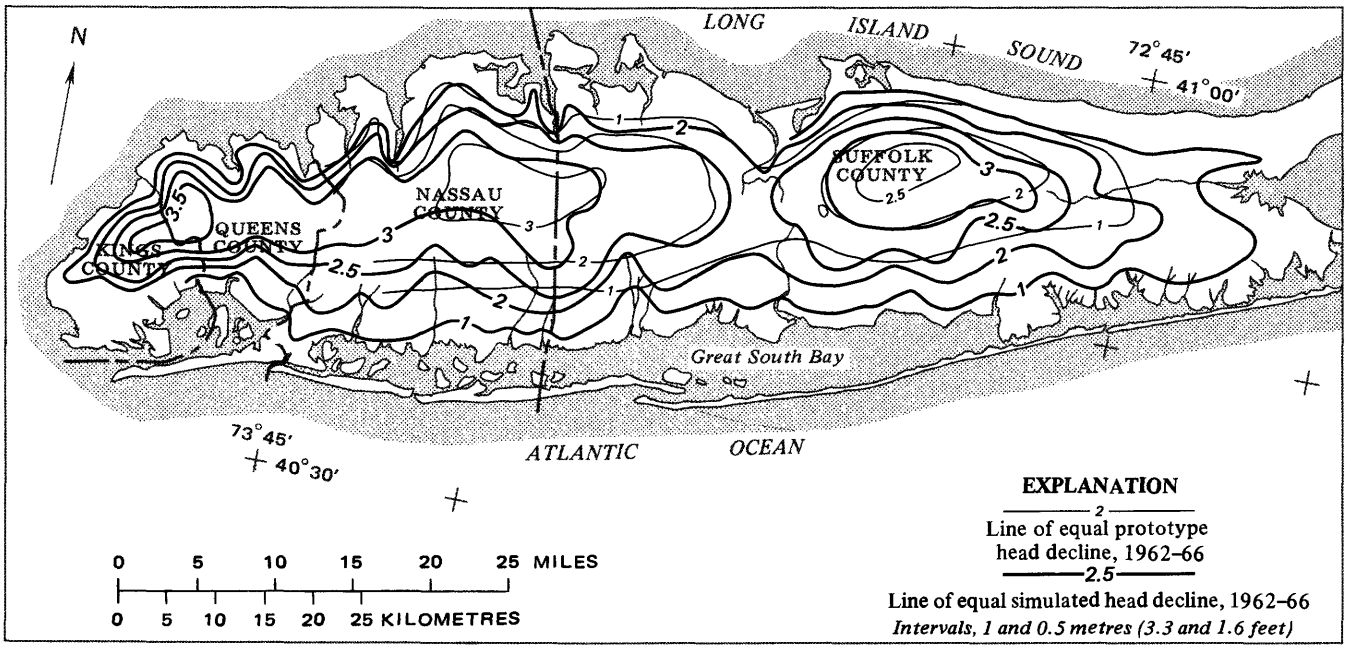

Base from U.S. Geological Survey, 1:250,000 series:
Hartford, 1962; New York, 1957; Newark, 1947

FIGURE 36.—Comparison of observed and simulated water-table declines as a result of the 1962–66 drought. (Prototype water-table decline from Cohen and others, 1969.)

the total stress during each time period was equal to the quantity indicated in figure 34.

Simulated response to the assumed stress situation is compared with the net-change map (fig. 36) presented by Cohen, Franke, and McClymonds (1969, fig. 10), who mapped the change in the water table between 1961 and 1966. Their map does not show net changes in New York City and western Nassau County because changes in water levels there are the result of other influences. Changes in recharge caused by pav-

TABLE 3.—*Net recharge (positive) and withdrawal (negative) at each model node used to simulate manmade historical stresses in western Long Island during the periods 1903–33, 1934–42, 1943–50, and 1951–63. Unstressed nodes are not listed*

[Accuracy of these measurements is about ±2 percent or ±40 cubic metres per day, whichever is greater]

	LEVEL 1				LEVEL 2				LEVEL 3			
YEARS → / MODEL NODE	1903-33	1934-42	1943-50	1951-63	1903-33	1934-42	1943-50	1951-63	1903-33	1934-42	1943-50	1951-63
	CUBIC METRES PER DAY				CUBIC METRES PER DAY				CUBIC METRES PER DAY			
10 BK	-12920.	-9940.	-5960.	-2980.	0.	0.	0.	0.	0.	0.	0.	0.
12 BG	-9940.	-8690.	-4970.	-2040.	0.	0.	0.	0.	0.	0.	0.	0.
14 BC	-8840.	-7750.	-4420.	-1790.	0.	0.	0.	0.	0.	0.	0.	0.
14 BE	-22160.	-18980.	-10680.	-4970.	0.	0.	0.	0.	0.	0.	0.	0.
14 BG	-7450.	-7950.	-6950.	-1490.	0.	0.	0.	0.	0.	0.	0.	0.
14 BI	-500.	-6950.	-5960.	0.	0.	-550.	-5460.	-1790.	0.	0.	0.	0.
16 BC	-20670.	-17730.	-9980.	-4620.	0.	0.	0.	0.	0.	0.	0.	0.
16 BE	-7950.	-6950.	-3970.	-1640.	0.	0.	0.	0.	0.	0.	0.	0.
16 BG	-5460.	-9940.	-7950.	-990.	0.	0.	0.	0.	0.	0.	0.	0.
16 BI	0.	0.	0.	0.	-990.	-7950.	-3480.	-200.	0.	0.	0.	0.
16 BK	-5020.	-4520.	-3530.	-500.	0.	0.	0.	0.	0.	0.	0.	0.
16 BN	-6460.	0.	0.	0.	0.	0.	0.	0.	0.	0.	0.	0.
17 BA	-12820.	-10980.	-6160.	-2880.	0.	0.	0.	0.	0.	0.	0.	0.
18 BB	-10180.	-8890.	-5070.	-2090.	0.	0.	0.	0.	0.	0.	0.	0.
18 BC	0.	0.	0.	0.	0.	-8450.	-10930.	-11920.	0.	0.	0.	0.
18 BE	0.	0.	0.	0.	0.	-450.	-4470.	-1490.	0.	0.	0.	0.
18 BG	0.	0.	0.	0.	-1990.	-12920.	-3970.	-500.	0.	0.	0.	0.
18 BI	-29810.	-13910.	-10930.	-1990.	0.	0.	0.	0.	0.	0.	0.	0.
19 AZ	-9240.	-8050.	-4620.	-1890.	0.	0.	0.	0.	0.	0.	0.	0.
19 BG	-4920.	-4420.	-3430.	-500.	0.	0.	0.	0.	0.	0.	0.	0.
20 AW	-3430.	-1940.	-1790.	-1940.	0.	0.	0.	0.	0.	0.	0.	0.
20 AY	-3530.	-2040.	-1840.	-2040.	0.	0.	0.	0.	0.	0.	0.	0.
20 BA	-9090.	-7950.	-4520.	-1840.	0.	0.	0.	0.	0.	0.	0.	0.
20 BC	-8350.	-7300.	-4170.	-1690.	0.	0.	0.	0.	0.	0.	0.	0.
20 BG	0.	0.	0.	0.	-3970.	-20860.	-9940.	-990.	0.	0.	0.	0.
20 BI	0.	0.	0.	0.	-5120.	0.	0.	0.	0.	0.	0.	0.
22 AU	-3230.	-1840.	-1690.	-1840.	0.	0.	0.	0.	0.	0.	0.	0.
22 AW	-8940.	-4470.	-4470.	-4470.	0.	0.	0.	0.	0.	0.	0.	0.
22 AY	-3480.	-1990.	-1840.	-1990.	0.	0.	0.	0.	0.	0.	0.	0.
22 BA	-3480.	-1990.	-1840.	-1990.	0.	0.	0.	0.	0.	0.	0.	0.
22 BG	-990.	0.	0.	0.	0.	0.	0.	0.	0.	0.	0.	0.
24 AU	-3680.	-2090.	-1940.	-2090.	0.	0.	0.	0.	0.	0.	0.	0.
24 BA	-3130.	0.	0.	0.	0.	0.	0.	0.	0.	0.	0.	0.
24 BG	0.	0.	0.	0.	0.	0.	0.	0.	-9940.	-600.	-300.	0.
26 BA	-1640.	0.	0.	0.	0.	0.	0.	0.	0.	0.	0.	0.
26 BC	-3130.	0.	0.	0.	0.	0.	0.	0.	0.	0.	0.	0.
26 BG	-6360.	-9090.	-12120.	-11570.	0.	0.	0.	0.	-3870.	-1940.	0.	0.
26 BI	0.	0.	0.	0.	0.	0.	0.	0.	-3870.	-1940.	0.	0.
28 BC	-1840.	0.	0.	0.	0.	0.	0.	0.	0.	0.	0.	0.
28 BE	-24840.	-4970.	-13410.	-13910.	0.	0.	0.	0.	-600.	-840.	-1040.	-2090.
28 BG	-5070.	-7300.	-9740.	-9290.	0.	0.	0.	0.	0.	0.	0.	0.
28 BI	-8450.	0.	0.	0.	0.	0.	0.	0.	0.	0.	0.	0.
30 BC	-21360.	-1990.	-990.	0.	0.	0.	0.	0.	0.	0.	0.	0.
30 BE	-7950.	-11920.	-12420.	-16390.	0.	0.	0.	0.	0.	0.	0.	0.
30 BG	-4970.	-7950.	-8940.	-11920.	0.	0.	0.	0.	0.	0.	0.	0.
30 BI	0.	0.	0.	0.	0.	0.	0.	0.	-6060.	-300.	-300.	0.
31 BI	-1490.	0.	0.	0.	0.	0.	0.	0.	0.	0.	0.	0.
32 BC	0.	0.	0.	0.	0.	0.	0.	0.	-600.	-840.	-1040.	-2090.
32 BG	0.	0.	0.	0.	0.	0.	0.	0.	-1990.	-990.	-1290.	-2380.
32 BI	0.	0.	0.	0.	0.	0.	0.	0.	-15900.	-5960.	-3780.	-990.
32 BQ	0.	0.	0.	0.	0.	0.	0.	0.	-3970.	-5560.	-4470.	-5560.
34 AY	-3970.	-4970.	0.	0.	0.	0.	0.	0.	0.	0.	0.	0.
34 BE	-11920.	-7950.	-8940.	-9940.	0.	0.	0.	0.	0.	0.	0.	0.
34 BI	-1990.	-500.	-500.	0.	0.	0.	0.	0.	-8450.	-4070.	-1190.	0.
36 AY	0.	0.	0.	0.	-4820.	0.	0.	0.	0.	0.	0.	0.

ing and building, ground-water withdrawals through pumping wells, and sewering have strongly affected the water table in the western part of Long Island. Considering the assumptions that underlie the recharge estimates (Cohen and others, 1968, p. 44), the extent of agreement between simulated and observed changes in the water table is quite satisfactory.

Although direct measurements of net recharge are not available—only gross estimates based on other components of the hydrologic cycle, some of which can only be approximated—the decline in recharge during a drought would probably be distributed unequally. The assumed distribution of stress (fig. 35) is not unrealistic because the erratic frequency and intensity of precipitation during the drought (Cohen and others, 1969, p. F8) resulted in much greater runoff than nor-

TABLE 3.—*Net recharge (positive) and withdrawal (negative) at each model node used to simulate manmade historical stresses in western Long Island during the periods 1903–33, 1934–42, 1943–50, and 1951–63. Unstressed nodes are not listed*—Continued

	LEVEL 1				LEVEL 2				LEVEL 3			
YEARS--	1903-33	1934-42	1943-50	1951-63	1903-33	1934-42	1943-50	1951-63	1903-33	1934-42	1943-50	1951-63
MODEL NODE	CUBIC METRES PER DAY				CUBIC METRES PER DAY				CUBIC METRES PER DAY			
36 BC	-350.	-4320.	-5120.	-6950.	0.	0.	0.	0.	0.	0.	0.	0.
36 BE	-5960.	-5960.	-6950.	-7950.	0.	0.	0.	0.	-790.	-2980.	-3830.	-8350.
36 BG	-350.	-4220.	-5020.	-6810.	0.	0.	0.	0.	0.	-2980.	-4170.	-8450.
36 BI	0.	0.	0.	0.	0.	0.	0.	0.	-700.	-2980.	-500.	100.
36 BK	-1490.	-500.	-500.	0.	0.	0.	0.	0.	-700.	-3970.	-4970.	-500.
36 BP	0.	0.	-1290.	-2140.	0.	0.	0.	0.	0.	0.	0.	0.
38 BC	0.	0.	0.	0.	0.	0.	0.	0.	0.	-990.	-990.	-990.
38 BE	-350.	-4370.	-5170.	-7050.	0.	0.	0.	0.	-790.	-2980.	-3830.	-8350.
38 BG	0.	0.	0.	0.	0.	0.	0.	0.	-700.	-2530.	-3280.	-7200.
38 BI	200.	990.	1090.	600.	0.	0.	0.	0.	-790.	-2980.	-3970.	-5960.
38 BK	-14900.	-4970.	-7450.	840.	0.	0.	0.	0.	-1990.	-2780.	-3080.	-5560.
38 BM	-9940.	4620.	4970.	4620.	0.	0.	0.	0.	-500.	-3480.	-4720.	-10930.
40 AS	0.	0.	0.	0.	0.	0.	0.	0.	-200.	-500.	-500.	-600.
40 AW	0.	0.	-1690.	-2830.	0.	0.	0.	0.	-1990.	-4970.	-4970.	-5960.
40 BA	-3680.	0.	0.	0.	0.	0.	0.	0.	-9940.	-9940.	-7950.	-4970.
40 BG	450.	2190.	2980.	100.	0.	0.	0.	0.	-1490.	-4970.	-5960.	-6950.
40 BI	250.	1140.	1690.	-300.	0.	0.	0.	0.	0.	0.	0.	0.
40 BK	3380.	2040.	2930.	2780.	0.	0.	0.	0.	-250.	-1590.	-1390.	-5120.
40 BM	-14900.	-5960.	-3970.	-5960.	0.	0.	0.	0.	0.	0.	0.	0.
40 BO	2680.	400.	450.	890.	0.	0.	0.	0.	0.	0.	0.	0.
42 AW	0.	0.	400.	2880.	0.	0.	0.	0.	0.	0.	-450.	-2730.
42 AY	0.	0.	400.	2580.	0.	0.	0.	0.	0.	0.	-350.	-2240.
42 BA	0.	550.	1840.	2140.	0.	0.	0.	0.	0.	0.	0.	0.
42 BC	500.	2240.	2830.	0.	0.	0.	0.	0.	-600.	-2290.	-2680.	-3480.
42 BE	500.	2240.	2880.	0.	0.	0.	0.	0.	0.	0.	0.	-2190.
42 BG	0.	0.	0.	1790.	0.	0.	0.	0.	0.	0.	0.	0.
42 BI	450.	2190.	2930.	0.	0.	0.	0.	0.	-600.	-2330.	-2780.	-3580.
42 BK	-2480.	0.	0.	0.	0.	0.	0.	0.	-250.	-1640.	-1440.	-5170.
42 BM	3330.	400.	0.	1640.	0.	0.	0.	0.	0.	0.	0.	0.
44 AO	0.	350.	350.	550.	0.	0.	0.	0.	0.	0.	0.	0.
44 AQ	0.	-990.	-1490.	-2480.	0.	0.	0.	0.	0.	0.	-450.	-1690.
44 AW	0.	450.	1640.	1740.	0.	0.	0.	0.	0.	0.	0.	0.
44 BA	350.	1490.	1940.	0.	0.	0.	0.	0.	-500.	-1590.	-1590.	-2480.
44 BE	0.	400.	200.	650.	0.	0.	0.	0.	0.	-600.	-600.	-1190.
44 BI	50.	1540.	2190.	1590.	0.	0.	0.	0.	-250.	-1540.	-1340.	-4970.
44 BK	0.	-1440.	0.	0.	0.	0.	0.	0.	0.	0.	0.	0.
44 BM	0.	1640.	1040.	-500.	0.	0.	0.	0.	0.	0.	0.	0.
44 BO	0.	0.	0.	0.	0.	0.	0.	0.	-700.	-3830.	-3830.	-4970.
45 BB	0.	450.	1590.	1690.	0.	0.	0.	0.	0.	0.	0.	0.
46 AS	500.	0.	0.	0.	0.	0.	0.	0.	0.	0.	0.	0.
46 AU	0.	0.	600.	2630.	0.	0.	0.	0.	0.	0.	0.	0.
46 AV	0.	0.	0.	0.	0.	0.	0.	0.	0.	0.	-550.	-1890.
46 AW	0.	0.	0.	0.	0.	0.	0.	0.	0.	0.	-250.	-990.
46 AX	0.	550.	2730.	4470.	0.	0.	0.	0.	0.	0.	0.	0.
46 AY	0.	0.	0.	0.	0.	0.	0.	0.	0.	0.	-350.	-1290.
46 BA	0.	0.	0.	0.	0.	0.	0.	0.	-400.	-1790.	-2980.	-3580.
46 BC	0.	0.	0.	0.	0.	0.	0.	0.	-400.	-1490.	-3080.	-7950.
46 BD	100.	1090.	150.	250.	0.	0.	0.	0.	0.	0.	0.	0.
46 BE	0.	0.	0.	0.	0.	0.	0.	0.	-100.	-1290.	-1690.	-3480.
46 BI	50.	1590.	2830.	1940.	0.	0.	0.	0.	0.	0.	0.	0.
46 BK	0.	-1540.	0.	0.	0.	0.	0.	0.	-790.	-4520.	-4570.	-5960.
46 BM	-2480.	-500.	-1990.	-2480.	0.	0.	0.	0.	0.	0.	0.	0.
47 AZ	0.	1640.	3280.	2480.	0.	0.	0.	0.	0.	0.	0.	0.
47 BB	0.	790.	1040.	1890.	0.	0.	0.	0.	0.	0.	0.	0.
47 BO	-990.	0.	0.	0.	0.	0.	0.	0.	0.	0.	0.	0.

mal. Most of the increased runoff was near the coast because the water table there is near land surface and closely spaced streams give good surface drainage. Also, storm-sewer systems near the coast route storm runoff directly to the surrounding bays. Inland, where streams are fewer and where there is a thick unsaturated zone, runoff and natural evapotranspiration are minor. In the central part of the island, even storm water quickly infiltrates beyond the reach of plant roots and solar heat, and runoff from buildings and paved areas is disposed of through dry wells and recharge basins; consequently, the irregular frequency of precipitation does not result in increased runoff. Thus, on the basis of observations, the assumed distribution

TABLE 3.—*Net recharge (positive) and withdrawal (negative) at each model node used to simulate manmade historical stresses in western Long Island during the periods 1903–33, 1934–42, 1943–50, and 1951–63. Unstressed nodes are not listed*—Continued

	LEVEL 1				LEVEL 2				LEVEL 3			
YEARS--	1903-33	1934-42	1943-50	1951-63	1903-33	1934-42	1943-50	1951-63	1903-33	1934-42	1943-50	1951-63
MODEL NODE	CUBIC METRES PER DAY				CUBIC METRES PER DAY				CUBIC METRES PER DAY			
48 AM	0.	0.	0.	0.	0.	0.	0.	0.	0.	0.	0.	-2580.
48 AW	100.	700.	940.	0.	0.	0.	0.	0.	-200.	-600.	-840.	-2290.
48 AY	0.	0.	0.	0.	0.	0.	0.	0.	-200.	-600.	-750.	-2190.
48 BC	250.	2430.	1690.	3280.	0.	0.	0.	0.	-400.	-2480.	-3380.	-5960.
48 BE	150.	1090.	200.	100.	0.	0.	0.	0.	-150.	-1290.	-1690.	-3480.
48 BG	0.	0.	0.	0.	0.	0.	0.	0.	-1790.	-8940.	-12420.	-14900.
48 BK	50.	1640.	2290.	1490.	0.	0.	0.	0.	-250.	-1590.	-1390.	-5070.
48 BM	100.	1740.	2380.	1690.	0.	0.	0.	0.	-500.	-3480.	-5220.	-11920.
48 BO	0.	0.	0.	0.	0.	0.	0.	0.	-6950.	-3970.	-4970.	-6950.
49 AY	100.	500.	500.	0.	0.	0.	0.	0.	0.	0.	0.	0.
49 BE	0.	1140.	1740.	2330.	0.	0.	0.	0.	0.	0.	0.	0.
49 BG	1440.	8150.	11280.	11230.	0.	0.	0.	0.	0.	0.	0.	0.
49 BM	0.	1640.	1090.	400.	0.	0.	0.	0.	0.	0.	0.	0.
50 AS	-500.	-2980.	-2480.	-2980.	0.	0.	0.	0.	-5960.	-2580.	-1990.	-2580.
50 AU	0.	0.	-500.	-500.	0.	0.	0.	0.	0.	0.	0.	0.
50 AW	0.	0.	0.	0.	0.	0.	0.	0.	-450.	-990.	-1390.	-3480.
50 AY	0.	250.	350.	0.	0.	0.	0.	0.	0.	-400.	-400.	-600.
50 BC	0.	0.	0.	0.	0.	0.	0.	0.	0.	0.	0.	0.
50 BE	0.	0.	0.	0.	0.	0.	0.	0.	-150.	-1390.	-1840.	-3730.
50 BK	100.	1740.	2330.	1440.	0.	0.	0.	0.	-250.	-1640.	-1440.	-5170.
50 BM	0.	0.	0.	0.	0.	0.	0.	0.	-500.	-2730.	-3230.	-3970.
51 AW	300.	1140.	1990.	0.	0.	0.	0.	0.	0.	0.	0.	0.
51 BC	0.	0.	-50.	1640.	0.	0.	0.	0.	0.	0.	0.	0.
52 AO	0.	0.	0.	0.	0.	0.	0.	0.	-600.	-890.	-1190.	-1640.
52 AQ	0.	0.	0.	0.	0.	0.	0.	0.	-600.	-890.	-1090.	-1540.
52 AU	0.	0.	-550.	-1590.	0.	0.	0.	0.	-150.	-550.	-550.	-1640.
52 AY	-300.	-2730.	-300.	-300.	0.	0.	0.	0.	0.	0.	0.	0.
52 BC	550.	1140.	1690.	5370.	0.	0.	0.	0.	-750.	-1490.	-2190.	-4870.
52 BI	0.	0.	0.	3580.	0.	0.	0.	0.	0.	0.	0.	-4870.
52 BK	0.	890.	1490.	5960.	0.	0.	0.	0.	0.	0.	0.	-4870.
52 BM	-5960.	-3970.	-3970.	-3970.	0.	0.	0.	0.	-500.	-2730.	-3230.	-3970.
53 BH	-300.	-2480.	-300.	-300.	0.	0.	0.	0.	0.	0.	0.	0.
53 BJ	0.	0.	0.	1490.	0.	0.	0.	0.	0.	0.	0.	0.
54 AM	100.	400.	4470.	1040.	0.	0.	0.	0.	0.	0.	0.	0.
54 AU	0.	0.	-450.	-1390.	0.	0.	0.	0.	-150.	-400.	-400.	-1190.
54 AW	100.	400.	300.	1440.	0.	0.	0.	0.	-150.	-500.	-500.	-1490.
54 AY	0.	550.	700.	0.	0.	0.	0.	0.	0.	-450.	-790.	-1290.
54 BA	0.	0.	0.	0.	0.	0.	0.	0.	-400.	-650.	-890.	-2330.
54 BC	0.	0.	0.	0.	0.	0.	0.	0.	-400.	-550.	-790.	-2140.
54 BI	0.	0.	0.	0.	0.	0.	0.	0.	0.	0.	0.	-7450.
54 BM	0.	0.	0.	0.	0.	0.	0.	0.	-1140.	-450.	-1040.	-200.
54 BO	-15900.	-11920.	-12420.	-2980.	0.	0.	0.	0.	-5020.	-2040.	-4720.	-890.
55 AT	-250.	-1990.	-250.	-250.	0.	0.	0.	0.	0.	0.	0.	0.
55 BB	550.	1140.	1640.	3870.	0.	0.	0.	0.	0.	0.	0.	0.
55 BF	-250.	-2330.	-250.	-250.	0.	0.	0.	0.	0.	0.	0.	0.
55 BH	0.	0.	0.	7450.	0.	0.	0.	0.	0.	0.	0.	0.
56 AL	100.	400.	3730.	990.	0.	0.	0.	0.	0.	0.	0.	0.
56 AM	100.	400.	4520.	1040.	0.	0.	0.	0.	0.	0.	0.	0.
56 AQ	0.	0.	0.	0.	0.	0.	0.	0.	0.	0.	0.	-400.
56 AT	-300.	-2480.	-300.	-300.	0.	0.	0.	0.	0.	0.	0.	0.
56 AZ	0.	750.	840.	3080.	0.	0.	0.	0.	0.	0.	0.	0.
56 BA	0.	0.	0.	0.	0.	0.	0.	0.	-300.	-500.	-500.	-2980.
56 BB	0.	0.	-150.	4770.	0.	0.	0.	0.	0.	0.	0.	0.
56 BC	0.	0.	0.	0.	0.	0.	0.	0.	0.	0.	-250.	-4920.
56 BE	0.	0.	0.	0.	0.	0.	0.	0.	0.	0.	0.	-1990.

(fig. 35) is defensible, and the simulated response shown in figure 36 provides a better comparison with prototype head decline than the other two cases that were tried. However, figure 36 indicates that a better match to observed water-table decline could have been obtained with a stress distribution intermediate between the one shown in figure 35 and a perfectly uniform distribution.

The second historical stress was obtained from pumping records that show a large increase in ground-water withdrawals in Kings County between 1899 and 1919. A similar increase occurred in Queens County during the mid 1930's and in Nassau County during World War II and the Korean War. Because of

TABLE 3.—*Net recharge (positive) and withdrawal (negative) at each model node used to simulate manmade historical stresses in western Long Island during the periods 1903–33, 1934–42, 1943–50, and 1951–63. Unstressed nodes are not listed*—Continued

	LEVEL 1				LEVEL 2				LEVEL 3			
YEARS-- / MODEL NODE	1903-33	1934-42	1943-50	1951-63	1903-33	1934-42	1943-50	1951-63	1903-33	1934-42	1943-50	1951-63
	CUBIC METRES PER DAY				CUBIC METRES PER DAY				CUBIC METRES PER DAY			
56 BG	0.	0.	400.	3970.	0.	0.	0.	0.	0.	0.	-350.	-3380.
56 BI	0.	0.	0.	990.	0.	0.	0.	0.	0.	0.	0.	-650.
56 BO	-9390.	-13060.	-6260.	-1540.	0.	0.	0.	0.	-600.	-600.	-2780.	-1990.
57 BE	0.	0.	250.	1640.	0.	0.	0.	0.	0.	0.	0.	0.
58 AR	100.	400.	400.	1690.	0.	0.	0.	0.	0.	0.	0.	0.
58 AY	100.	400.	350.	1290.	0.	0.	0.	0.	-150.	-500.	-500.	-1490.
58 BA	0.	0.	0.	0.	0.	0.	0.	0.	0.	0.	0.	-1990.
58 BE	0.	0.	350.	5510.	0.	0.	0.	0.	0.	0.	-250.	-5020.
58 BG	0.	0.	-990.	1390.	0.	0.	0.	0.	0.	0.	-350.	-3530.
58 BI	0.	0.	0.	0.	0.	0.	0.	0.	0.	0.	-400.	-3970.
58 BK	0.	0.	0.	0.	0.	0.	0.	0.	0.	0.	0.	-9940.
58 BM	0.	0.	-100.	9490.	0.	0.	0.	0.	0.	0.	0.	-5370.
58 BO	-8490.	-11770.	-5660.	-1440.	0.	0.	0.	0.	0.	0.	0.	0.
59 BI	0.	0.	300.	2480.	0.	0.	0.	0.	0.	0.	0.	0.
60 AQ	250.	-990.	-990.	-1490.	0.	0.	0.	0.	0.	0.	0.	0.
60 AY	100.	400.	350.	1340.	0.	0.	0.	0.	-100.	-400.	-400.	-1090.
60 BA	0.	0.	400.	7310.	0.	0.	0.	0.	0.	0.	0.	-4970.
60 BI	0.	0.	0.	550.	0.	0.	0.	0.	0.	0.	-500.	-4470.
60 BK	-300.	-2430.	-300.	-300.	0.	0.	0.	0.	0.	0.	0.	0.
60 BM	-11920.	-11920.	-8450.	-990.	0.	0.	0.	0.	0.	0.	0.	-2190.
60 BW	0.	0.	0.	0.	0.	0.	0.	0.	-200.	-890.	-600.	-1040.
61 BN	-10980.	-11970.	-8490.	-2480.	0.	0.	0.	0.	0.	0.	0.	0.
62 BA	0.	0.	0.	1640.	0.	0.	0.	0.	0.	0.	0.	-1540.
62 BC	0.	0.	0.	3630.	0.	0.	0.	0.	0.	0.	0.	0.
62 BI	0.	0.	0.	0.	0.	0.	0.	0.	0.	0.	0.	-400.
62 BJ	0.	0.	0.	1040.	0.	0.	0.	0.	0.	0.	0.	0.
62 BK	0.	0.	0.	0.	0.	0.	0.	0.	0.	0.	0.	-350.
62 BL	-250.	-2330.	-250.	-250.	0.	0.	0.	0.	0.	0.	0.	0.
62 BM	0.	0.	0.	0.	0.	0.	0.	0.	0.	0.	0.	-1190.
62 BO	0.	0.	0.	0.	0.	0.	0.	0.	-200.	-200.	-400.	-200.
62 BW	0.	0.	0.	0.	0.	0.	0.	0.	-200.	-840.	-600.	-940.
63 BF	0.	0.	350.	0.	0.	0.	0.	0.	0.	0.	0.	0.
63 BL	0.	0.	0.	2430.	0.	0.	0.	0.	0.	0.	0.	0.
63 BN	-10880.	-11870.	-8400.	-2480.	0.	0.	0.	0.	0.	0.	0.	0.
64 AQ	0.	0.	0.	0.	0.	0.	0.	0.	0.	0.	0.	-650.
64 AW	100.	400.	400.	1490.	0.	0.	0.	0.	-200.	-600.	-600.	-1840.
64 AY	0.	0.	0.	0.	0.	0.	0.	0.	-200.	-600.	-600.	-1790.
64 BA	0.	0.	0.	1740.	0.	0.	0.	0.	0.	0.	0.	-790.
64 BC	0.	0.	0.	0.	0.	0.	0.	0.	0.	0.	0.	-550.
64 BE	0.	0.	0.	0.	0.	0.	0.	0.	0.	0.	0.	-990.
64 BG	0.	450.	790.	750.	0.	0.	0.	0.	0.	-450.	-790.	-1290.
64 BM	0.	0.	500.	1340.	0.	0.	0.	0.	0.	0.	0.	0.
64 BI	0.	0.	0.	0.	0.	0.	0.	0.	0.	0.	-200.	-990.
64 BK	0.	0.	0.	0.	0.	0.	0.	0.	0.	0.	0.	-940.
64 BM	0.	0.	0.	2730.	0.	0.	0.	0.	0.	0.	0.	-3630.
64 BO	-11920.	-13910.	-8940.	-990.	0.	0.	0.	0.	0.	0.	0.	-4720.
64 BP	0.	890.	1490.	1140.	0.	0.	0.	0.	0.	0.	0.	0.
64 BW	0.	0.	0.	0.	0.	0.	0.	0.	0.	0.	0.	-100.
65 BD	0.	-2480.	-2480.	1440.	0.	0.	0.	0.	0.	0.	0.	0.
66 AS	0.	0.	0.	0.	0.	0.	0.	0.	0.	0.	0.	-1590.
66 AT	0.	0.	0.	2830.	0.	0.	0.	0.	0.	0.	0.	0.
66 AV	0.	0.	0.	0.	0.	0.	0.	0.	0.	0.	0.	-1390.
66 AW	0.	0.	0.	1090.	0.	0.	0.	0.	0.	0.	0.	-1340.
66 AY	100.	400.	450.	1540.	0.	0.	0.	0.	0.	0.	0.	0.
66 BE	0.	0.	0.	0.	0.	0.	0.	0.	0.	0.	0.	-990.

deteriorating water quality, many wells in Kings County were abandoned during the periods 1932–36 and 1940–42. For simulation, changes in pumping were assumed to occur instantaneously at 1903, 1934, 1943, and 1951. The complexity of this model stress (228 pumping areas in model levels 2 and 3, each changing discharge rates at four different times, table 3) cannot be adequately represented on a map. Nevertheless, the complexity of the prototype stress is considerably greater than the model stress.

After being used for cooling, water from many wells was returned to the ground through basins or shallow wells. Before 1961, most sewage in Nassau County was disposed of through cesspools and septic tanks. Water

TABLE 3.—*Net recharge (positive) and withdrawal (negative) at each model node used to simulate manmade historical stresses in western Long Island during the periods 1903–33, 1934–42, 1943–50, and 1951–63. Unstressed nodes are not listed*—Continued

	LEVEL 1				LEVEL 2				LEVEL 3			
YEARS—	1903-33	1934-42	1943-50	1951-63	1903-33	1934-42	1943-50	1951-63	1903-33	1934-42	1943-50	1951-63
MODEL NODE	CUBIC METRES PER DAY				CUBIC METRES PER DAY				CUBIC METRES PER DAY			
66 BG	0.	0.	0.	-150.	0.	0.	0.	0.	0.	0.	0.	0.
66 BK	0.	0.	0.	1190.	0.	0.	0.	0.	0.	0.	0.	-650.
68 AU	0.	0.	0.	2830.	0.	0.	0.	0.	0.	0.	0.	0.
70 AY	0.	0.	0.	0.	0.	0.	0.	0.	0.	0.	0.	-940.
70 BA	0.	0.	0.	1190.	0.	0.	0.	0.	0.	0.	0.	-940.
70 BG	0.	0.	0.	50.	0.	0.	0.	0.	0.	0.	0.	0.
70 BK	0.	0.	0.	250.	0.	0.	0.	0.	0.	0.	0.	0.
70 BN	0.	0.	0.	100.	0.	0.	0.	0.	0.	0.	0.	0.
71 AY	0.	0.	0.	940.	0.	0.	0.	0.	0.	0.	0.	0.
72 AW	0.	0.	0.	1140.	0.	0.	0.	0.	0.	0.	0.	-1090.
72 AY	0.	0.	100.	5170.	0.	0.	0.	0.	0.	0.	0.	-4970.
72 BM	0.	0.	0.	0.	0.	0.	0.	0.	0.	0.	0.	-600.
73 BL	0.	0.	0.	700.	0.	0.	0.	0.	0.	0.	0.	0.
75 AR	0.	0.	0.	3330.	0.	0.	0.	0.	0.	0.	0.	0.
76 AS	0.	0.	0.	0.	0.	0.	0.	0.	0.	0.	0.	-3280.
76 BK	0.	0.	0.	1340.	0.	0.	0.	0.	0.	0.	0.	-940.
78 AS	0.	0.	0.	150.	0.	0.	0.	0.	0.	0.	0.	-100.
78 BE	0.	0.	0.	1290.	0.	0.	0.	0.	0.	0.	0.	-1190.
78 BK	0.	0.	0.	100.	0.	0.	0.	0.	0.	0.	0.	-100.
80 AW	0.	0.	0.	300.	0.	0.	0.	0.	0.	0.	0.	-350.
80 BK	0.	0.	0.	0.	0.	0.	0.	0.	0.	0.	0.	-100.
80 BM	0.	0.	0.	350.	0.	0.	0.	0.	0.	0.	0.	-700.
81 BL	0.	0.	0.	150.	0.	0.	0.	0.	0.	0.	0.	0.
82 AS	0.	0.	0.	650.	0.	0.	0.	0.	0.	0.	0.	-650.
82 BC	0.	0.	0.	0.	0.	0.	0.	0.	0.	0.	0.	-350.
82 BD	0.	0.	0.	250.	0.	0.	0.	0.	0.	0.	0.	0.
82 BI	0.	0.	0.	0.	0.	0.	0.	0.	0.	0.	0.	-100.
83 BA	0.	0.	0.	150.	0.	0.	0.	0.	0.	0.	0.	0.
84 BL	0.	0.	0.	150.	0.	0.	0.	0.	0.	0.	0.	0.
84 BM	0.	0.	0.	0.	0.	0.	0.	0.	0.	0.	0.	-150.
84 BY	0.	0.	0.	0.	0.	0.	0.	0.	0.	0.	0.	-150.
86 AT	0.	0.	0.	700.	0.	0.	0.	0.	0.	0.	0.	0.
86 AU	0.	0.	0.	0.	0.	0.	0.	0.	0.	0.	0.	-650.
88 BI	0.	0.	0.	150.	0.	0.	0.	0.	0.	0.	0.	-150.
88 BY	0.	0.	0.	0.	0.	0.	0.	0.	0.	0.	0.	-150.
90 BY	0.	0.	0.	0.	0.	0.	0.	0.	0.	0.	0.	-150.

was returned to the ground in the model through 112 recharge areas, whose rates of recharge changed simultaneously with changes in pumping rate. Estimates of recharge are much less precise than estimates of pumping. On the basis of available information, the following assumptions were made: (a) Recharge from cooling water equals 90 percent of water pumped for this purpose; (b) recharge from domestic and commercial water equals 20 percent of water pumped for these purposes in sewered areas; (c) recharge from domestic and commerical water equals 75 percent of water pumped for these purposes in unsewered areas; (d) the remaining water is lost to evaporation or discharged to tidewater and does not return to the ground-water reservoir; and (e) all recharge water goes to the shallow aquifer. Changes in islandwide recharge, pumping, and net stress are given for the period 1903–63 in figure 37.

Pumping and recharge were simulated without streams. On western Long Island, where most of the pumping was done, the streams were mostly small; many of them had already disappeared by the time a regular stream-gaging program was begun. Thus, the contribution to ground water from diverted streamflow is largely unknown but is probably small. Inclusion of streams in this simulation was considered unnecessary, but ommission of streams adversely affected model accuracy in some areas.

Response to historical pumping and recharge is mapped in figures 38 and 39. Figure 38 and table 4 compare observed head changes with those measured on the model. Figure 38 shows good general agreement between model and prototype head changes, but many details are lost because of the coarse grid of the model. Local defects in simulation also result from the large time steps between changes in pumping rates. The difference between prototype and model drawdown in northwest Queens County (fig. 38) indicates some type

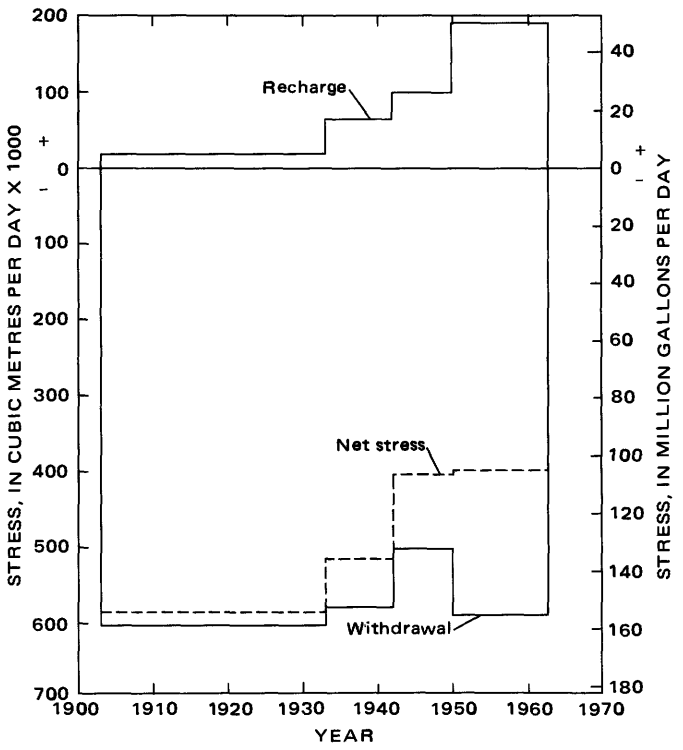

FIGURE 37.—Estimated islandwide changes in pumping, manmade recharge, and net stress between 1903 and 1963. These estimates were used in unsteady-state calibration of the model. They do not include water returned to the same node from which it is pumped.

of model or data deficiency. Comparison of figures 38 and 39 suggests that this deficiency is due to inadequate pumping data. Prototype data for 1961 (fig. 38) shows localized drawdown of 8 m (26 ft) and more in northwest Queens County. This drawdown is not seen in the model data for 1961 but is seen in the model data for 1942 (fig. 39). Apparently, pumping data for 1942–61 are incomplete, probably because drainage pumped from railroad tunnels was not included in pumping data. Model and prototype drawdowns for 1942 cannot be compared because of insufficient prototype data for that year. The author did not attempt to modify the stress to obtain a better comparison between model and prototype drawdowns. Near the north shore (northeastern Queens County, for example) are many localized faults in the simulation, which can be seen in most model tests. These faults result from inability of the coarse model grid to match the fine-scale variations in boundaries. However, ice-margin deformation of the sediments along the north shore creates local barriers to ground-water flow that were not modeled.

The general trend of model drawdown in Kings and Queens Counties, where most of the pumping on Long Island was done, matches the overall pattern in prototype drawdown quite well, not only in 1961 (fig. 38) but also at several other times as well. If the differences between the 1903 prototype water table and the steady-state model results in these counties (fig. 29) had been the result of poor model design, one would expect the unsteady-state model response to differ from prototype response by 50–100 percent, as was seen in the steady-state comparison. Averaging prototype drawdowns over areas of several square miles results in better agreement between prototype and model drawdowns than is shown in figure 38. Good comparison of unsteady-state model and prototype response is evidence that the discrepancy in the comparison of steady-state model and prototype response is chiefly the result of pre–1903 pumping, which the steady-state model did not simulate.

In the preceding test, the model was operating in the unsteady-state mode without natural recharge. Model streams were not flowing. The simulation is noticeably inaccurate where it does not account for diverted streamflow. In prototype situations, where wells were close to streams, they received part of their discharge from diverted streamflow. Wells 36, 37, 45, and 47 (table 4; fig. 40) are examples of this type of inaccuracy.

SUMMARY AND CONCLUSIONS

Problems in water resources evaluation that cannot be analyzed directly can be analyzed through model simulation. The Long Island ground-water reservoir was simulated by a three-dimensional analog model. Experience has shown that ground-water flow in thick, anisotropic aquifer systems such as the system on Long Island cannot be adequately described by two-dimensional methods but can be satisfactorily described by a three-dimensional model.

Boundaries of the Long Island ground-water reservoir are three dimensional, and the resulting natural patterns of ground-water flow are three dimensional. When wells and other human influences affect only the upper surface of the ground-water reservoir, some of the three-dimensional aspects of the natural flow system can be ignored; but the present state of ground-water development on Long Island, which superposes a new three-dimensional flow pattern on the preexisting, three-dimensional, natural flow system, requires three-dimensional analysis. Three-dimensional analysis is not only more difficult than two-dimensional analysis; it is less certain because data on hydraulic conductivity normal to the strata are much less abundant than data on hydraulic conductivity parallel to the strata and because compensating errors make evaluation of three-dimensional simulation more uncertain than evaluation of two-dimensional

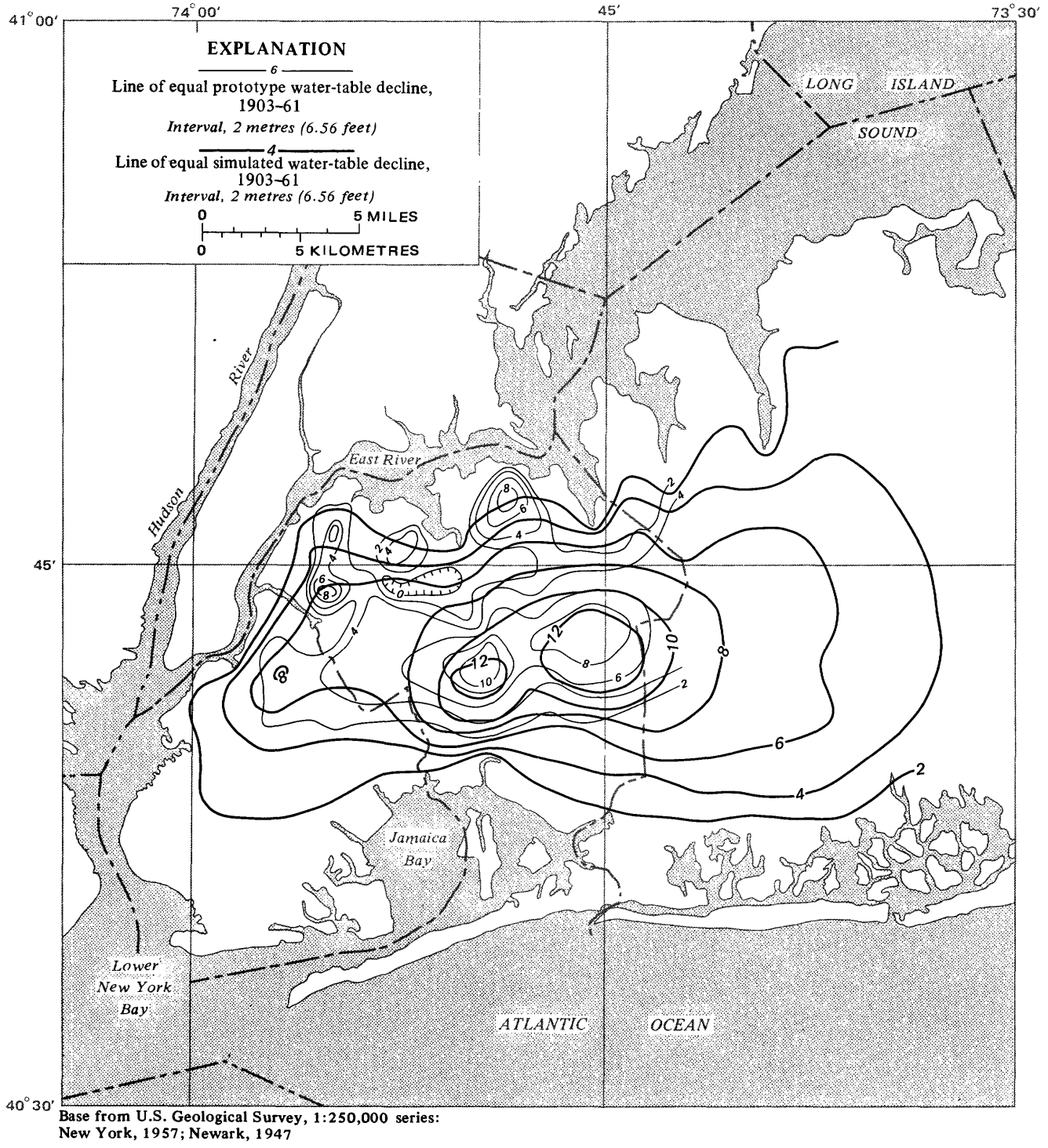

FIGURE 38.—Comparison of simulated decline in water table between 1903 and 1961 on western Long Island with observed decline. (Prototype data modified from Perlmutter and Soren, 1962.)

simulations.

Model-prototype comparisons indicate that this model simulates the Long Island ground-water reservoir adequately, but that care is required in modeling some types of stresses. Good results cannot be obtained when stresses cause significant changes in saturated thickness of the ground-water reservoir. Any change in saturated thickness causes a change in an aquifer's transmissivity that this modeling technique cannot simulate; when the change exceeds 10–15 percent of

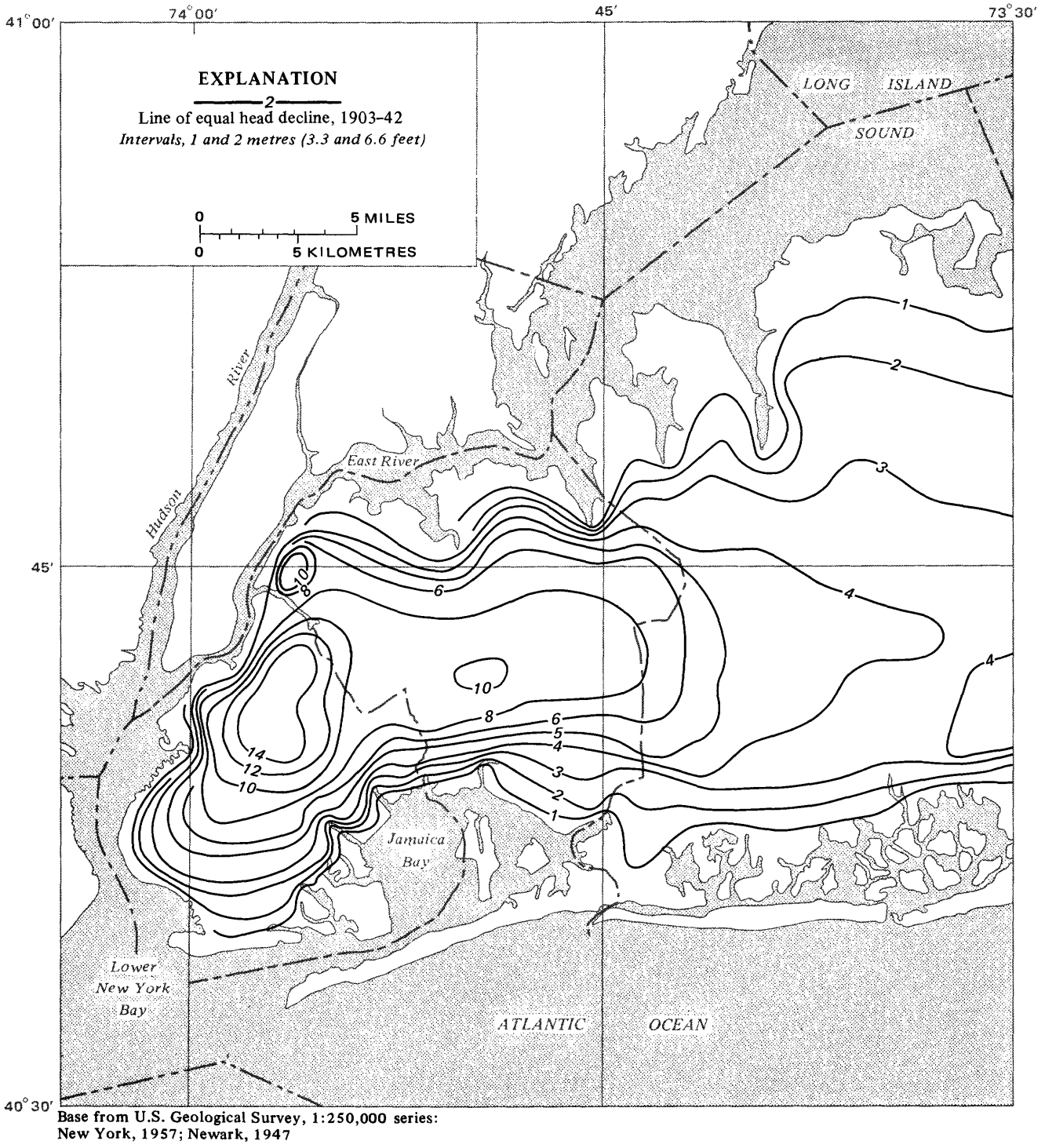

FIGURE 39.—Simulated decline in water table due to pumping on western Long Island between 1903 and 1942.

the total saturated thickness (about 15 m or 50 ft of drawdown for most of Long Island), the error resulting from the divergence of prototype and simulated transmissivity becomes significant. Offshore head measurements in the model are not reliable; boundary conditions there are not well understood. Several different circuits were used to simulate stream-aquifer relationships, but because these circuits were developed empirically, not on the basis of open-channel flow equations, the usefulness of each type of stream circuit is limited to a few stress situations. Extremely localized stresses near the mouths of streams can give

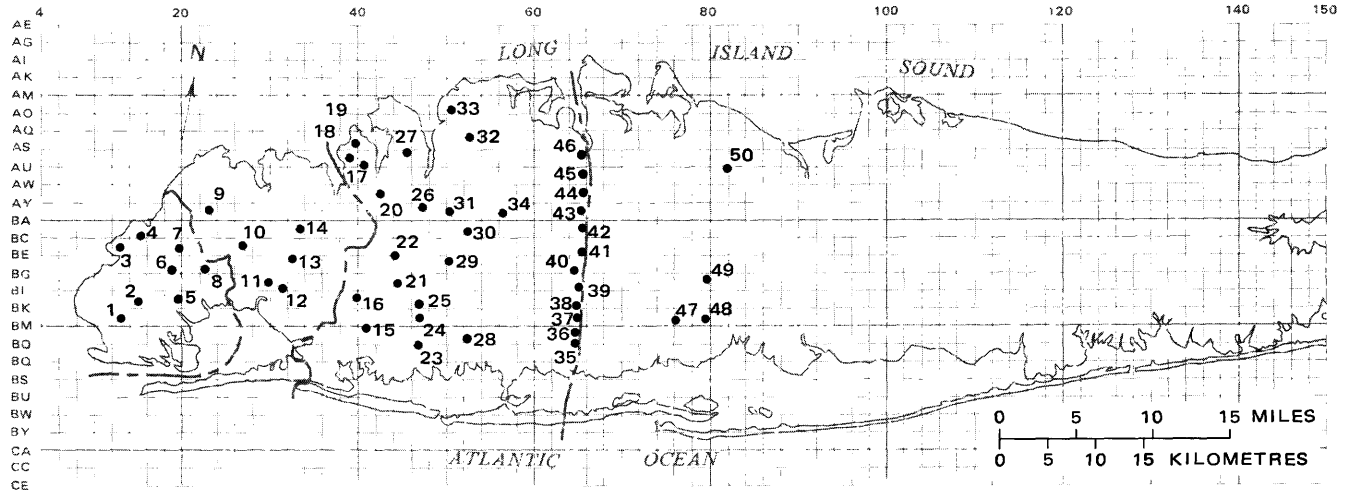

FIGURE 40.—Locations of wells used for water-level changes in table 4.

TABLE 4.—*Comparison of model and prototype water-level changes for selected wells between 1951 and 1963*

Well[1]	Prototype change (m)	Model change (m)	Well	Prototype change (m)	Model change (m)
1	[2]0.20	1.7	26	−2.0	−1.8 to −2.4
2	1.5	4.4	27	−.10	.10 to −.40
3	.50	0 to [3]1.0	28	.0	0 to .80
4	5.1	4.0	29	−.20	−1.2
5	1.0	2.0 to 3.0	30	−1.0	−.60
6	3.0	4.8 to 5.8	31	−1.0	−1.8
7	4.5	4.0 to 5.0	32	.0	−.50 to .60
8	2.0	1.2 to 2.0	33	−.30	0 to −.40
9	1.2	.80 to 1.0	34	−.60	0 to −.20
10	−.20	.10 to −.60	35	.03	1.0 to 1.8
11	−.40	0 to −.60	36	.06	1.0 to 1.8
12	−.50	−.60 to −.80	37	.30	.80 to 1.2
13	−3.0	−1.8 to −3.0	38	.40	.80
14	−4.0	−1.4 to −2.4	39	.30	.40 to .50
15	−.70	−1.4 to −1.6	40	.0	.20 to .40
16	−2.0	−2.2 to −2.6	41	.40	0 to .40
17	−1.0	−.24	42	.30	.20
18	−1.0	0 to −.24	43	.40	.20 to .30
19	−2.0	0 to −.18	44	.30	.20 to .30
20	−1.5	−1.0	45	−.40	.20
21	−.20	−2.4 to −2.6	46	.0	0 to .02
22	−2.5	−2.6	47	−.03	.22 to .26
23	−.20	−1.2	48	.03	.14 to .16
24	−.30	−2.0	49	.10	.12 to .14
25	−1.2	−1.4 to −2.0	50	.80	.04

[1]Well locations shown in figure 40.
[2]Positive changes indicate increasing water levels between 1951 and 1963; negative changes indicate decreasing water levels.
[3]Range of values indicates that prototype well lies between two model nodes having different changes in water level.

a distorted picture of stream discharge with almost any stream circuit.

The apparent inability of the steady-state model to match the 1903 water table in western Queens County is shown (by good unsteady performance in that area) to result from pumping interference in 1903, not from incorrect conductivities or boundaries in the model. This model, however, cannot simulate the fine structure of the hydrologic features in the north shore area; predictive results near the north shore may not be satisfactory.

The desired end product of model design, construction, and calibration is predictive capability. The ultimate purpose of the model is to predict response of the ground-water flow system to future stresses. Three types of stresses are considered: (a) Natural stresses, such as prolonged drought; (b) stresses caused by human activity, which are unforeseen or unplanned, including changes in recharge rate that result from paving and other construction activities such as dams, quarries, landfills, and recharge basins; and (c) planned water-management schemes. Examples of water-management alternatives are discussed briefly by Cohen, Franke, and Foxworthy (1968, p. 94–105); two plans are discussed exhaustively in Greeley and Hansen (1971) and Holzmacher, McLendon, and Murrell (1968). Several examples of each type of stress have been modeled. Results of these model tests and a description of the hydrologic and electrical assumptions underlying the tests are contained in other reports.

REFERENCES CITED

Bermes, B. J., 1960, An electric analog model for use in quantitative hydrologic studies: U.S. Geol. Survey open-file rept.

Burr, W. H., Hering, Rudolph, and Freeman, J. R., 1904, Report of the Commission on additional water supply for the city of New York: New York, Martin B. Brown Co., 980 p.

Cohen, Philip, Franke, O. L., and Foxworthy, B. L., 1968, An atlas of Long Island's water resources: New York Water Resources Comm. Bull. 62, 117 p.

Cohen, Philip, Franke, O.L., and McClymonds, N. E., 1969, Hydrologic effects of the 1962–66 drought on Long Island, New York: U.S. Geol. Survey Water-Supply Paper 1879–F, 18 p.

Collins, M. A., and Gelhar, L. W., 1970, Ground water hydrology of the Long Island aquifer system: Dept. Civil Eng., Massachusetts Inst. Technology, Hydrodynamics Lab. Rept. No. 122, 185 p.

Collins, M. A., Gelhar, L. W., and Wilson, J. L., III, 1972, Hele-Shaw

model of Long Island aquifer system: Am. Soc. Civil Engineers Proc., Jour. Hydraulics Div., v. 98, no. HY6, p. 1701–1714.

Collins, R. E., 1961, Flow of fluids through porous materials: New York, Reinhold Publishing Co., 270 p.

Cooper H. H., Jr., 1959, A hypothesis concerning the dynamic balance of fresh water and salt water in a coastal aquifer: Jour. Geophys. Research, v. 64, no.4, p. 461–467.

Dana, J. D., 1890, Long Island Sound in the Quaternary age, with observations on the submarine Hudson River channel: Am. Jour. Sci., 3d ser., v. 40, p. 425–437.

De Varona, I. M., 1896, History and description of the water supply of the city of Brooklyn: Brooklyn Commissioner of Public Works, 306 p.

Fetter, D. W., Jr., 1971, The hydrogeology of the south fork of Long Island, New York: Indiana University, unpub. Ph. D. thesis, 236 p.

Franke, O. L., and Cohen, Philip, 1972, Regional rates of groundwater movement on Long Island, New York: U.S. Geol. Survey Prof. Paper 800–C, p. C271–C277.

Franke, O. L., and Getzen, R. T., 1975, Evaluation of hydrologic properties of the Long Island ground-water reservoir using cross-sectional electric-analog models: U.S. Geol. Survey open-file report 75–679, 80 p.

Freeman, J. R., 1900, Report upon New York's (city) water supply: New York, Martin B. Brown Co., 587 p.

Freeze, R. A., and Witherspoon, P. A., 1967, Theoretical analysis of regional groundwater flow, II: Effect of water table configuration and subsurface permeability variations: Water Resources Research, v. 3, no. 2, p. 623–634.

Fuller, M. L., 1914, Geology of Long Island, New York: U.S. Geol. Survey Prof. Paper 82, 231 p.

Getzen, R. T., 1974, The Long Island ground-water reservoir; a case study in anisotropic flow: Urbana-Champaign, Ill., University of Illinois, unpub. Ph. D. thesis, 130 p.

Glover, R. E., 1959, The pattern of fresh-water flow in coastal aquifers: Jour. Geophys. Research, v. 64, no. 4, p. 457–459.

Greeley and Hansen, 1971, Report on comprehensive public water supply study, county of Nassau, New York: Contract CPWS–60 by Greeley and Hansen, Engineers, for country of Nassau and New York State Department of Health, 243 p.

Hollick, Arthur, 1893, Preliminary contributions to our knowledge of the Cretaceous formation of Long Island and eastward: New York Acad. Sci. Trans., v. 12, p. 222–237.

———1894, Some further notes on the geology of the north shore of Long Island: New York Acad. Sci. Trans., v. 13, p. 122–130.

Holzmacher, R. G., McLendon, S. C., and Murrell, N. E., 1968, Report on comprehensive public water supply study, Suffolk County, New York: Contract CPWS–24 by Holzmacher, McLendon, and Murrell, Consulting Engineers, for county of Suffolk and New York State Department of Health, 224 p.

Hubbert, M. K., 1940, The theory of ground-water motion: Jour. Geology, v. 48, no. 8, p. 785–944.

Isbister, John, 1959, Ground-water levels and related hydrologic data from selected observation wells in Nassau County, Long Island, New York: New York State Water Power and Control Comm. Bull. GW–41, 42 p.

———1966, Geology and hydrology of northeastern Nassau County, Long Island, New York: U.S. Geol. Survey Water-Supply Paper 1825, 89 p.

Jacob, C. E., 1939, Fluctuations in artesian pressure produced by passing railroad trains as shown in a well on Long Island, New York: Am. Geophys. Union Trans., v. 20, pt. 4, p. 666–674.

———1941, Notes on the elasticity of the Lloyd sand on Long Island, New York: Am. Geophys. Union Trans., v. 22, pt. 3, p. 783–787.

———1945, Correlation of ground-water levels and precipitation on Long Island, New York: New York State Water Power and Control Comm. Bull. GW–14, 20 p.

Jensen, H. M., and Soren, Julian, 1972, Hydrogeologic data from selected wells and test holes in Suffolk County, Long Island, New York: Long Island Water Resources Bull. 3, 35 p.

———1974, Hydrogeology of Suffolk County, Long Island, New York: U.S. Geol. Survey Atlas HA–501, 2 sheets.

Karplus, W. J., 1958, Analog simulation: New York, McGraw-Hill Book Co., 434 p.

Karplus, W. J., and Soroka, W. W., 1959, Analog methods [2d ed.]: New York, McGraw-Hill Book Co., 483 p.

Kimmel, G. E., 1971, Water-level surfaces in the aquifers of western Long Island, New York, in 1959 and 1970: U.S. Geol. Survey Prof. Paper 750–B, p. B224–B228.

———1972, The water table on Long Island, New York, in March 1970: Long Island Water Resources Bull. 2, 8 p.

Lubke, E. R., 1964, Hydrogeology of the Huntington-Smithtown area, Suffolk County, New York: U.S. Geol. Survey Water-Supply Paper 1669–D, 68 p.

Lusczynski, N. J., 1952, The recovery of ground-water levels in Brooklyn, New York, from 1947 to 1950: U.S. Geol. Survey Circ. 167, 29 p.

Lusczynski, N. J., and Swarzenski, W. V., 1966, Saltwater encroachment in southern Nassau and southeastern Queens Counties, Long Island, New York: U.S. Geol. Survey Water-Supply Paper 1613–F, 76 p.

McClymonds, N. E., and Franke, O. L., 1972, Water-transmitting properties of aquifers on Long Island, New York: U.S. Geol. Survey Prof. Paper 627–E, 24 p.

Mather, W. W., 1843, Geology of the first geological district, *in* Geology of New York, pt. 1. Nat. History of New York, pt. IV, New York State Mus. Nat. History: Albany, N.Y., Carroll and Cook, 653 p.

Mills, H. D., and Wells, P. D., 1974, Ice-shove deformation and glacial stratigraphy of Port Washington, Long Island, New York: Geol. Soc. America Bull., v. 85, p. 357–364.

Miller, J. F., and Frederick, R. H., 1969, The precipitation regime of Long Island, New York: U.S. Geol. Survey Prof. Paper 627–A, 21 p.

Perlmutter, N. M., and Geraghty, J. J., 1963, Geology and groundwater conditions in southern Nassau and southeastern Queens Counties, Long Island, New York: U.S. Geol. Survey Water-Supply Paper 1613–A, 205. p.

Perlmutter, N. M., and Soren, J., 1962, Effects of major water-table changes in Kings and Queens Counties, New York City: U.S. Geol. Survey Prof. Paper 450–E, p. E136–E139.

Perlmutter, N. M., and Todd, Ruth, 1965, Correlation and Foraminifera of the Monmouth Group (Upper Cretaceous), Long Island, New York: U.S. Geol. Survey Prof. Paper 483–I, 24 p.

Pluhowski, E. J., and Kantrowitz, I. H., 1964, Hydrology of the Babylon–Islip area, Suffolk County, Long Island, New York: U.S. Geol. Survey Water-Supply Paper 1768, 119 p.

Salisbury, R. D., 1902, Description of New York City: U.S. Geol. Survey, Geol. Atlas, Folio 83.

Skibitzke, H. E., 1961, Electronic computers as an aid to the analysis of hydrologic problems: Internat. Assoc. Sci. Hydrology, Pub. 52, p. 706–742.

Soren, Julian, 1971, Ground-water and geohydrologic conditions in Queens County, Long Island, New York: U.S. Geol. Survey Water-Supply Paper 2001–A, 39 p.

Suter, Russell, de Laguna, Wallace, and Perlmutter, N. M., 1949, Mapping of geologic formations and aquifers of Long Island, New York: New York State Water Power and Control Comm. Bull., GW–18, 212 p.

Swarzenski, W. V., 1963, Hydrogeology of northwestern Nassau and

northeastern Queens Counties, Long Island, New York: U.S. Geol. Survey Water-Supply Paper 1657, 90 p.

Upham, Warren, 1879, Terminal moraines of the North Atlantic ice sheet: Am. Jour. Sci., 3d ser., v. 18, p. 81–92, 197–209.

Upson, J. E., 1966, Relationships of fresh and salty ground water in the northern Atlantic Coastal Plain of the United States: U.S. Geol. Survey Prof. Paper 550–C, p. C235–C243.

———1970, The Gardiners Clay of eastern Long Island, New York—a reexamination: U.S. Geol. Survey Prof. Paper 700–B, p. B157–B160.

U.S. Geological Survey, 1972, Water resources data for New York, Part 1, Surface water records, 1971: U.S. Geol. Survey open-file rept., 302 p.

Veatch, A. C., Slichter, C. S., Bowman, Isaiah, Crosby, W. O., and Horton, R. W., 1906, Underground water resources of Long Island, New York: U.S. Geol. Survey Prof. Paper 44, 394 p.

Walton, W. C., and Prickett, T. A., 1963, Hydrogeologic electric analog computers: Am. Soc. Civil Engineers Proc., Jour. Hydraulics Div., v. 89, no. HY6, p. 67–91.

Wilson, J. W., III, 1970, A Hele-Shaw model for the study of the Long Island ground water system: Cambridge, Mass., Massachusetts Inst. Technology, unpub. M.S. thesis, 89 p.

Woodworth, J. B., 1901, Pleistocene geology of portions of Nassau County and Borough of Queens: New York State Mus. Bull., no. 48, p. 618–679.

☆ U.S. GOVERNMENT PRINTING OFFICE: 1976 - 789-025/26